ADDIS ABABA UNIVERSITY
SCHOOL OF EARTH SCIENCE

APPLICATION OF INTEGRATED GEOPHYSICAL TECHNIQUES FOR MAPPING GROUND WATER RESOURCE AT THE TISABALIMA SUB BASIN, EASTERN AMHARA REGIONAL STATE, ETHIOPIA.

A thesis Submitted to the School of Graduate Studies

of the Addis Ababa University

In partial fulfillment of the requirements for the Degree of Science Applied Geophysics

By

Tewodros Mulugeta

July, 2017 Addis Ababa

Declaration

I,the undersigned, hereby declare that the thesis entitled with **"**Application of integrated geophysical techniques for mapping ground water resource at the Tisabalima sub basin, eastern Amhara regional state, Ethiopia.**"** is my original work carried out under the supervision of Prof. Tigistu Haile and has not been presented a thesis for a degree program in any other university and all resources of materials used for the thesis are duly acknowledged.

Name: Tewodros Mulugeta

Signature ……..

The Thesis has been submitted for examination with my approval as university advisor.

Name: Prof. Tigistu Haile

Signature ……..

Place and date of submit ion: School of graduate studies

Addis Ababa University

Addis Ababa

July, 2017

Addis Ababa University

School of Earth Sciences

Geophysics Stream

APPLICATION OF INTEGRATED GEOPHYSICAL TECHNIQUES FOR MAPPING GROUND WATER RESOURCE AT THE TISABALIMA SUB BASIN, EASTERN AMHARA REGIONAL STATE, ETHIOPIA.

By: Tewodros Mulugeta

School of Earth Sciences

Approved by board of examiners:

	_____	_____
Chairman	**Signature**	**Date**
Prof. Tigistu Haile	_____	_____
Advisor	**Signature**	**Date**
	_____	_____
Internal Examiner	**Signature**	**Date**
Dr. AberaAlemu	_____	_____
Internal Examiner	**Signature**	**Date**
	_____	_____

ACKNOWLEDGEMENTS

I would like to acknowledge those people (expertise) for their contributions for letting me to share their extensive experience and knowledge during the preparation of this thesis as:

I would like to express my gratitude for my advisor prof.Tigistu Haile for his patience, advice and support during the long preparation this thesis. With your perspective as an advisor this thesis is mainly possible with your great experience on geophysical methods of ground water exploration and identification of ground water contaminants. You have been a trace in geophysical exploration for many students as well as researchers thank you again.

I would like to acknowledge staff members of Water Works Design and Supervision Enterprise Ato Engida Zemedagegnehu (chief hydro geologist) for his support for letting me to involve in Pressurized Irrigation Projectat Kobo-Robit-Minjar Valley. Practical knowledge of field works and interpretation has been possible with the help of geophysicists Ato Yigrem Assefa, thanks for your support for letting me to share your great experience on field geophysics. Further hydrogeologist Ato Kidanemaream, your contribution is so great in full filling the thesis with basic reference of bore hall data and ground water potential report the study areas.

Further to my friends and staff members (National Metrology Institute of Ethiopia) Ato Getachew Melaku, Neseredin Nezir and Henok Mengestu thank you for your support throughout this time.

My family,especial thank you for your believe in education; you have been so great to support me throughout my life.

ABSTRACT

This work which focuses on geophysical study at Tisabalima sub basin has the aim of identifying the groundwater potential zone of the sub basin and locate potential sites for the drilling of test and production boreholes. During this study, Electrical Sounding and Magnetic data were collected, processed and interpreted using additional inputs from geological and borehole data.

The electrical survey results have mapped the geeoelctrical/geological units and possible water bearing horizons in the area and these have enabled the selection of drilling sites for each traverse lines that showed the area to have high groundwater potential dominated by a confined aquifer. The area is identified as having alluvial deposits of sand, gravel and clay with a maximum thickness of 205 m.

The magnetic results showed that the area is highly affected by regional tectonic settings such as NE-SW and E-W trending faults that could be the main controlling factors for the source of groundwater occurrences and as a discharge zone in the area.

The electrical and magnetic results are seen to correspond very well especially in mapping vertical (near vertical) discontinuities like faults and weak zones in the area.

TABLE OF CONTENTS

LIST OF FIGURES

LIST OF TABLES

CHAPTER ONE

INTRODUCTION

1.1 General Introduction

Groundwater resource for Pressurized Irrigation Project at Kobo-Robit-Minjar Valley are currently being implemented in Eastern Amhara Development Corridor in parts of the Awash Basin by Ethiopian Construction, Design and Supervision Works Corporation (ECDSWC) Bureau previously known by Water Works, Design and Supervision Enterprise (WWDSE).The Project mainly focuses on the evaluation of the groundwater potential in parts of the Awash Basin. The project as such involves the assessments of the groundwater resources potential of three areas i.e., Woldiya, Mersa, Wirgesa and Tisabalima areas, Gerado, Kombolcha and Harbu areas, Kemissie and Chefa areas. Out of these three areas, the current research work involves the study on the potential area of Tisabalima area within the Woldiya, Mersa, Wirgesa and Tisabalima watershed.

In the past, geophysics has either been used as a tool for groundwater resource mapping or as tool for groundwater character discrimination. For groundwater resource mapping it is not the groundwater itself that is the target of the geophysics rather it is the geological situation in which the water exists. Integrated geophysical techniques, vertical electrical sounding and magnetic, have proved very popular in ground water exploration due to due to the simplicity of the technique and the ruggedness of the instrumentation.

Geoelectrical methods are applied to map the resistivity structure of the underground. Rock resistivity is of special interest for hydrogeological purposes: it allows, e.g., to discriminate between fresh water and salt water, between soft-rock sandy aquifers and clayey material, between hardrock porous/fractured aquifers and low-permeable claystones and marlstones, and between water-bearing fractured rock and its solid host rock (Reichard, 2009).

Magnetic survey measurement along the surface of the earth measure the resultant magnetic field which includes: dipole field, external field and rock magnetism. In magnetic surveying, rock magnetism is one of the interests because it relates to the existence of subsurface rocks of contrasting susceptibilities (high or low magnetic susceptibilities).Magnetic measurements can be used to locate subsurface rocks having high magnetic susceptibilities by mapping variations in the

strength of the magnetic field at the Earth's surface. The magnetic method can be used in groundwater exploration mapping of fractures in crystalline rocks and bedrock aquifers under alluvial cover, delineating volcano-sedimentary belts concealed by recent formations, and associated to local tectonic structures (faults, fractures/shears).

Every research project has its strength and weaknesses and the choice of the best topic is sometimes difficult. The selection of research project was made mainly based on criteria which are primarily the interest and willingness of researcher, availability of field site activities to collect primary geophysical data (electrical resistivity sounding and magnetic).Further, integerated geophysical investigation in the area (Tisabalima sub basin) has never been done until now. In this respect, the application of integrated geophysical techniques in ground water resource mapping and identifying the geological structures in which the water exists at Tisabalima sub basin (parts of Eastern Amhara Regional State) is selected for MSc thesis study.

During this study, resistivity [Vertical Electrical Sounding (VES)] secondary data collected by Ethiopian Construction, Design and Supervision Works Corporation and primary magnetic data have been used to define the ground condition of the subsurface.. Since the area is not well studied, this thesis will be an important contribution for defining the ground water condition of the sub basin.

The thesis has been organized in Five Chapters. The First Chapter is Introduction and presents general insight on the location, objective and general geologic, hydrogeologic and tectonic aspects of the study area. Chapter Two discusses the basic principles of the geophysical methods resistivity and magnetics. Chapter Three discusses data acquisition, processing and presentation. Finally Chapter four discussions about the field work, data reduction, interpretation, conclusion and recommendation of the studies.

1.2 Description of the Study Area

1.2.1 Location and topography

The study area is located within Eastern Amhara Regional State which is part of the Awash River catchment (Figure 1.1). The study area lies on UTM Geographical coordinate between latitudes Northing 1257436 to 1270701 and longitudes Easting 562692 to 571800 in meter.

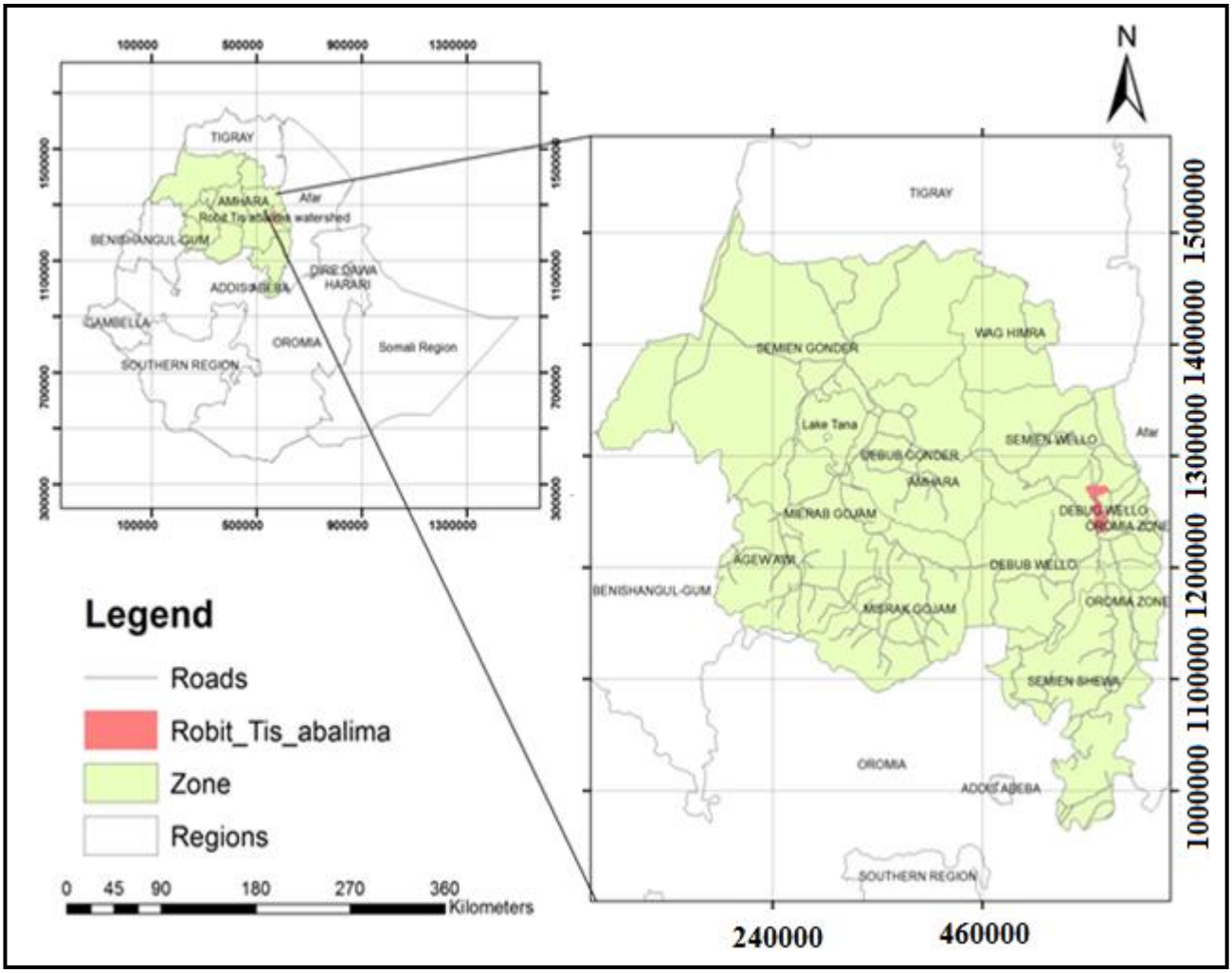

Figure 1.1 Location map of Tisabalima, the study area in the research work.

1.3 Objectives and Scope of the Study

1.3.1General Objective

The main objective of the study is identifying the groundwater potential zone of Tisabalima sub basin and locates potential sites for the drilling of test boreholes that are favorable for sustainable yield of ground water.

1.3.2 Specific Objectives

The specific objectives of the research work include

- Identify the major subsurface geoelectrical/geological units in the area and map possible water bearing horizons.
- Mapping subsurface structure like faults, fractures and fissures that acts conduits or barriers for groundwater flow.
- Identify potential sites for the drilling of test boreholes that are favorable for sustainable yield of ground water.

1.4 Previous Works

Geophysical studies namely Vertical Electrical Sounding (VES) surveys were conducted by Amhara Design and Supervision Works Enterprise, with the aim of identifying the groundwater potential assessment for test and/or production well drilling and also provision of subsurface information. The geoelectric section developed along two profiles TPV 1, TPV 2, TPV 3 and TPV 6, TPV 2, TAPV 4, TAPV 8 shown in Figure 1.2 and 1.3 revealed that the area has four to five major layers. The locations of these sounding profiles and the sounding points are indicated in Figure 3.1.

The first profile along TPV 1, TPV 2, and TPV 3 comprises of:

- Top dry soil
- sand and gravel layer
- silt layer
- weathered and fractured basalt layer
- bottom paleo soil (clay)

These layers layer vary in thickness from1-5 m, 40-50 m, 75-125 m, 125-150 m respectively. Whereas geo-electric section produced along VES points TPV 6, TPV 2, TAPV 4, and TAPV 8 reveal top dry clay soil having a resistivity 10 to 25 ohm-m underneath, the second layer comprises of sandy layer, with resistivity range 6-16 ohm- m and gravel (boulder) layer with resistivity range 30-64 ohm- m.

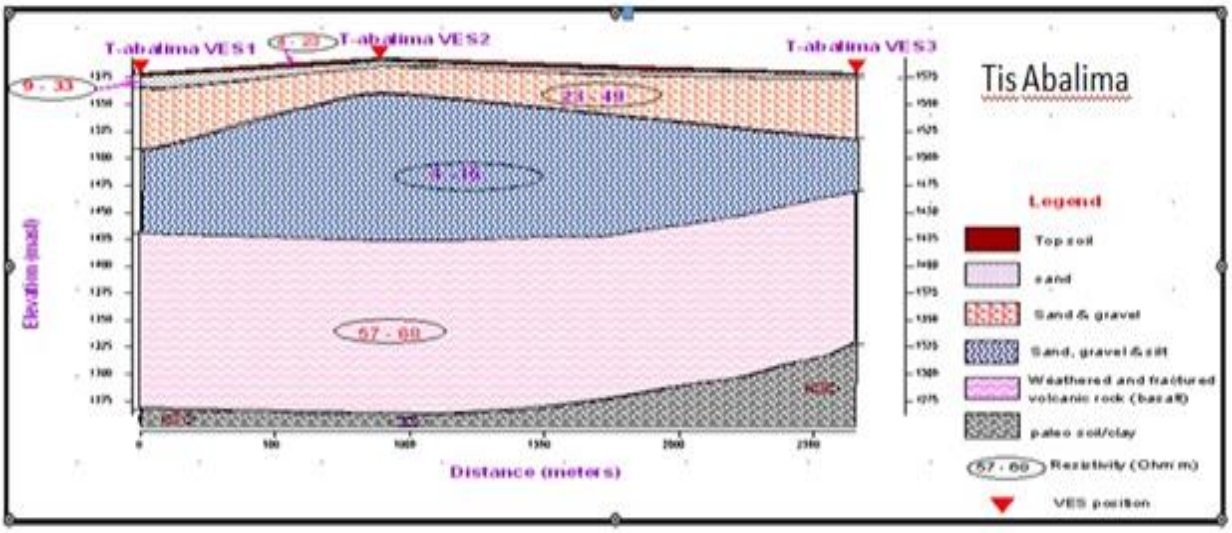

Figure 1.2 Geoelectrical Sections along the survey traverse consisting of VES pointsTPV 1, TPV 2 and TPV 3, Tisabalima sub basin (from AmharaDesignand Supervision Works Enterprise, 2013).

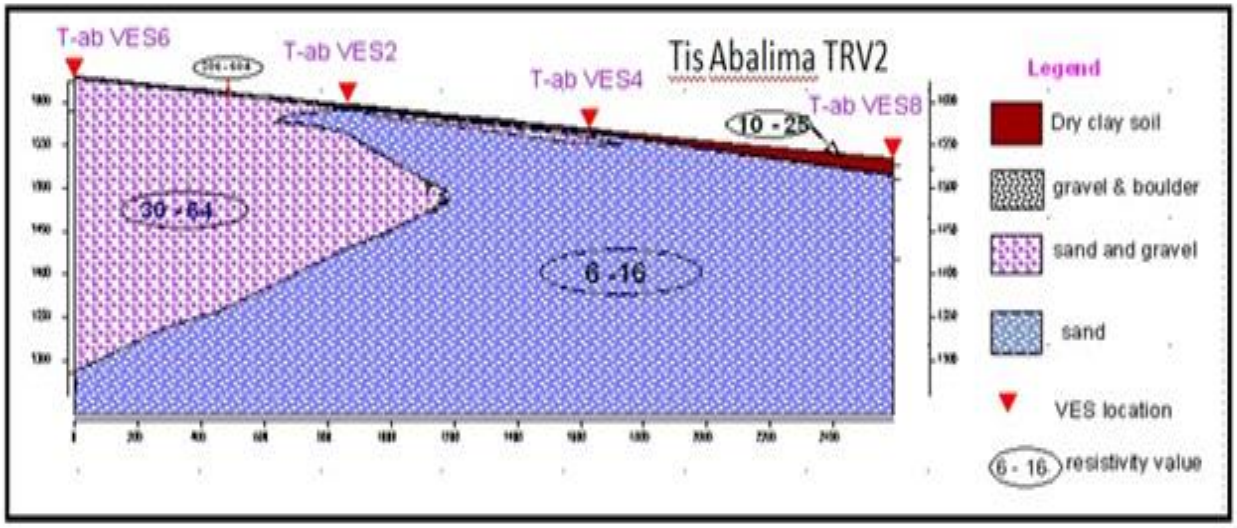

Figure 1.3 Geoelectrical Sections along the survey traverse consisting of VES points TPV 6, TPV 2, TAPV 4, TAPV 8, Tisabalima sub basin (from AmharaDesign and Supervision Works Enterprise, 2013).

This study is limited on electrical sounding survey along two profiles which makes it difficult to define zones of saturation (aquifer) of the study area. Due to a limitation in financial resources, an in integrated geophysical technique electrical and magnetic is mainly made to study the area that are located in between easting from 563553 to 569313 and northing 1264188 to 1271489 UTM geographical coordinate. To study the regional ground water flow in the area further magnetic survey should have to be made.

CHAPTER TWO

GEOLOGICAL, STRUCTURAL AND HYDROLOGICAL REVIEW

2.1 Regional Geology and Tectonic Setting of the Study Area

The ground water potential assessment of Kobo-Robit-Minjar unpublished report 2013 is reviewed for the study area as a reference. The general lithological units identified in the Kobo, Dessie,

Kemissie sheet are shown in Figure 2.1 revealing 23 rock types with separate lithological code. These units are shown on the geological maps of the study area. These mappable lithological rock units are listed below: -

- Upper sandstone (Ka)
- Ashange basalt (E3as)
- Aiba basalt (E2ai)
- AlajiSirro rhyolite, trachyte, ignimbrite & tuff (E2ajs)
- AlajiMolale rhyolite, trachyte, ignimbrite & tuff (E2ajm)
- Anchar basalt (NlAn)
- Termaber – Guassa basalt (E3tg)
- Dermaber – Megezez basalt (E3tm)
- Ataye Rhyolite & domes (Nlar)
- Granite Intrusion (Nlgt)
- Kessem formation (Nlkf)
- Fursa Rhyolite (NlFs)
- Mabla rhyolite (Nlma)
- Albuko rhyolite (Nlab)
- Dalha basalt (Nldh)
- Rasa basalt (Nlrb)
- Balchi rhyolite, ignimbrite, tuff (Nlbr)

- GaraBokan older rhyolitic domes & flows (QlGb)
- K'one Felsic volcanics (lavas, domes, pyroclastics) (Q1kv)
- Recent basalt flows & scoria cones (Q2rb)
- Fluvio-lacustrine sediments (Q1us)
- Alluvium (Qus)

Of these rock units, the dominant lithological units that feature in the Tisabalima area are the Alluvium (Qus) deposits.

Alluvium deposits (Qus)

This deposit is observed to occur in almost all of the marginal grabens of Tisabalima areas. The sub-basins have thick unconsolidated deposit that overlay the bedrock. The loose and unconsolidated sediments that are re-deposited in the sub-basins are thick enough to have implications on groundwater availability and movement. These deposits are very young sedimentary materials that are transported by the river that exists in the area.

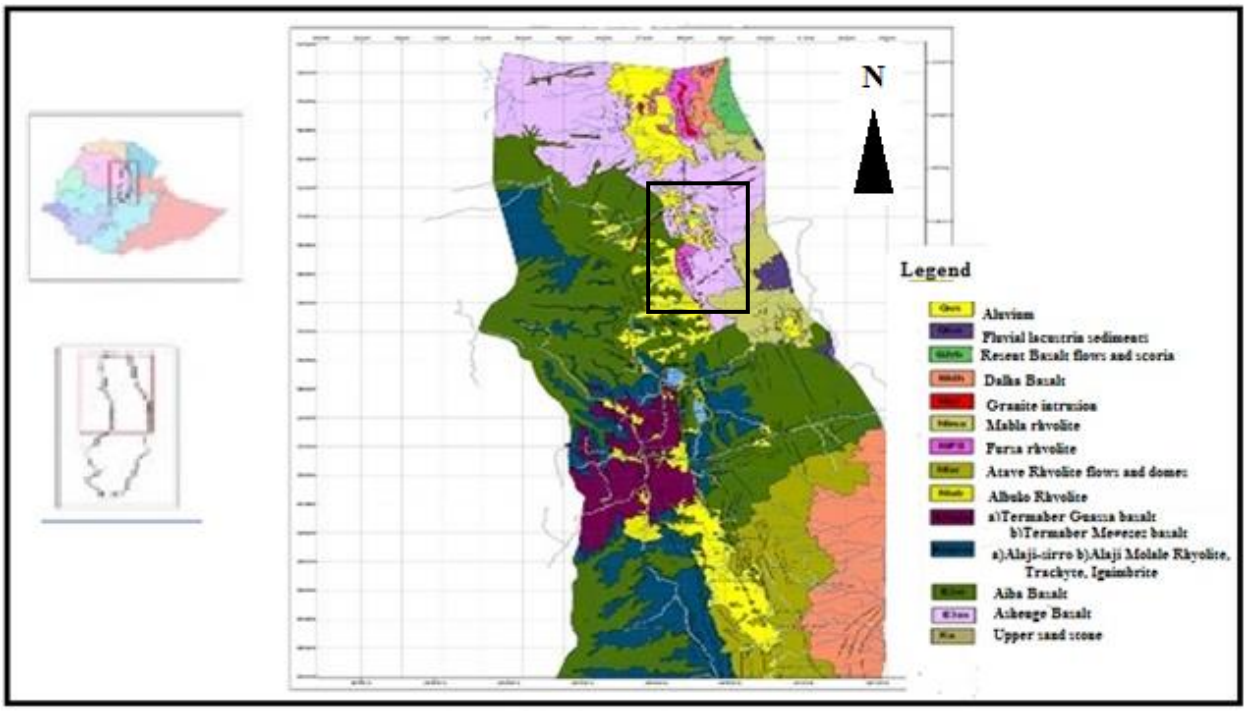

Figure 2.1 Geological Map of Kobo, Dessie, Kemissie Sheet, 1:250, 000scale (from Amhara Design and Supervision Works Enterprise, 2013).

Rivers have the capacity to erode, transport and deposit earth materials such as rocks and sediments. Fluvial processes are related to the hydrosphere and belong to the exogenous processes that shape the relief, sometimes by acting constructively land creation through accretion and other times by acting destructively, resulting in lowering of relief (erosion).

The formation of the drainage network in the marginal grabens or basins begins with the down faulting of the rifting processes. When the initial inclinations of the resulting escarpment are small, erosion processes are limited. With time, the escarpment continues to rise up its inclination dramatically, thus erosion becomes more intense and fluvial deposits more abundant. In general the river or stream flow directions are west to east from the plateau and bordering escarpments drain towards the rift.

When the solid supply of a stream is high and the transfer capacity is not adequate for the transportation of the corresponding solid material, flow speed is reduced and deposition of the heavier solid material (boulders, gravels) begins to be deposited in the upstream areas (towards the western sector of the marginal grabens near the Escarpments). As one goes towards downstream due to a decrease in inclination of the terrain, a decrease of a water stream's transfer capacity occurs and as a result finer and lighter materials (sand, silts, and clays) are deposited on the eastern part of the marginal grabens forming wide alluvial plains.

2.2 Geological structures

Several researchers agree that crustal extension had been commenced by 18Ma in the southern Main Ethiopian Rift (MER), but most of the present rift morphology was developed after 12 Ma. The age of the first stage basins in the northern Main Ethiopian Rift (MER) is considered to be 11 Ma; whereas the basins in the Southern Red Sea are 15 Ma older than those in the northern MER. The Main Ethiopian Rift is a narrow rift segment of 700 Km long, 80km wide volcanically active rift situated between the northwestern and southeastern Ethiopian plateaus bordered by the great border faults. The eastern margin border faults are characterized by rift-ward en échelon; right-stepping normal faults with a NNE-SSW & NE-SW strike directions. They are defined by multiple faults with cumulative displacement greater than100m on each of the fault, where as the

western margin is marked by a elevated escarpment with an exposed throw of 1.5 Km. Between these border faults, the central rift valley is marked by approximately 20 km-wide right-stepping, en echelon chains of eruptive volcanic centers, extension cracks, fissures and N15E striking, small offset normal faults. These right stepping en échelon faults, fissures and chains of Quaternary eruptive centers were collectively referred to as the Wonji Fault Belt (WFB).

Three distinct structural patterns are depicted in Kobo-Robit-MINJAR area are shown in Figure 2.2. These are, NNW to SSE trending structures are observed starting from Kobo up to Kara Kore area that is parallel to Red Sea Rift, the NE – SW structures that corresponds to the Main Ethiopian Rift trend, which characterizes the southern part, and N – S trending border faults from Kara-Kore up to Debresina-Ankober area where both the Main Ethiopian Rift and Red Sea Rift interact. Additionally ENE -WSW trending structures of the Gerado,-Meticolo – Degan- Bati areas and Ambo - Kessem fault that parallels the Gulf of Aden Ridge are also observed.

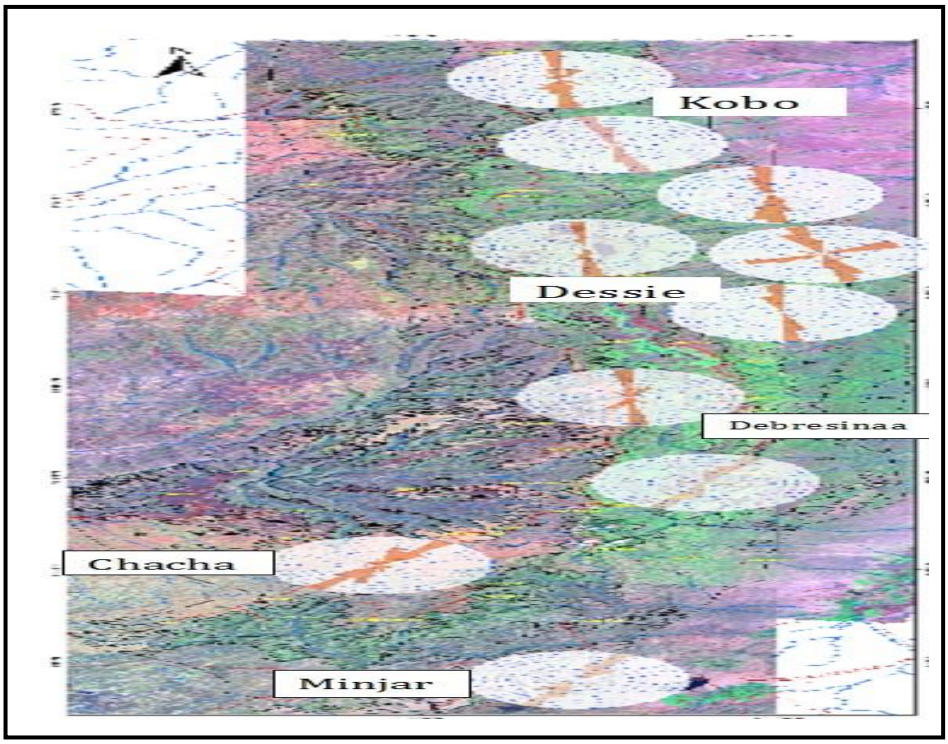

Figure 2.2 Strike variation of the major faults trend within the Kobo, Robit and Minjar(from Amhara Design and Supervision Works Enterprise, 2013).

2.3 Hydrogeology

2.3.1 Recharge and discharge area

Generally, the major sources of groundwater recharge are mainly high land plateau, fault block high lands and escarpments, shield volcanoes, high land plateau, isolated domes within the valleys, whereas marginal graben basins, low land and faulted plains are the discharge areas where groundwater is released in various ways.

2.3.2 Hydrogeological Set up of Tisabalima Sub basin

This area is located downstream of Kete stream catchment. It is wide E-W elongated intermountain valley plain area started from the foot of Ambassel Mountain (Tisabalima) along Mille stream up to Seglen area. Kete, Nibo (Chirecha) &Gomora streams begin from south west of Tisabalima area and join at about 2 km SW of Jarri village and form one big stream called Mille. This stream flows to north direction through highly faulted gorge to Tis Abalima plain area and later bends east to Seglen area. Since the western escarpment of Rift valley is highly affected by tectonic activities; most of the streams follow weak zone and transport huge volume of rock fragment (boulder, pebble, coble, sand, silt and clay). These transported earth material settle gradually at plain area based on grain size and fills intermountain valleys. Wide plain area south of Wuchale town and around Tisabalima town have coarser deposit and the base flow from the plain area of the unconsolidated sediments feeds the Mille stream. Rhyolitic and basaltic ridges around Wuchale town, Mille bridge, south and south west of Jari area, along the road to Marye-silassie, had been highly affected and crushed by north – south trending parallel faults and this situation provides a highly permeable condition for groundwater recharge and circulation. The presence of Bededo, Itecha, Passo-Mille, Jari and other high discharge springs indicate the role of tectonic effect on the groundwater recharge and circulation in the area.

Other intermountain valley plain area is along Burka intermittent stream begins north of Haik Lake and flows NE to Mille stream. This plain area starts from Kistane and extend to Seglen area with good prevailing geological and morphological circumstances for groundwater occurrence.

CHAPTER THREE

GEOPHYSICAL METHODS

3.1 General

3.2 Electrical Methods of Prospecting

3.2.1. Vertical Electrical Sounding (VES) Principle

In Vertical Electrical Sounding (VES), the positions of electrodes are changed with respect to a fixed point (known as the sounding point) and the measured values reflect the vertical distribution of resistivity values on a geologic section.

Vertical electrical sounding consists of a symmetrical electrode array used to determine the resistivity of the subsurface which is assumed to be consisting of horizontally stratified layers. The procedure is used to determine the variations in resistivity in the vertical direction and is also called electrical drilling or commonly vertical electrical sounding (VES). By expanding symmetrically the distance between current electrodes about a point called the sounding point, while keeping the potential electrodes MN at the same position, provides a sounding curve corresponding to the apparent resistivity versus depth of the location. As the spacing between the current electrode increases, the investigated depth will also increase. The two most commonly used arrays in electrical sounding survey are the Wenner and Schlumberger arrays. In this work, the data which was collected by using the Schlumberger electrode array techniques. When the Schlumberger array is used, the distance between the potential electrodes is not greater than one tenth of the current electrodes spacing. The advantage of this array is that initially only the spacing between the current electrodes is increased. However, at large current electrode spacing,

The measured potential becomes very low and the distance between the potential electrodes is increased. Increasing the potential electrode spacing produces a ‘step’ in the apparent resistivity curve and it is good practice to obtain an overlap between the curve segments by obtaining two readings at different potential electrode spacing for two adjacent current electrode spacing. Segments obtained at larger potential electrode spacing can be shifted in order to produce a smooth curve (Gibson and George, 2003). In electrical prospecting to determine the depth and electrical resistivity of a series of horizontal or nearly horizontal ground, it is difficult to measure

both parameters. In order to solve this problem, we should calculate the potential and the electric field, due to a point source of current, at any point on the surface of a stratified earth. This has advantages because of enables one to use axial symmetry of the potential filed about the vertical axis through the current source and the additive property of the potential is also be used. Let us choose a cylindrical system of coordinate with the origin at the point source a direct current located on the surface. The subsurface consists of infinite number of layers separated by horizontal boundary planes, the deepest layer existing to infinite depth and the other layers have finite thickness $h_i = h_1, h_2, h_3 \ldots h_n$ and resistivity's $\rho_i = \rho_1, \rho_2, \rho_3, \ldots, \rho_n$. Each of the layers is electrically homogeneous and isotropic.

The derivative of the potential based on the above conditions was first due to (Stefanescus et al., 1930).

The electrical potential field V for direct current satisfies the differential equation of Laplace, which is

$$\frac{\partial 2_V}{\partial x^2} + \frac{\partial 2_V}{\partial y^2} + \frac{\partial 2_V}{\partial z^2} = 0 \qquad (2.1)$$

The potential field has a cylindrical symmetry with respect to the vertical axis line through the current source. Therefore, Laplace equation in cylindrical coordinate is most appropriate.

For a solution symmetrical with respect to the vertical axis $\frac{\partial V}{\partial \theta} = \frac{\partial^2 v}{\partial \theta^2} = 0$ so,

$$\frac{\partial^2 V}{\partial X^2} + \frac{1}{r}\frac{\partial V}{\partial r} + \frac{\partial^2 V}{\partial Z^2} = 0 \qquad (2.2)$$

The particular solution of equation (2.2) can be obtained using the method of separation of variables and can be assumed to be of the form

$$V(r,z) = U(r)W(z) \qquad (2.3)$$

Substituting equation (2.3) to (2.2) and divide throughout by the product U(r) W (z) gives

$$\frac{1}{U(R)}\frac{\partial^2 U(r)}{\partial r^2}+\frac{1}{rU(r)}\frac{\partial U(r)}{\partial r}+\frac{1}{W(z)}\frac{\partial^2 W(Z)}{\partial z^2}=0 \qquad (2.4)$$

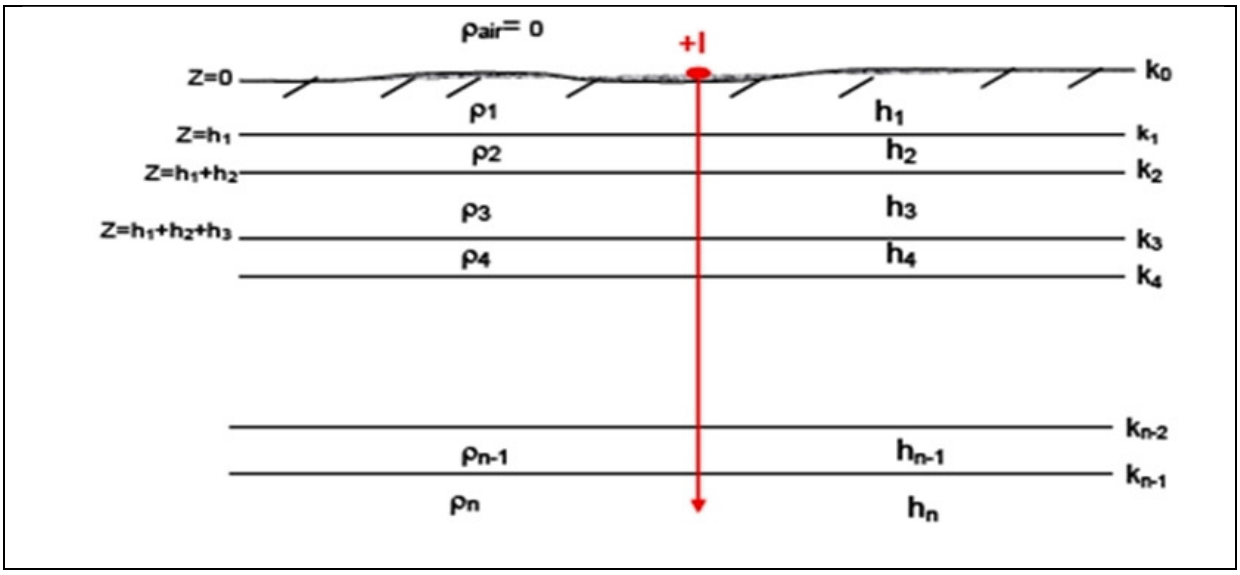

Figure 3.1 Problem presentation for sounding over multi-layered Earth**.**

This equation is satisfied if and only if

$$\frac{1}{U(R)}\frac{\partial^2 U(r)}{\partial r^2}+\frac{1}{rU(r)}\frac{\partial U(r)}{\partial r}=\lambda^2\ and \qquad (2.5)$$

$$\frac{1}{W(z)}\frac{\partial^2 W(Z)}{\partial z^2}=-\lambda^2 \qquad (2.6)$$

where λ is an arbitrary constant. The solution of equation (2.6) may be given as:

$$W(z)=C_1e^{-\lambda z}andW(z)=C_1e^{+\lambda z} \qquad (2.7)$$

and that of equation (2.5) is given as

$$U(r)=C_3J_O(\lambda r) \qquad (2.8)$$

where **J0**is the Bessel function of order zero.

The combination of equation (2.7) and (2.8) gives the particular solution of the differential equation given by equation (2.9), which is

$$V(r,z) = C_4 e^{+\lambda z} J_O(\lambda r) \; and \qquad (2.9)$$
$$V(r,z) = C_4 e^{-\lambda z} J_O(\lambda r)$$

where**c** and $\lambda$are both constants in the last of these equations.

Since, by theory of differential equation, every linear combination of the particular solution is also a solution, one can make λ to rough all possible values from zero toinfinity and allowing the constant "c" to very independence of λ the general solution of equation (2.2) can be obtained as

$$V(r,z) = \int_0^\infty [\phi(\lambda)\, e^{+\lambda z} + \psi(\lambda) e^{-\lambda z}]\, J_O(\lambda r) d\lambda \qquad (2.10)$$

Here$\phi(\lambda)$ and $\psi(\lambda)$are arbitrary functions of the boundary conditions control the special form of these equations. From basic theory, the potential generated by a single point source of current intensity "I" located at the surface of an electrically homogeneous earth is given by

$$V = \frac{I\rho}{2\pi} \frac{1}{\sqrt{r^2+z^2}} \qquad (2.11)$$

Where ρ is the resistivity of homogeneous Earth. Equation (2.11) can be written in integral form by using the so-called Lipchitz integral (also called the Weber Integral Formula) in theory of Bessel function as

$$\int_0^\infty e^{-\lambda z} J_O(\lambda r) d\lambda = \frac{1}{\sqrt{r^2+z^2}} \qquad (2.12)$$

So that equation (2.12) gives

$$V = \frac{I\rho}{2\pi} e^{-\lambda z} J_O(\lambda r) d\lambda \qquad (2.13)$$

Equation (2.13) is also a solution of equation (2.12). Therefore, the combined solutions will also be a solution to the equation, that is

$$V(r,z) = \frac{I\rho}{2\pi}\int_0^{\infty}[e^{-\lambda z} + X(\lambda)e^{+\lambda z} + \Theta(\lambda)\, e^{+\lambda z}]J_O(\lambda r)d\lambda \qquad (2.14)$$

Where $\Theta(\lambda)$ and $X(\lambda)$ are arbitrary function. Solutions of equation (2.14) are valid in all the layers of the subsurface. However, necessarily it is the same in different layers of the subsurface. Therefore, the potential due to a point source of current at the surface of a horizontally layered earth must in each layer satisfy

$$V_I = \frac{I\rho}{2\pi}\int_0^{\infty}[e^{-\lambda z} + X_i(\lambda)e^{+\lambda z} + \Theta_i(\lambda)\, e^{+\lambda z}]J_O(\lambda r)d\lambda \qquad (2.15)$$

This equation is called the Stefanescu Integral, with 'i' referring to the several layers of the subsurface.

Boundary conditions

For a potential set up by a single source of current at the surface of a horizontally stratified earth, the following boundary conditions are fulfilled.

1. At each of the boundary planes in the subsurface, the electrical potential must be the same

$$V_i = V \; at \; Z = h_i \qquad (2.16)$$

2. The vertical component of the current density must be continuous on each boundary plane (the current density normal to the boundary planes …)

$$(J_I)_N = (J_{i+1})_N$$

$$\frac{1}{\rho_i}\frac{\partial v_i}{\partial z} = \frac{1}{\rho_{i+1}}\frac{\partial v_{i+1}}{\partial z} \qquad (2.17)$$

the current source. In air J air = 0 and from condition (2.17), the vertical component of the current density at depth zero must be zero. Near the current source the potential must not approach infinity (must remain finite) as

$$V = \frac{I\rho}{2\pi}\frac{1}{\sqrt{r^2+z^2}} \qquad (2.18)$$

3.2.2 Basic Principles of Resistivity for Groundwater

- Groundwater, through the various dissolved salt it contains, is ionic ally conductive and enables electric currents to flow into the ground. By measuring the ground and subsurface resistivity therefore gives the possibility to identify conditions necessary for the presence or absence of water. In resistivity surveying, especially in vertical electrical sounding (VES), conduction in rocks is mainly due to pore fluids acting as electrolytes. Water in its pure form is poor conductor but most water contains dissolved salts which facilitate current flow. Resistivity of rocks generally depends on the water content (porosity), the resistivity of the water, the clay content and the content of metallic minerals (Bernard, 2003). The following considerations help in the determination of the resistivity of rocks.

- A hard rock without pores or fractures is very resistive to the flow of electric current. This is generally observed in hard fresh Precambrian rocks.

- Dry sand without water is very resistive.

- Porous or fractured rock bearing free water has resistivity, which depends on the resistivity of the water and on the porosity of the rock.

- Impermeable clay layer, which is wet, has low resistivity but may not contain enough yields for successful groundwater exploitation.

- Mineral ore bodies (iron, sulphides) have very low resistivity due to their electronic conductions; usually lower or much lower than 1 Ohm-m(Bernard, 2003).

To identify the conditions necessary for the presence of groundwater from resistivity measureme nts, the absolute value of the ground resistivity must be considered. Usual target for aquifer resistivity can be between 50 Ohm-m to 2000 Ohm-m (Bernard, 2003).

- In hard rock environment, which is considered very resistant to the flow of electric Current, a low resistivity anomaly will be the target for groundwater.

- In a clayey or salt environment that is normally considered conductive, a comparatively high resistivity anomaly will most probably correspond to fresh wate r and thus will be the target in the case for groundwater exploration for domestic use.

Resistivity values of earth materials cover a wide range (Table 3.1). The variety of resistivity has been the essential reason why the technique can be used for different applications (Loke, 2001).

In resistivity measurements, highest resistivities are associated with igneous rocks. Sedimentary r ocks tend to be most conductive due to their high fluid content. Metamorphic rocks have intermediate resistivity. Granites and quartzite have high resistivity ranges; sandstone and shale have intermediate resistivity ranges (Bernard, 2003). The resistivity therefore in a particular geological environment has an influence on the aquifer resistivity. Numerical values for various types of water are outlined (Table 3-2).

In resistivity measurements current is injected into the ground via electrodes and the resulting potential is measured also by electrodes in the ground. The outer electrodes shows the current electrodes for injecting current into the ground and the inner electrodes are the potential electrodes connected to the voltmeter. Consider that a direct current of strength, I, is introduced in to a homogeneous and isotropic earth by means of two point electrodes as shown in the Figure 2.2. The potential difference between the two points P1 and P2 on the surface is given by using equation (2.19).

The Potential at $V_{P1} = \frac{I}{2}\frac{\rho}{\Pi}\left(\frac{1}{r_1} - \frac{1}{r_2}\right)$

Similarly, the potential at $V_{P2}=\frac{I}{2}\frac{\rho}{\Pi}\left(\frac{1}{r3}-\frac{1}{r_4}\right)$

Table 3.1 Resistivity of some common rocks, minerals and soils (Loke, 2004)

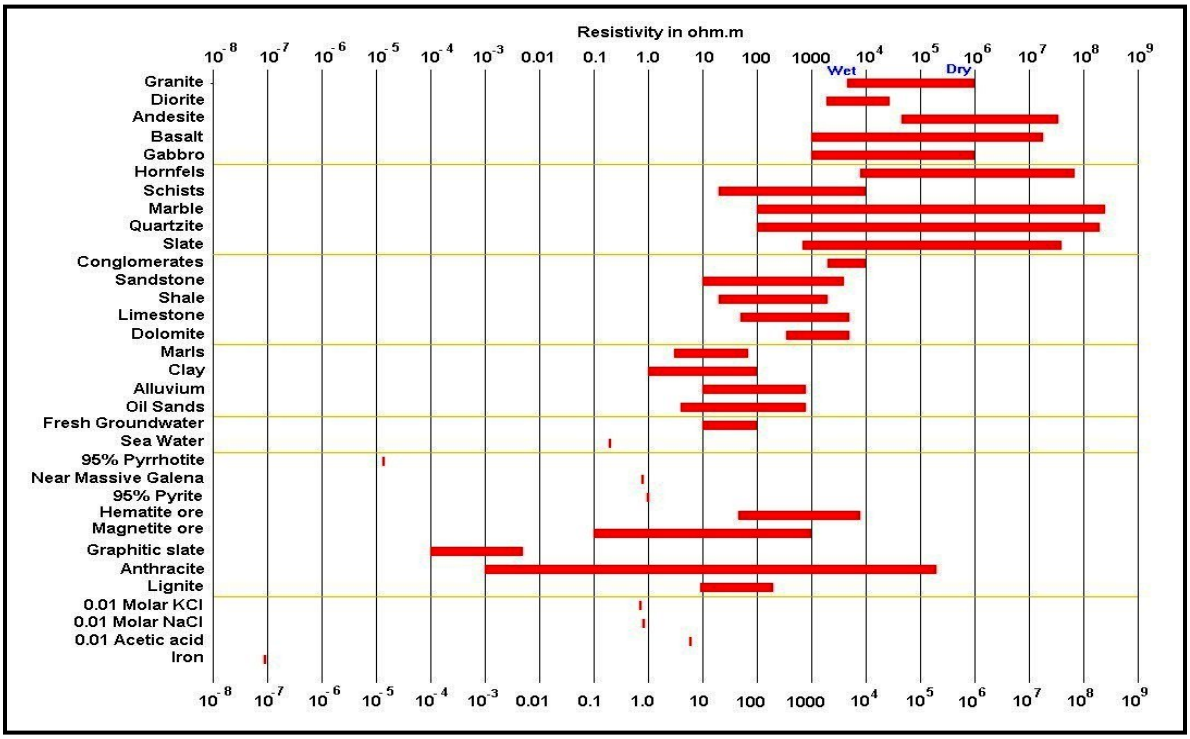

Table 3.2 Numerical values for various types of water (modified from Bernard, 2003).

Type of Water	**Resistivity(ohm-m)**	**Conductivity(micros/cm)**	**Salinity (mg/l)**
Fresh	20	500	150
Salted	10	1000	700
Sea water	0.3	30000	35000

The potential difference

$$\Delta V=\frac{I}{2}\frac{\rho}{\Pi}\left(\frac{1}{r1}-\frac{1}{r_2}-\frac{1}{r3}+\frac{1}{r_4}\right) \quad (2.19)$$

where r_1, r_2, r_3 and $r_4$distances in meters, whereas V_{P1} and $V_{P2}$are the potential at distance point P_1 and P_2.

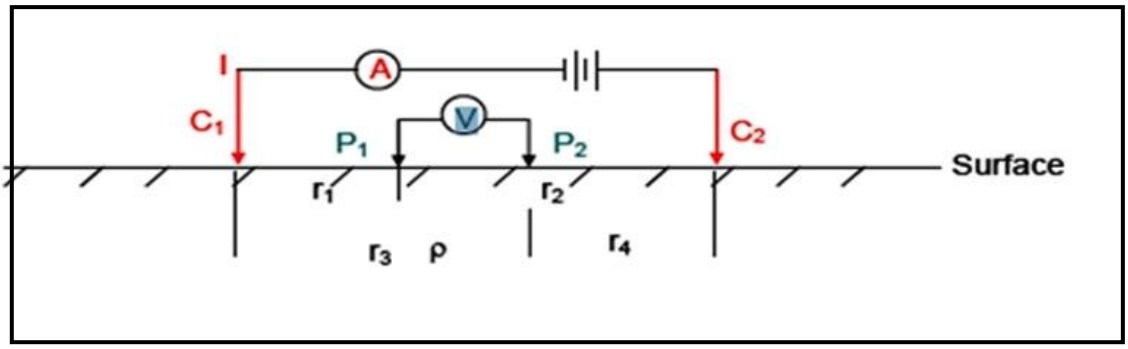

Figure 3.2 The arrangement of current and potential electrodes in a four-electrode system.

3.3 Magnetic Method of Prospecting

The other method employed in the work is the magnetic method of prospecting. Geomagnetic methods can be used in a wide variety of applications and range from small-scale investigations to locate pipes, cables and metallic objects in the very near surface, and engineering site investigations, through to large scale regional geological mapping to determine gross structure, such as in hydrocarbon exploration (Reynolds, 1997).

3.3.1 Basic concepts and units of Geomagnetism

Within the vicinity of a bar magnet a magnetic flux is developed which flows from one end of the magnet to the other (Figure 2.6).This flux can be mapped from the directions assumed by a small compass needle suspended within it. The points within the magnet where the flux converges are known as the poles of the magnet. A freely-suspended bar magnet similarly aligns in the flux of the Earth's magnetic field.

The pole of the magnet which tends to point in the direction of the Earth's North Pole is called the north-seeking or positive pole, and this is balanced by a south-seeking or negative pole of identical strength at the opposite end of the magnet (Kearey et al., 2002).

Magnetic poles always exist in pairs of opposite sense to form a dipole. When one pole is sufficiently far removed from the other so that it no longer affects the other, the single pole is referred to as a monopole (Reynolds, 1997).

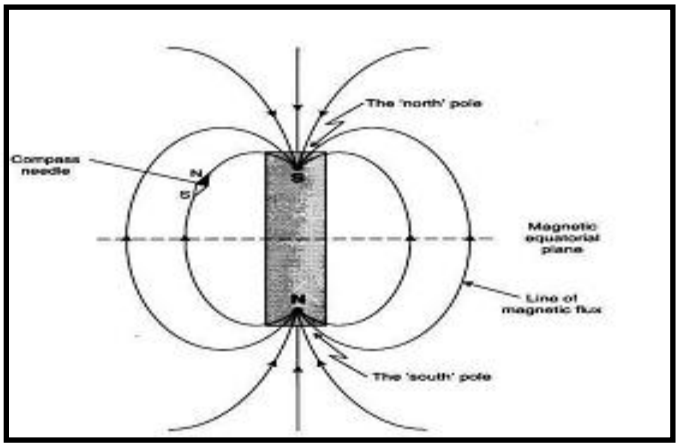

Figure 3.3 Lines of magnetic flux around a bar magnet (after Reynolds, 1997).

The force F between two magnetic poles of strengths m_1 and m_2 separated by a distance 'r' is given by

$$F = \frac{\mu_0 m_1 m_2}{4\pi\mu_R r^2} \tag{2.20}$$

where μ_0 and μ_R are constants corresponding to the magnetic permeability of vacuum and the relative magnetic permeability of the medium separating the poles (Kearey et al., 2002).The force is attractive if the poles are of different sign and repulsive if they are of like sign.

The magnetic field B due to a pole of strength m at a distance r from the pole is defined as the force exerted on a unit positive pole at that point

$$B = \frac{\mu_0 \mathrm{m}}{4\pi\mu_\mathrm{R}\mathrm{r}^2} \quad (2.21)$$

Magnetic fields can be defined in terms of magnetic potentials in a similar manner to gravitational fields. For a single pole of strength *m*, the magnetic potential *V* at a distance *r* from the pole is given by

$$V = \frac{\mu_0 m}{4\pi\mu_R r} \quad (2.22)$$

The magnetic field component in any direction is then given by the partial derivative of the potential in that direction.

The SI unit of B is expressed in Vsm^{-2}(Weber (Wb)m^{-2}). The unit of the Wbm^{-2} is designated the Tesla (T). The c.g.s unit of magnetic field strength is the gauss (G), numerically equivalent to 10^{-4}T.

Common magnets exhibit a pair of poles and are therefore referred to as dipoles. The *magnetic moment M* of a dipole with poles of strength *m* a distance *l* apart is given by

$$M = ml \quad (2.23)$$

The magnetic moment of a current-carrying coil is proportional to the number of turns in the coil, its cross sectional area and the magnitude of the current, so that magnetic moment is expressed in Am^2.

The intensity of induced magnetization J_i of a material is defined as the dipole moment per unit volume of material:

$$J_i = \frac{M}{LA} \quad (2.24)$$

Where M is the magnetic moment of a sample of length L and cross-sectional area A. J_i is consequently expressed in Am^{-1}.

The induced intensity of magnetization is proportional to the strength of the magnetizing force H of the inducing field:

$$J_i = kH \tag{2.25}$$

where k is the magnetic susceptibility of the material. Since J_i and H are both measured in Am^{-1}, susceptibility is dimensionless in the SI system.

In a vacuum the magnetic field strength B and magnetizing force H are related by $B=\mu_0 H$ where μ_0 is the permeability of vacuum ($4\pi \times 10^{-7} Hm^{-1}$). Air and water have very similar permeability to μ_0 and so this relationship can be taken to represent the Earth's magnetic field when it is undisturbed by magnetic materials (Kearey et al., 2002).

When a magnetic material is placed in this field, the resulting magnetization gives rise to an additional magnetic field in the region occupied by the material, whose strength is given by $\mu_0 J_i$. Within the body the total magnetic field, or magnetic induction, B is given by

$$B = \mu_0 H + \mu_0 J_i \tag{2.26}$$

Substituting equation (2.26)

$$B = \mu_0 H + \mu_0 kH = (1 + k)\mu_0 H = \mu_R \mu_0 H \tag{2.27}$$

where μ_R is a dimensionless constant known as the relative magnetic permeability. The magnetic permeability μ is thus equal to the product of the relative permeability and the permeability of vacuum, and has the same dimensions as μ_0. For air and water μ_R is thus close to unity.

3.3.2 Nature of the Geomagnetic Field

The geomagnetic field of the Earth is composed of three parts:

- The main field or Dipole field $\mathbf{B_D}$, which is produced in the fluid outer core of the earth and accounts for the very large regional variations in the total field intensity and direction.

- The external magnetic field $\mathbf{B_{ext}}$, which is produced by electric currents in the earth's ionosphere consisting of particles ionized by solar radiation and put into motion by the solar tidal force.

- The anomalous magnetic field which is produced by ferromagnetic minerals and rocks in the earth's crust or rock magnetism $\mathbf{B_{rm}}$.Therefore the Earth's total magnetic field $\mathbf{B_T}$ is given by

$$B_T = B_{ext} + B_D + B_{rm} \tag{2.28}$$

3. 3.3 The Earth's Magnetic Elements

A vector is used to represent the earth's magnetic field at an observation site. At any point on the Earth's surface, the magnetic field **B** has some strength and points in some direction. This vector quantity has a vertical component **Z** and a horizontal component **H** in the direction of the magnetic north. The horizontal component **H** of the magnetic field **B** can be further decomposed into a component **X** in the geographic north direction and a component **Y** in the geographical east direction. The terms which are used to describe the direction of the magnetic field **B** are declination (**D**), the angle between geographic and the magnetic north. The angle of declination is measured positive through east and varies from 0 to 360 degrees, and inclination (**I**), the angle between the horizontal **H** and field **B**. Angle of inclination **I** varies from -90^0 to 90^0. These seven magnetic elements are related in the following ways (Figure 3.4).

3.4 Data Reduction and Processing

Data reduction and processing is the series steps taken to remove both signal and spurious noise from the data that are not related to the geology of the site. This process there by prepares the dataset for interpretation by reducing the data to only contain signal relevant to the task. These steps are summarized below:

i. **Data checking and editing:** involves the removal of spurious noise and spikes from the data that was caused by high tension power cable.

ii. **Diurnal removal:** corrects for the temporal variation of the Earth's main field which was achieved by subtracting the time synchronized signal, recorded at a stationary base magnetometer from the survey data.

iii. **IGRF removal:** removes the strong influence of the Earth's main field. This was achieved by subtracting a calculated of main field from the diurnal corrected survey data.

$$B^2 = H^2 + Z^2 = X^2 + Y^2 + Z^2 \quad \mathrm{B}^2 = \mathrm{H}^2 + \mathrm{Z}^2 = \mathrm{X}^2 + \mathrm{Y}^2 + \mathrm{Z}^2$$

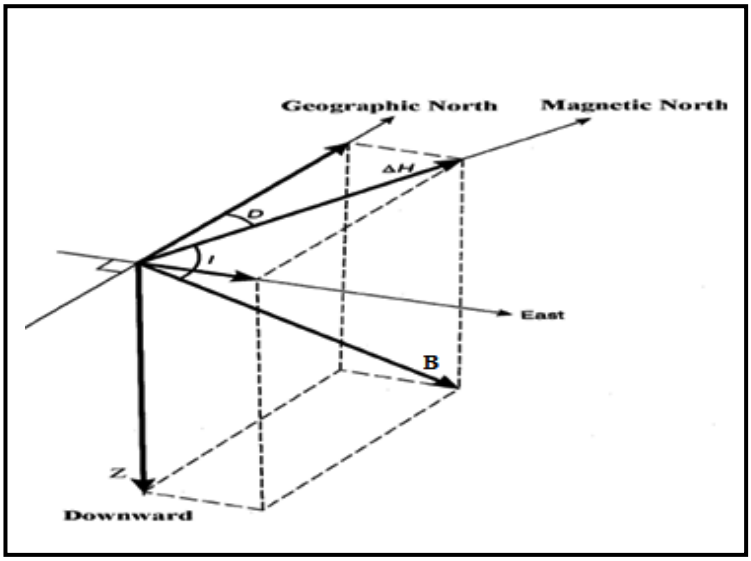

$$\mathrm{H} = \mathrm{B}\cos \mathrm{i}$$

$$\mathrm{Z} = \mathrm{B}\sin \mathrm{i}$$

$$\tan \mathrm{i} = \mathrm{Z} / \mathrm{H} \quad (3.22)$$

$$\mathrm{X} = \mathrm{H}\cos \mathrm{D}$$

$$Y = H \sin D$$

Figure 3.4 The Earth's magnetic field elements (from Reynolds1997).

CHAPTER FOUR

DATA ACQUISITION, PROCESSING AND PRESENTATION

4.1 The Resistivity Method

4.1.1 Field procedure and data acquisition

The Schlumberger array is mostly used in vertical electrical sounding for its better depth penetration and that it is less sensitive for lateral inhomogeneities because the potential electrodes remain fixed during a number of successive measurements with expanding current electrodes.

For this study the symmetrical Schlumberger array which is the secondary data which is vertical electrical sounding (VES) among 4 lines are shown in Figure 4.1. The VES were carried out with maximum current electrode spacing (AB/2) of 750 m by injecting electrical current in to the ground by means of two outer electrodes, and the resulting potential difference were measured by a second pair of potential electrodes placed near the center of the outer electrodes.

Electrical resistivity survey using ABEM SAS 1000 Terrameter was used to collect the data within an average distance of 880 m. The current electrode spacing AB/2: 1.5, 2.1, 3.0, 4.2, 6.0, 9.0, 13.5, 20.0, 30.0, 45.0, 66.0, 100.0, 150.0, 220.0, 330.0,500.0 and 750.0 meter and the potential electrodes spacing were MN/2 1.0, 12.0 and 90.0 were used to collect data during field work. The overlap readings AB/2: 20.0, 30.0, 150.0 and 220.0 m were taken in order to avoid the ambiguity of in homogeneity of the subsurface.

4.1.2 Data reduction

The apparent resistivity values are plotted on logarithmic transparent paper. In processing of the collected data, the apparent resistivity values were written on the ordinate and the electrode separation (AB/2) on the abscissa. The resistivity measurements were made by progressively increasing the potential electrode distance (MN/2) relatively large increment of the current

electrode distance (AB/2).In most cases the sounding curve is segmented due to overlap measurement and cannot be interpreted as it is. To have precise interpretations the segmented curves were shifted to the small MN curve points, so that the effect could be quantified and corrections could be made in order to obtain a single smooth curve that could be processed with the computer software known as "RESIXIP" software.

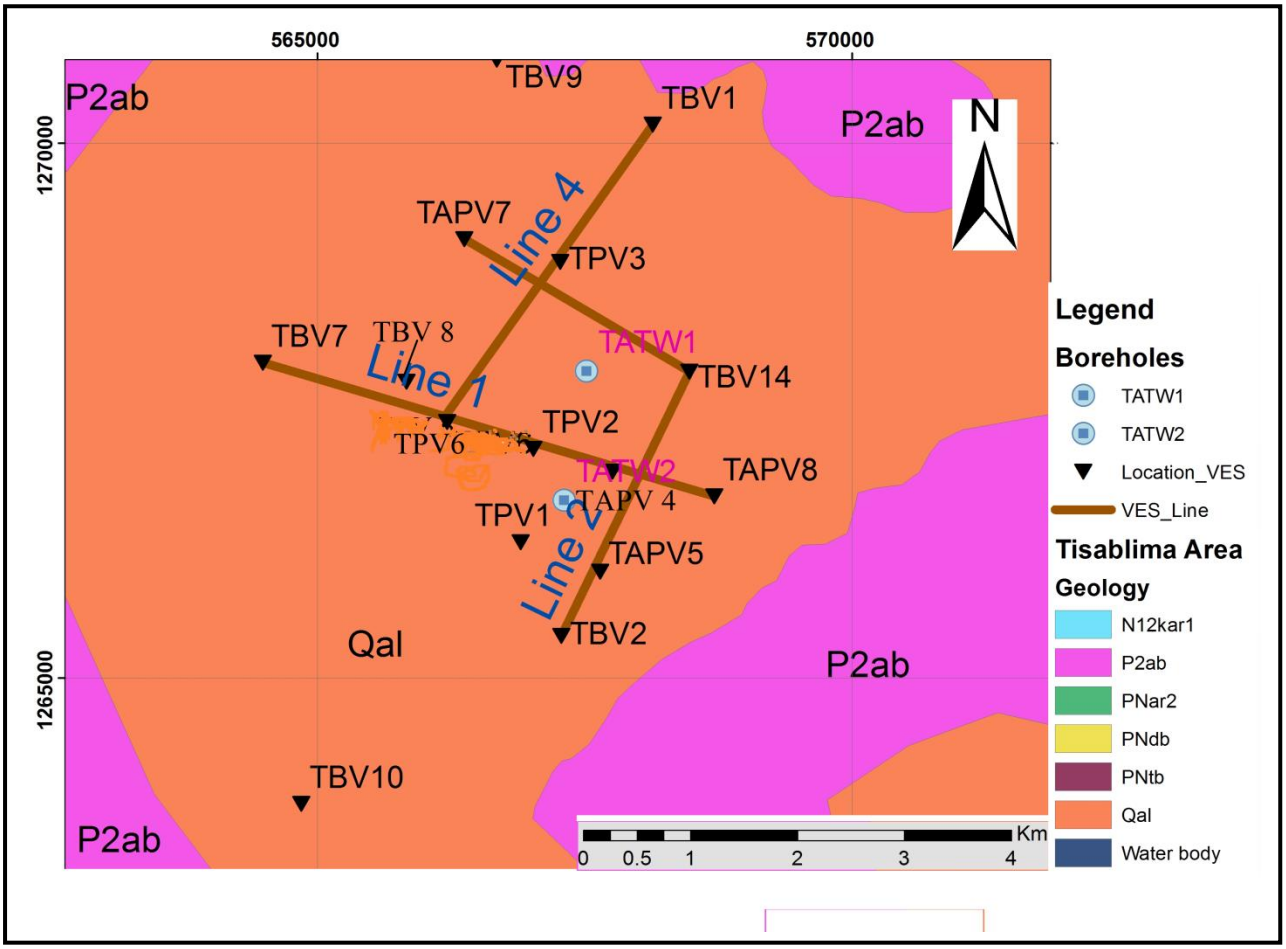

Figure 4.1 Location of the Vertical Electrical Sounding (VES) points along the four traverse lines at Tisabalima sub basin, Eastern Amhara Regional State Ethiopia.

4.1.3 Data processing and presentation

The electrical sounding data collected in the field work were plotted on a bi- logarithmic paper and interpreted by using two layer master curves and auxiliary charts to find out initial model parameters for the thickness and electrical resistivity of the possible layers mapped with survey. These

parameters obtained from curve matching techniques arranged and analyzed with litho logical units of existing boreholes were used as initial model in the WIN RESIST inversion software which resulted in improved and reliable electrical parameters under the area of investigation as depicted in the interpreted sounding resist curves. Consequently, from the results of these interpreted geoelectric parameters. The depth, thickness and resistivity parameters acquired by the mentioned software program of vertical electrical sounding curves were used to construct geoelectric sections for each VES to show the distribution of different lithological unit in vertical direction using the software AutoCAD, 2007 programs. Geoelectric Sections are constructed according to the traverses they positioned. Available lithological logs from boreholes TATW 1 and TATW 2 in proximity of the surveyed traverses have been used for calibration and further refining the results. Thus, interpreted VES points at existing well sites are employed for calibrating the sounding points with in the area.

4.2 The Magnetic Methods

4.2.1 Field procedures and data acquisition

To gain the field target (anomaly), Total magnetic field measurements with spacing interval 50 meter along traverse line 1, line 2, line 3 and line 4 was made. These traverses are on the same lines as that of the VES points as can be seen in the figure 3.1.During each measurement GPS location and time of measurements were taken. Total magnetic field measurements with GSM-19 magnetometer having a resolution 0.01 nT has been used. For each survey a base station was carefully selected and established in an area away from the magnetic noise like stores, iron sheet buildings. The location of the base station is within the study area in order to facilitate easy and quick reoccupation. At each station the location, time and reading were recorded, as well as any relevant topographic or geological information and details of any visible or suspected magnetic sources. Readings at the base stations were taken within an hour are used to correct the diurnal variation of the earth magnetic field.

The GSM-19 is a portable high-sensitivity Overhauser effect magneto meter designed for hand-held, towed or base station use. In contrast to a standard proton magnetometer sensor that uses a proton-rich liquid, an Overhauser Effect sensor has a free radical added. This free radical ensures the presence of free unbound electrons that couple with protons, producing a two-spin system. A strong RF magnetic field is used to disturb the electron-proton coupling. By saturating free

electron resonance lines, the polarization of protons in the sensor liquid is greatly increased. The Overhauser effect offers a more powerful method of proton polarization than standard DC polarization (GSM 19 v7.0 Instruction Manual, 2008).

The diurnal variation was removed from the observed magnetic field data using the Microsoft excel 2007. The main magnetic field at the base station is obtained from the International Geomagnetic Reference Field (IGRF). The IGRF value at the base station is subtracted from the diurnal corrected total magnetic field of each station. The magnetic field anomaly map was gridded and contoured using the Geosoft Oasis Montaj mapping software.

4.2.2 Data processing and presentation

During a survey, magnetic base readings were taken within intervals of two hours, so that diurnal corrections for total magnetic field readings along the profiles were corrected using Microsoft excel 2007. Additionally by using Microsoft excel 2007 IGRF correction for each total magnetic reading along the profiles were corrected by referring to online IGRF calculator.

The corrected magnetic data were processed using a standard Geosoft Oasis Montaj were used program and presented as: Total magnetic field intensity map, Residual map Magnetic analytic signal map are presented in chapter 4.These maps are used to define qualitative interpretations in terms subsurface anomalous magnetic source that are favorable for ground water occurrences.

4.2.3 Data enhancement

Data enhancement techniques for residual magnetic anomaly field data like analytical methods were used for highlighting the contrast between magnetic anomalies generated by deep-seated and shallow origin anomalous geologic bodies. The residual magnetic map was used to enhance the analytical signal magnetic map of the study area and the resulting plots were interpreted in terms of the objectives of the work.

CHAPTER FIVE

RESULTS, DISCUSION AND INTERPRETATION

5.1 Results and Interpretation of Resistivity Data

To gain the greatest amount of change over the anomaly, a total of 15 vertical electrical soundings (VES) data are used to develop five survey lines are shown in Figure 3.1. Four of the survey lines that form a grid are used to identify the major subsurface geological units in the area and map possible water saturated horizons.

From the interpreted individual VES curves, the results of geoelectrical surveys along the lines are presented and discussed in the presiding sections in terms of interpreted individual VES curves, apparent resistivity pseudodepth sections, and geoelectric sections. The apparent resistivity pseudodepth section along the selected lines are mapped from raw data using surfer 10 software and the resistivity sounding geoelectric sections along the selected line are constructed from the interpreted layer parameters of each VES points(sample interpretations of the individual VES are shown in Annex-1). In the preside sections, Interpretation of a sample curve VES-TPV 2, the apparent resistivitypseudodepth and geoelectric sections on each line are presented and discussed separately.

5.1.1 Interpreted VES curves

A typical interpreted sounding curve, for example VES-TPV 2 of Line 1 is as shown in the Figure 4.1. By plotting the apparent resistivity with electrode spacing on a bi-log scale the initial model of VES-TPV 2 is obtained using RESIXIP and IPI2Win software. Further by using the nearby borehole TATW 2 (Annnex-2) the initial model parameter such as static water level of the study area 7.9 m, the depth of the boulder layer 6-36 m, gravel layer 36-66 m and clayey sediments within a depth 66-112 m are used as a standard to calibrate VES-TPV 2.Finally by using the inversion software (WINRESIST)and litho-logical description final model parameters are defined in terms of geo-electric layers and its depth obtained by the resistivity survey.
The interpretation of the resistivity data revealed five layers with resistivity contrast between 24.6 and 127.3 Ohm-m (Figure 4.1).The first tiny layer having a thickness 1m and resistivity

value 48 Ohm-m is interpreted to be top clayey layer. Below it two consecutive layers located at a depth of 4.8 m and 51.1 m having resistivity value 127.3and 35.1 Ohm-m is characterized by highly permeable gravel and boulder layers. Similarly beneath these layers, the fourth layer clayey gravel shows low resistivity response (15.6 Ohm-m) than the underlying unit gravel.

Generally the interpreted VES-TPV 2 represents a five layer subsurface each of varying thickness and resistivity. A very good data quality and interpretation is obtained with RMS error of 2.4 %.

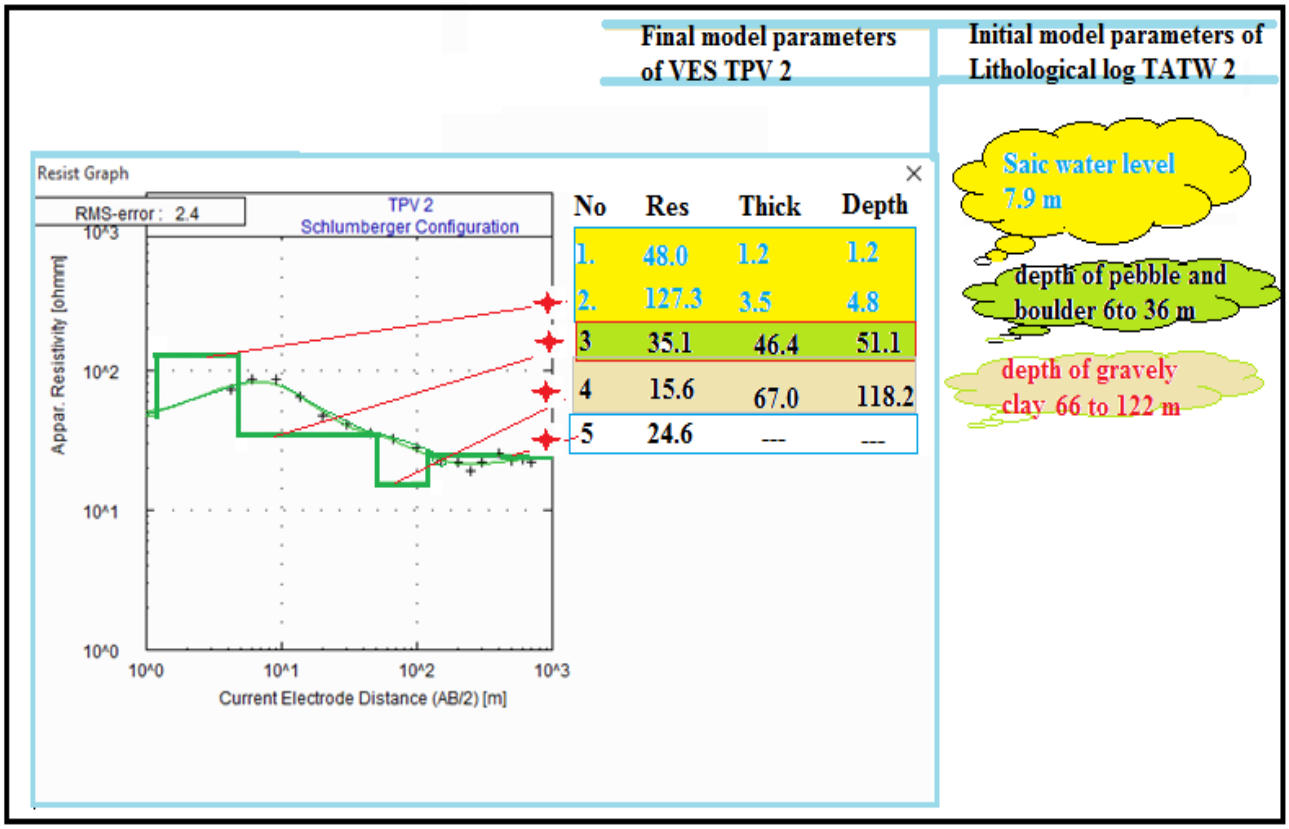

Figure 5.1 An example of interpreted sounding curve VES-TPV 2, on Line 1, Tisabalima Eastern Amhara Regional State, Ethiopia.

5.1.2 Pseudo depth section and Geoelectric Section of the Profiles

Using the 15 VES, Pseudodepth and geoelectric sections mapped along profilelines 1 to line 4 are constructed from software surfer 10 and Auto CAD, 2007 respectively. On average each VES

points distant within 1204 m are used to represent the area. The designations of VES on each line and its location are given in the Table 5.1.

5.1.2.1 Traverse Line 1

Traverse line-1 positioned near the middle of the basin is oriented NW to SE direction. This line with total length 4487 m consists of 6 VES points that lie on the traverse. Each VES with average spacing 747 m has an advantage to cross the widest part of the anomaly.

Table 45.1 Location of the VES sounding points along each traverse and total traverse length.

Line		UTM Location			Total line/Profile lengths in meter
		Easting	Northing	Elevation(m)	
1	TBV 7	564489	1267947	1725	4500
	TBV 8	565834	1267769	1639	
	TPV 6	566212	1267395	1625	
	TPV 2	567020	1267144	1593	
	TAPV 4	567758	1266931	1565	
	TAPV 8	568710	1266699	1530	
2	TBV 2	567281	1265395	1565	2823
	TAPV 5	567643	1265995	1550	
	TAPV 4	567758	1266931	1565	
	TBV 14	568477	1267866	1555	
3	TAPV 7	568477	1267866	1555	2500
	TPV 3	567270	1268889	1579	
	TBV 14	566374	1269101	1657	
4	TPV 6	566212	1267395	1625	3380
	TPV 3	567270	1268889	1579	
	TBV 1	568137	1270173	1610	

A. Pseudodepth section of traverse Line 1

From Pseudodepth section shown in Figure 5.2. Except the top layer mapped between VES point TBV7 and TBV8 along the traverse Line 1; all layers are covered by lower resistivity values. Overall, the vast portions of the section are covered by low resistivity values that lie between 3 to 23 Ohm-m. These layers are expected to be a high yield aquifer for ground water exploration.

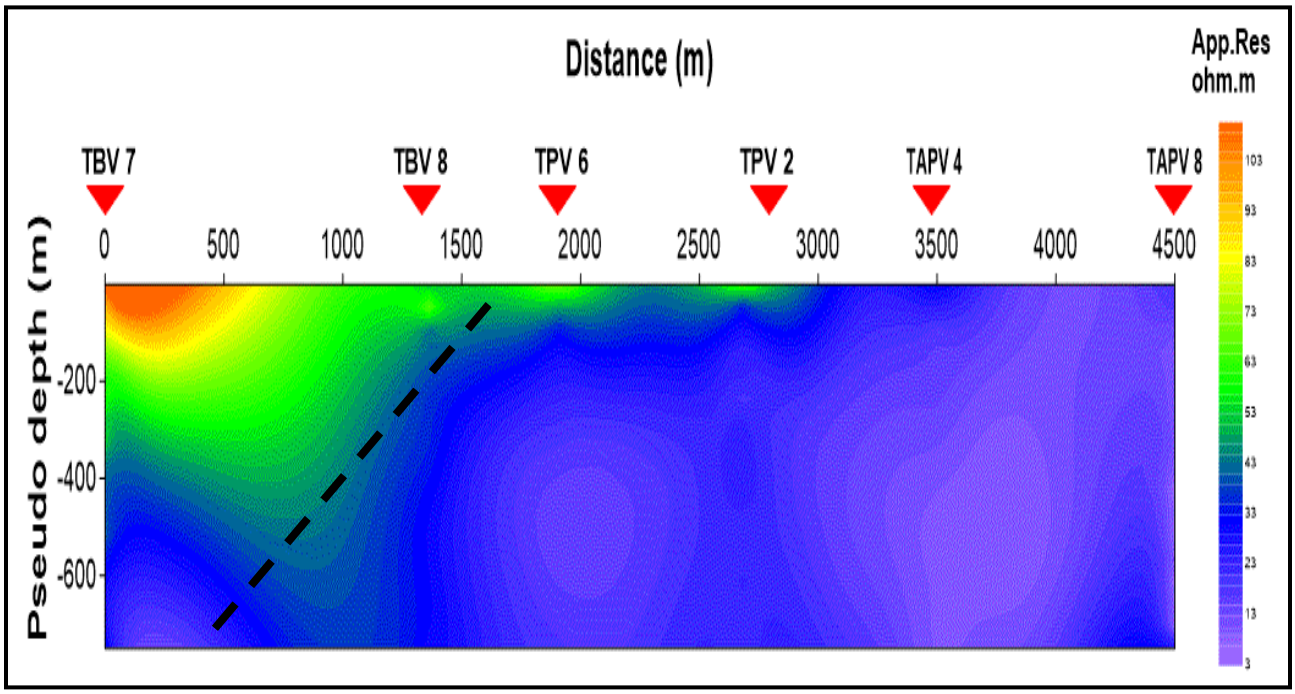

Figure 45.2.Apparent resistivity pseudodepth section along traverse Line 1,Tisabalima Eastern Amhara Regional State, Ethiopia.

B. Geoelectric section along traverse Line 1

Geoelectric section along traverse Line 1 shown in Figure 5.3 is constructed from the interpreted layer parameters of six VES. Among these, discussion on sample interpretations of VES curve TPV 2 which is near the bore hall TATW 2 is given on appendix-2.. As the standard VES TPV 2 has been used as an initial model to interpret and model VES TBV 8, TPV 6 and TAPV 4.Where as other VES-TBV 7 and VES- TAPV 8 are interpreted initially using two layers Master curve. Finally geoelectric section along traverse line 1 is mapped using a priori information (data) such as bore hall, thickness of the aquifer static water level 7.9 m, and thickness of alluvial deposit dominantly coarse size of sand, gravel and boulder 220 m to 238 m are adopted from Kobo-Robit-Minjar project report (ADSWE, 2013).The geoelectric section developed along traverse line 1 are discussed as follows:

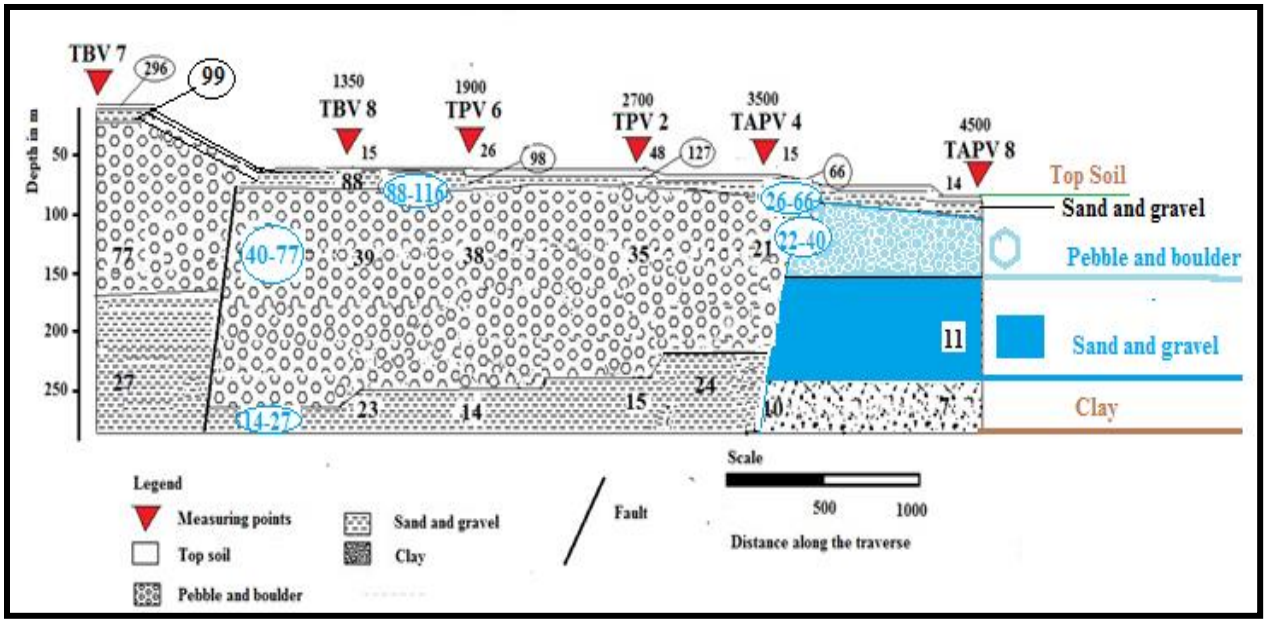

Figure 5.3 Geoelectric section along traverse Line 1, Tisabalima Eastern Amhara Regional State, Ethiopia.

The geoelectric section along the traverse Line 1 is represented by four to five layers of simple structures which dip along the traverse. The first layer having variable resistivity ranges 14 to 126 Ohm-m is represented by top clay soil. This layer extends on the top of traverse has an average thickness of 1 m.

The second layer located within VES point TBV 7 and TPV 2 has resistivity ranges from 88 to 116 Ohm-m is characterized by highly permeable sand and gravel. This layer having an average thickness 17 meter is highly porous and has an advantage in ground water recharging. Beyond the VES point TPV 2, this layer with resistivity range 26 to 66 Ohm-m extends down has a thickness from 4 to 20 meter.

The third layer oriented from VES point TBV 7 and TBV 6 is represented by pebble and boulder additional of sediments with a proportion nearly one fourth has high resistivity value within a range 40 to 77 Ohm-m. This layer with an average thickness 160 meter dominated the region is best situated area for ground water circulation within the neighboring layers. Due to a variation in moisture content of sub surface soil, this layer decreases its resistivity to range 22 - 40 Ohm-m indicated that moisture content increases along the region from VES point TPV 6 to TAPV8.

The fourth layer beyond the depth of 167 m decreases its resistivity from 14 to 27 Ohm-m beneath VES point TBV 7 to TAPV 8.The resistivity value indicates the layer to be a high yield aquifer sand and gravel. Below this layer, the fifth layer located between VES point TAPV 4 and TAPV 8; has a very low resistivity range 7 to 9 Ohm-m is considered to be moist clay.

Of all the layers mapped with the survey over this traverse, the fourth layer which is located beneath VES-TAPV4 and TAPV 8 within depth interval of 43m-140m and 20m-126m respectively, are suggested to be more promising for ground water exploration.

5.1.3Traverse Line 2

Traverse Line 2 oriented on direction of SW-NE has a total length of 2800 m. This line consists of 4 VES points that lay within an average VES point spacing 933 m.

A. Pseudodepth section along Line 2

Four VES points shown in Figure 5.4 aligning namely TBV 2, TAPV 5, TAPV 4 and TBV 14 are used in defining the Pseudodepth section along the traverse line 2.

Except the region at the top of VES TPV 2 and bottom of VES TBPV 14, all regions is covered by low resistivity zone. This low resistivity region having alluvial deposit is expected to have ground water potential in the region. In contrast, the high resistivity region beneath VES point TBV 2 is expected to be slightly weathered and fractured basalt.

B. Geoelectric section along traverse line 2

The geoelectric section along traverse Line 2 shown in Figure 5.5 reveals four main layers. Except in the middle of the profile, the upper most layer is covered by high resistive dry top soil .This layer having an average thickness 2 m; is considered to be variable in moisture content of the sub soil changes within resistivity of range of 7 to 44 Ohm-m.

Except between VES point TBV 2 and TAPV 5, the second layer having high resistive 21 to 66 Ohm-m is interpreted as pebble and boulder. This layer increases its thickness along the profile from 42 m at VES point TAPV 4 to 12 m at TBV 14.

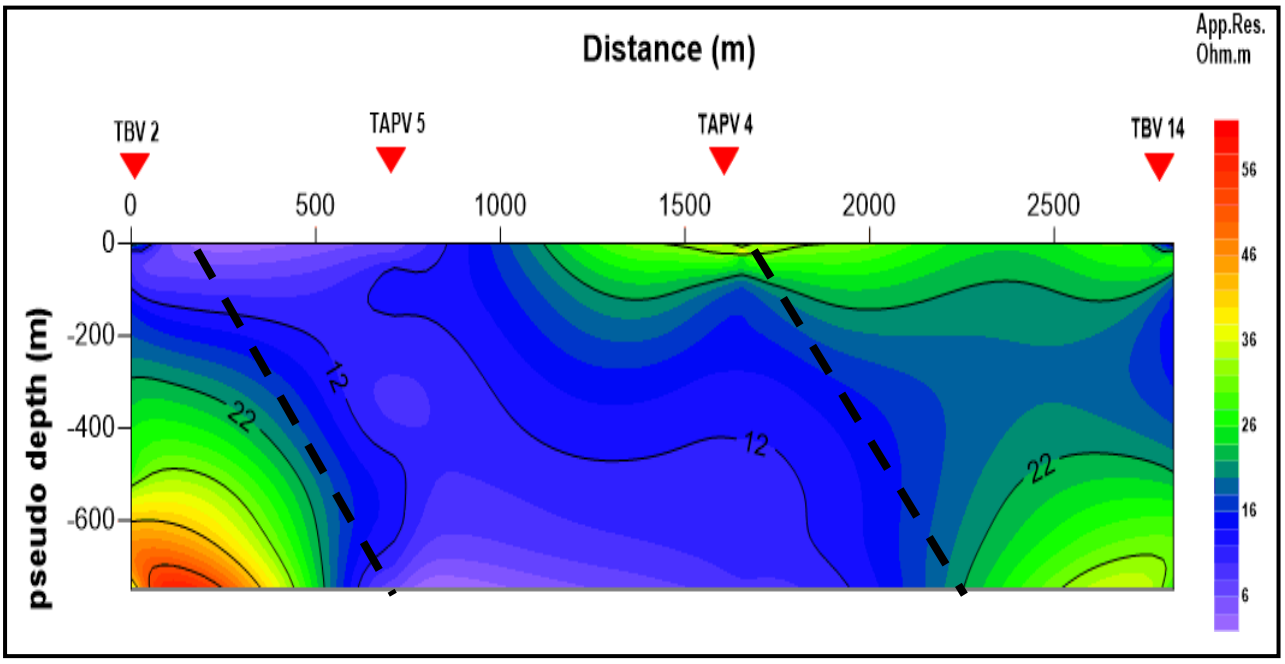

Figure 5.4 Pseudodepth sections along traverse Line 2, Tisabalima Eastern Amhara Regional State, Ethiopia.

In contrast, the third layer located between VES point TAPV 5 and TAPV 4 is dominated by unconsolidated thick gravely clay layer (46 to 120 m). This layer with resistivity range 12-15 Ohm-m is defined to be a high yield aquifer for ground water exploration.

Except beneath VES point TAPV 5 and TAPV 4, the forth layer with resistivity 35 and 41 Ohm-m) is characterized highly weathered and fractured basalt. Whereas beneath the point TAPV 5 and TAPV 4, low resistive mineralized clay (9 Ohm-m) is sandwiched by highly weathered and fractured basalt. The variation in resistivity indicates the possible position of structure can be depicted in between VES point TBV 2 and TAPV 4.

For ground water exploration purpose the third gravely clay layer which is located between the VES point TAPV 5 and TAPV 4 is the best position where ground water can be tapped.

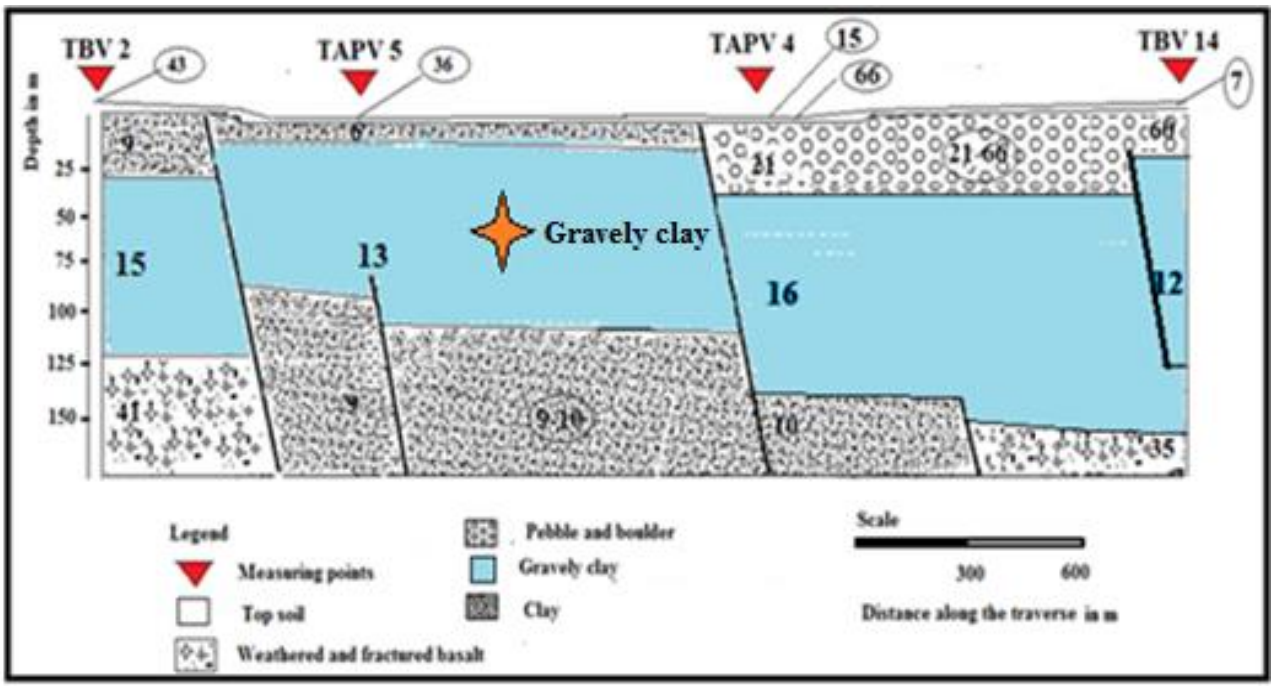

Figure 5.5 Geoelectric section along traverse Line 2, Tisabalima Eastern Amhara Regional State Ethiopia.

4.1.4 Traverse Line 3

This line shown in figure1.3 is oriented in NW to SE direction. This with a total length of 2506 m is identified by 3 VES points namely TAPV7, TPV3 and TBV14 .The average distance between each VES point is nearly equal to be 1253 m.

A. Pseudodepth section along traverse line 3

AT the shallower depth level between VES point TAPV 7 and TAPV 3 (Figure 4.6.), the region are dominated by high resistivity value which corresponds to dry silt and clay.

At deeper depth point VES TBV14, it is covered by high resistivity value which corresponds to fresh basalt. In contrast the low resistivity region is related to geological formation having high yield aquifer.

B. Geoelectric section along traverse Line 3

The geoelectric section along the traverse Line 3 (Figure 5.7.) is represented by three or four layers of simple structures which dip along the traverse. The first layer with resistivity ranges 7 to 28 Ohm-m is represented by dominantly top soil clay. This layer extends on the top of traverse varies with thickness from 1.3 m to 6.4 m is considered to be so thin that its contribution for ground water distribution is inconsiderable.

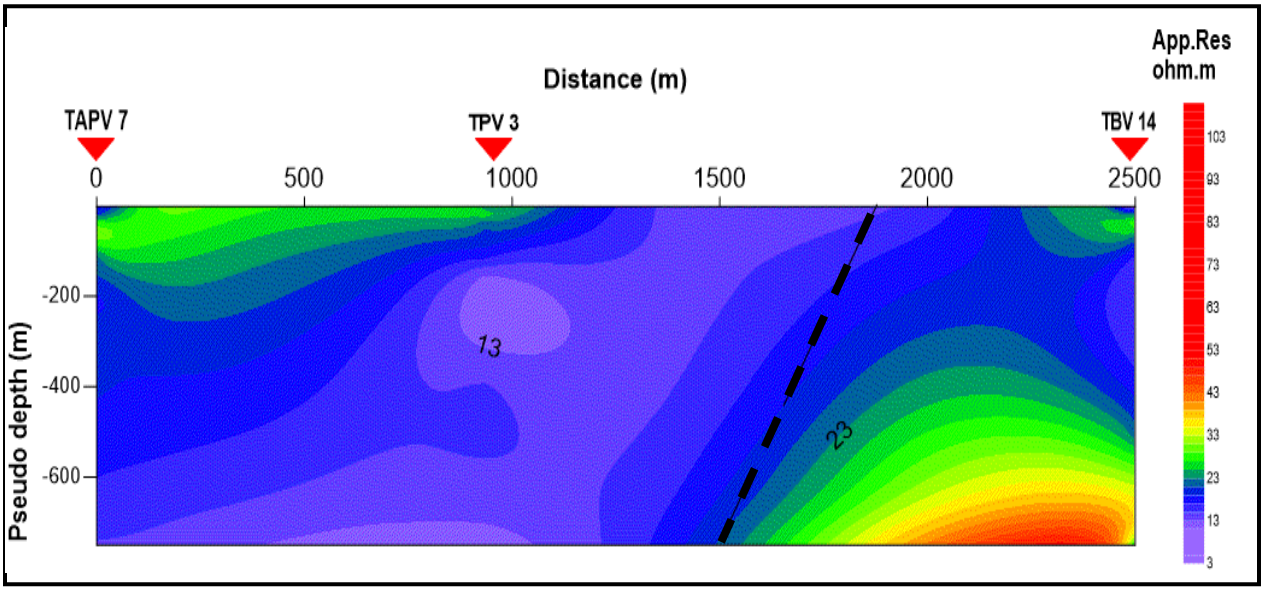

Figure 5.6 Apparent resistivity pseudodepth section along traverse Line 3, Tisabalima Eastern Amhara Regional State Ethiopia.

The second layer with resistivity ranges 25 to 40 Ohm-m is characterized by highly permeable pebble and boulder. This layer with average thickness of 31 m covers the whole traverse dips in the NE direction. Due to its permeability, this layer may acts like a conduit for ground water movement dawn to the traverse line.

At deeper depth point below VES TBV 14, the last layer is covered by resistivity value 40 Ohm-m which corresponds to slightly weathered and fractured basalt. In contrast the low resistivity layer below VES TAPV 7 and TPV 3 has resistivity range 8 to 16 Ohm-m is related to geological formation having high yield aquifer sand, gravel and clay (Gravely).

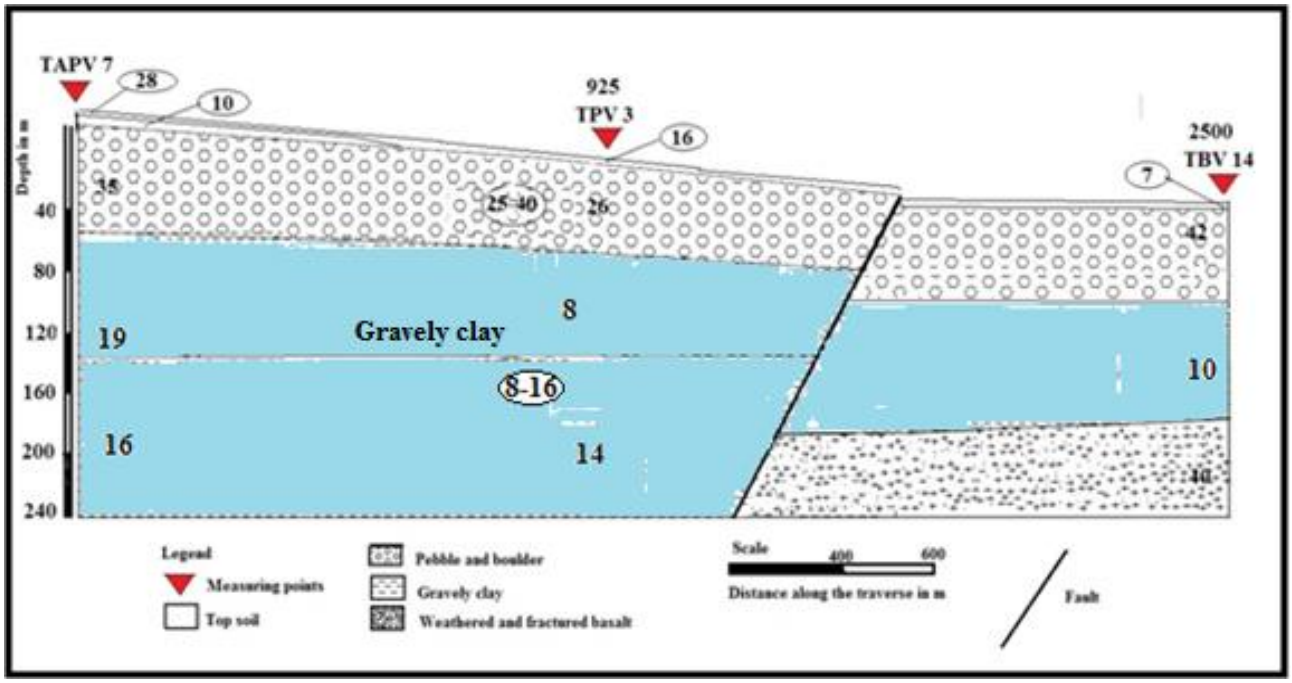

Figure 5.7 Geoelectric section along traverse Line 3, Tisabalima Eastern Amhara Regional State, Ethiopia.

4.1.5 Traverse line 4

This line is oriented in south west to north east direction. The line has a total length of about 3381m and having 3 VES points namely VES point TPV6, TPV3 and TBV1.The average distance between each VES point is nearly equal to 1253 m.

A. Pseudo depth section along Line 4

AT the shallower depth level between VES point TPV6 and TPV3 is dominated by high resistivity value which corresponds to dry silt and clay. At deeper depth VES point TBV1 there is a high resistivity value which corresponds to fresh basalt. The contrast between low to high resistivity region is related to top dry soil and the bed rock is an indication of faults which is located at a distance of 1500 m and 3000 m on the survey line.

B. Geoelectric section along traverse line 4

The geolelectric section developed along traverse line 4 is characterized by litho logical unit clay, boulder, sand (gravel) and weathered or fractured basalt.

The first geoelectric layer with resistivity range 26 to 35 Ohm-mis defined to be top soil clay. This layer which covers the upper most geoelectric section with an average thickness 1m is considered to have less effect for ground groundwater occurrences in the area. Beneath this layer, the second geoelectric layer located beneath VES point TPV 6 having a thickness 16 m showed highly resistive pebble and boulder layer (98 Ohm-m).It spans horizontally within a distance of 800 m act as a medium for ground water recharging.

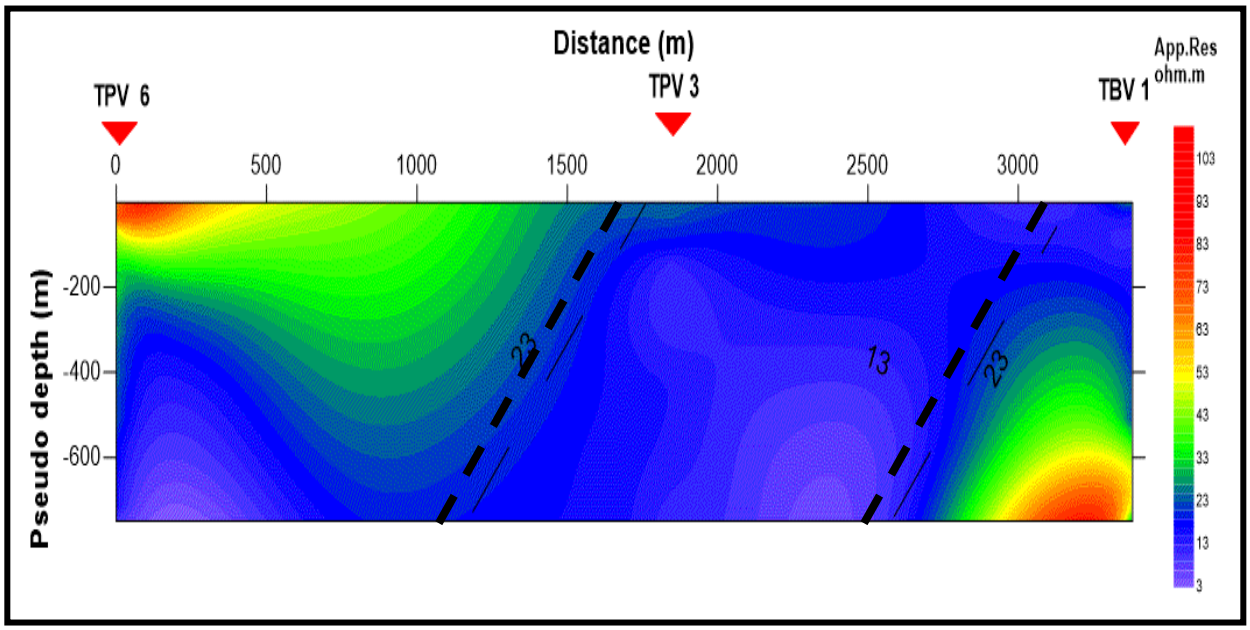

Figure 5.8.Pseudodepth sections along traverse Line 4, Tisabalima Eastern Amhara Regional State, Ethiopia.

Whereas the third geoelectric layer having variable thickness 9 to 137 m cover the whole section from VES point TPV 6 to TBV 1 .This layer with resistivity range 16 to 38 Ohm-m is interpreted to be sand and gravely layer.

Except at end of VES point TBV 1, the fourth geoelectric layer is characterized by having very low resistive clayey layer with a range 8 to 14 Ohm-m. This layer which is located beneath the VES point TPV 6, TPV 3 and TBV 1 respectively can serve as a dam for accumulation of ground water. In contrast the fourth layer is highly resistive (60 Ohm-m) and it is interpreted to be slightly weathered and fractured basalt.

From the geoelectric section shown the third layer lying between the VES point TPV 6 and TPV 3 is considered to be potential source for ground water (aquifer zones).This layer having resistivity value 38 Ohm-m is considered to be a high yield aquifer. This layer which is sandwiched by overlain highly permeable boulder layer and underlain clayey layer makes it preferable for ground water exploration.

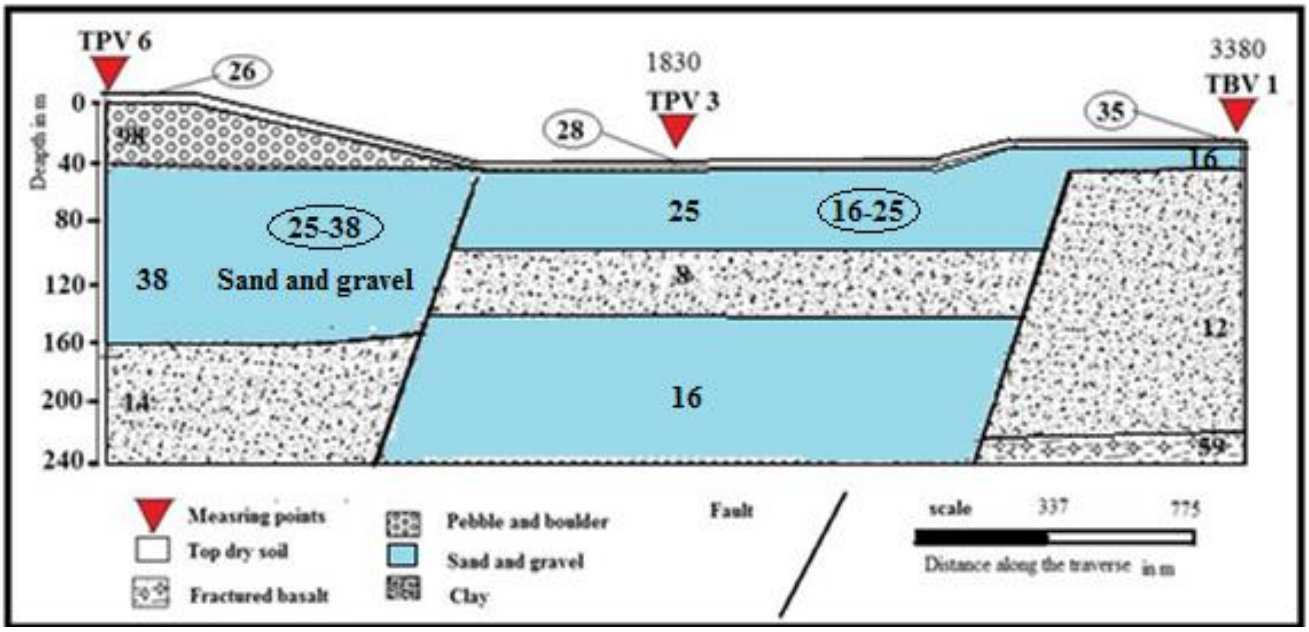

Figure 5.9 Geoelectric section along traverse Line 4, Tisabalima Eastern Amhara Regional State Ethiopia.

5.2 RESULT AND INTERPRETATION OF MAGNETIC DATA

5.2.1 Total magnetic field anomaly and analytical signal maps

The total magnetic field intensity map plotted shown in Figure 5.10, are corrected for diurnal variation shows variation of rock magnetization at their respective locations. The total magnetic field intensity map can be revealed within three magnetic anomaly patterns. The first pattern which is represented in region **A** shows low magnetic intensity 35444 nT to 35787 nT is represented to be sediment geological formation. In contrast, the high magnetic intensity (36096 nT to 36459 nT) located within a region **C;** is related to be tertiary volcanic rocks .This region is highly affected by dislocation trends SW-NE direction. Between a region **A** and **C**, an intermediate magnetic intensity35787nT to36096nTdepicted in region B (green and yellow pattern) define the directions of the lineaments to be SW-NE, SE-NW and E-W.

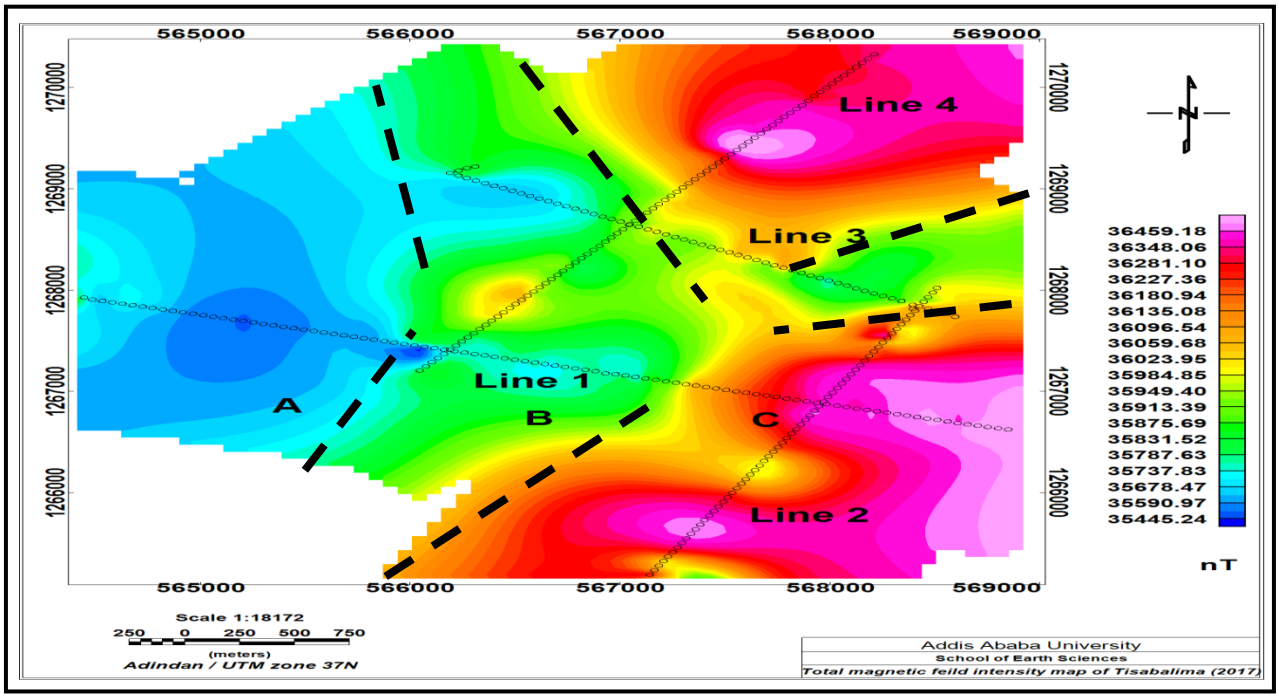

Figure 5.10 Total magnetic field intensity map of Tisabalima, Eastern Amhara Regional State, Ethiopia.

5.2.2 Residual magnetic field anomaly map

Magnetic anomalies, on the other hand, are a function of two independent parameters: the subsurface distribution of susceptibility and the orientation of the Earth's main magnetic field. Change one of these parameters will change the resulting magnetic anomaly. That is magnetic anomalies over the same susceptibility distribution will be different if the distribution is in a different location, say one located beneath the equator versus one located beneath the north pole. Additionally, the magnetic anomaly over a two-dimensional body will look different depending on the orientation of targeted object.

Strong remanent magnetization is abundantly observed with young volcanic rocks, while in sedimentary and metamorphic rocks the remanent magnetization is in general much lower than the induced magnetization (Reinhard et al., 2009).

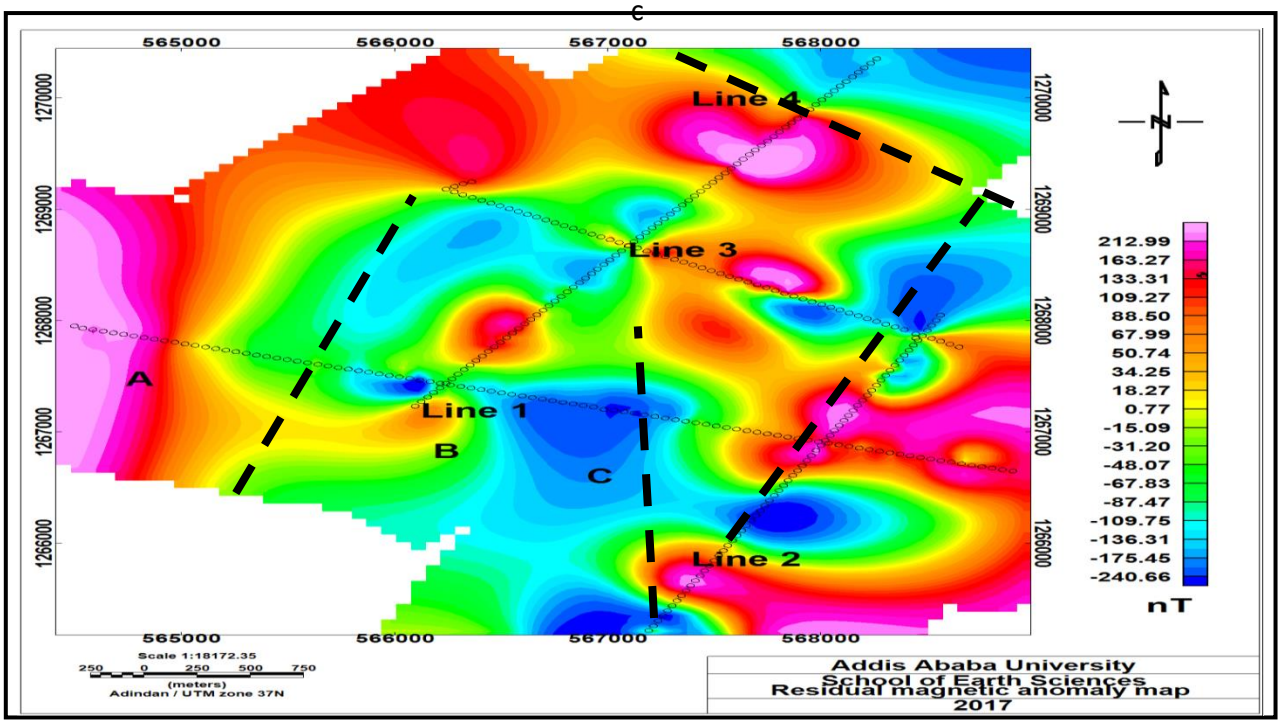

Figure 5.11Residual magnetic anomaly map of Tisabalima, Eastern Amhara Regional State, Ethiopia.

The residual magnetic anomaly map Figure 5.11 and 5.12 of the study area are compiled by applying a linear fit and Gaussian residual filter to the diurnally corrected total magnetic field intensity map of the study area (Figure 5.10).

These map shows relatively high residual magnetic anomaly represented in the region **A** (red and yellow pattern). This high magnetic response is could be magnetization of tertiary volcanic rocks basalt which is represented in the area. Whereas, the low magnetic responses represented by blue and green pattern B and C, could arise due to alluvial deposits located in the region. From the ground potential report of Kobo-Robit-Minjar, the alluvial deposits of the study area can reach from 100 to 200 m depth is dominant with coarse grain size (boulders, gravels and coarse sand).

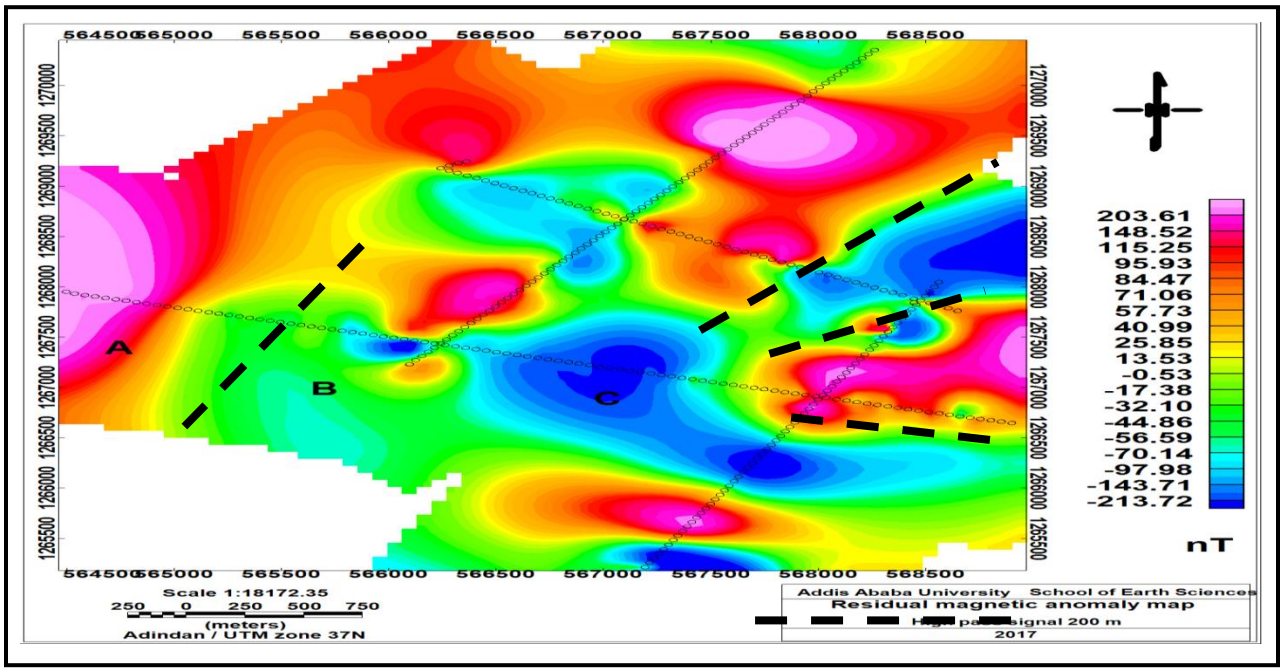

Figure 5.12 High pass filtered (200m cut off frequency) residual magnetic anomaly map of Tisabalima, Eastern Amhara Regional State, Ethiopia.

5.2.3 Residual magnetic anomaly trend along selected profiles

Residual magnetic anomaly profiles along the traverse line 1, 2 and 3 shown in Figure 5.12, 5.13 and 5.14are constructed from the residual magnetic anomaly map. These profiles are intended to

define faulted plains or a possible geological contact that acts as discharge areas for ground water release.

Residual magnetic profile line 1shown in Figure 5.12 is intended to define the faults that lie within Ethiopian Main Rift. Along the profile line 1 shown in Figure 5.12, high residual magnetic contrast to low evidence SSW-NNE two trending faults are confirmed to lie within Ethiopian Main Rift.

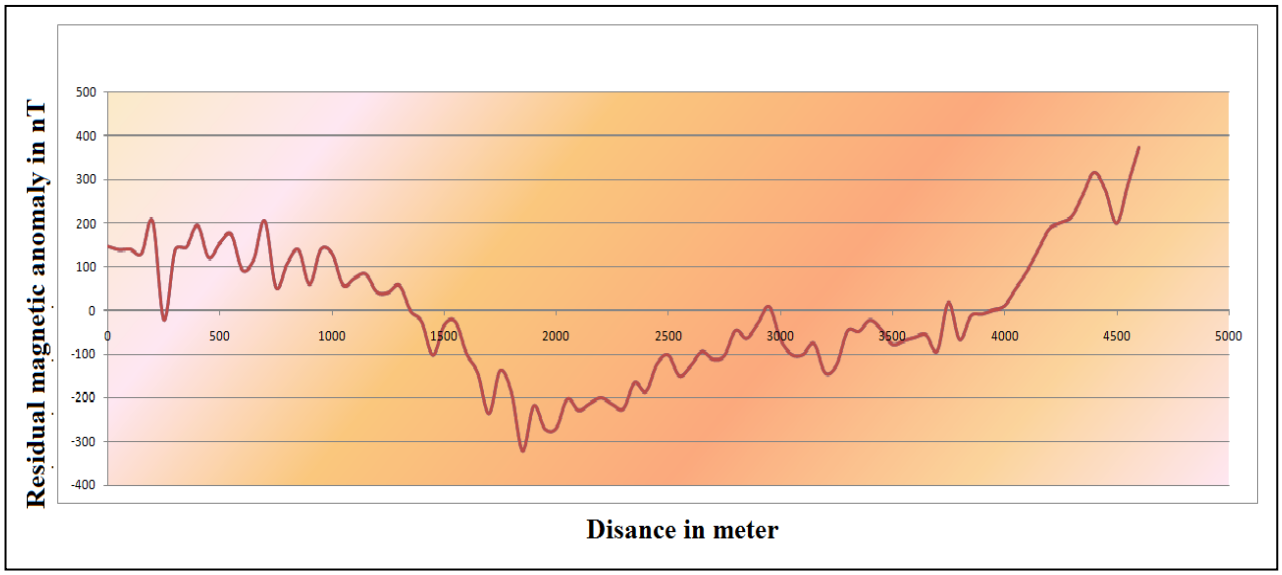

Figure 5.13 Magnetic profile plot along Line 1.

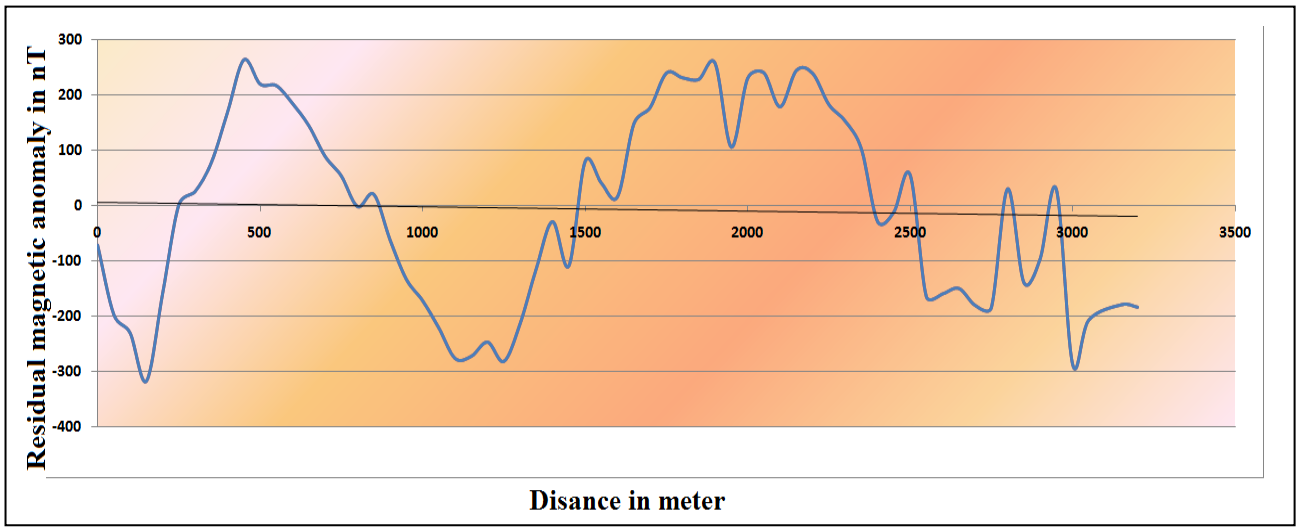

Figure 5.14 Magnetic profile plot along line 2.

Whereas, the contrast between high residual magnetic profiles (line 2) to low shown in Figure 5.13 define four possible geologic contacts. This is mainly caused by E-W trending faults elongated in a direction along the Gulf of Aden Ridge. Similarly residual magnetic profile of line 4 confirms four geologic contacts oriented in E-W.

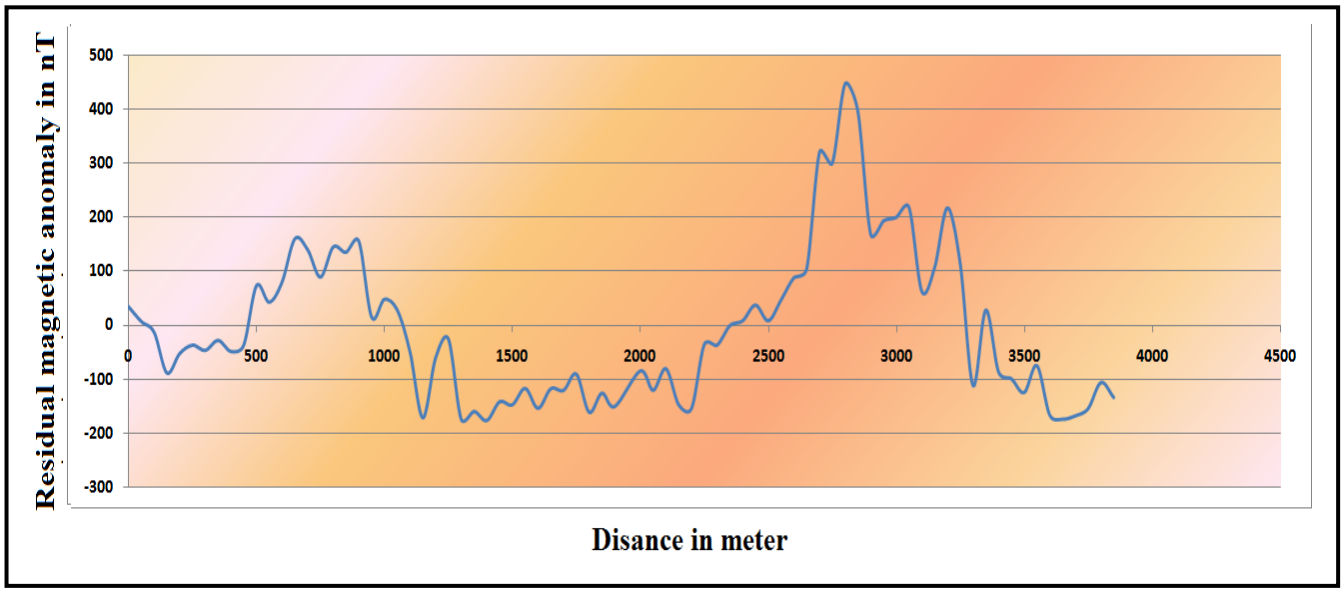

Figure 5.15 Magnetic profile plot along Line 4.

5.2.4 Magnetic analytical signal map

The analytical signal map Figure 5.16 is formed through a combination of horizontal and vertical gradients of a residual magnetic anomaly map. The analytic signal has a form over causative bodies that depend on the locations of the bodies but not their directions of magnetization.

The analytic signal method, known also as the total gradient method, as defined here produces a particular type of calculated gravity or magnetic anomaly enhancement map used for defining in a map sense the edges (boundaries) of geologically anomalous density or magnetization distributions (e.g., basement fault block boundaries, basement lithology contacts, fault/shear zones, igneous and salt diapirs, etc.).

The amplitude of analytic signal of the magnetic anomaly of a 3D source can be given by the following formula:

$$|AS(x,y,z)| = \sqrt{(\frac{\partial M}{\partial x})^2 + (\frac{\partial M}{\partial y})^2 + (\frac{\partial M}{\partial z})^2}$$

In contrast to the sediments deposited in the area, High analytical signal gradient oriented in a direction SSW-NNE and W-E is caused by High Susceptibility contrast of basalt. Whereas low magnetic anomalies values around region **c,** located in residual anomaly map; shows contrasting high analytical signal values. This is believed to be a structure that oriented towards NNE direction can acts like a barrier for ground water circulation.

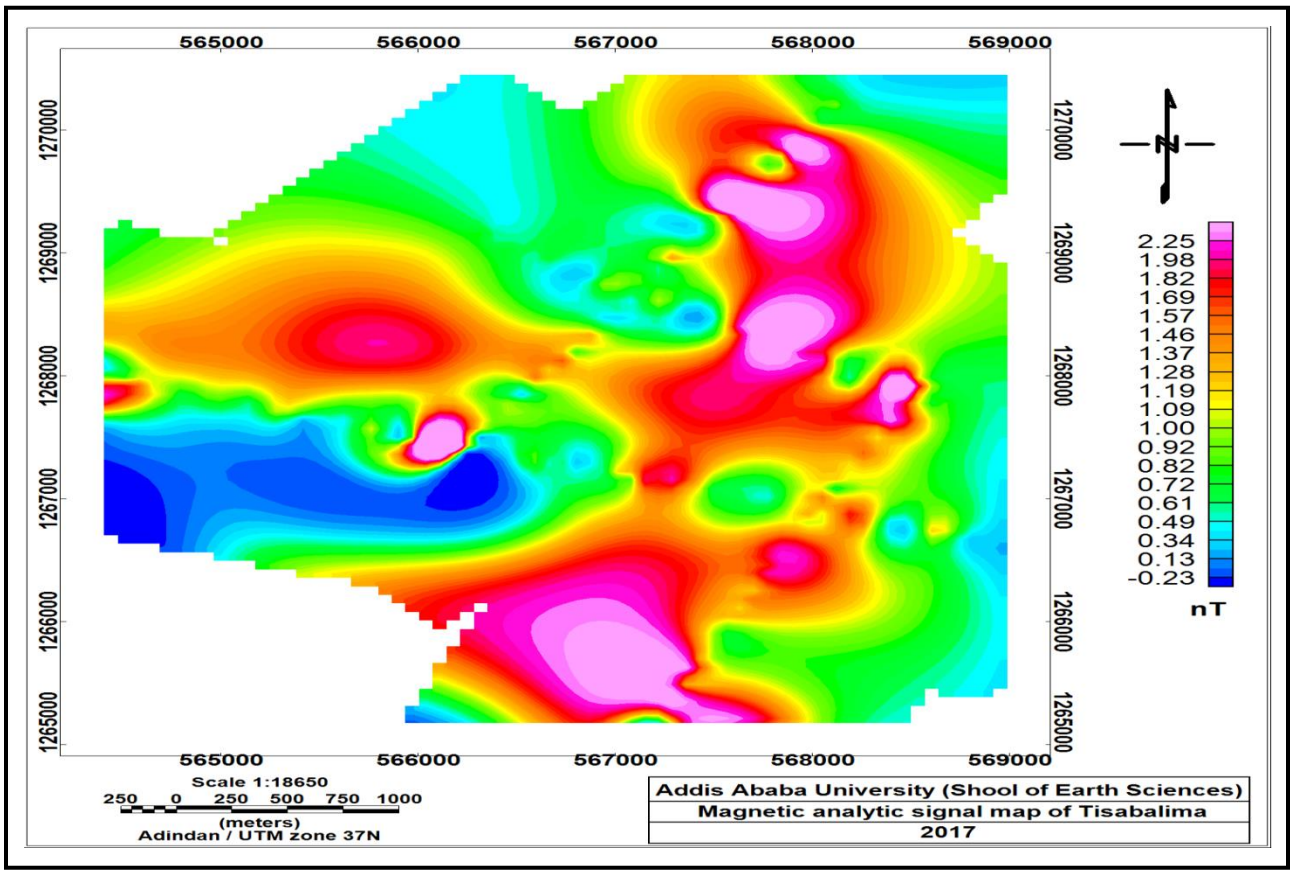

Figure 5.16 Magnetic analytical signal map of Tisabalima, Eastern Amhara Regional State, Ethiopia.

CHAPTER SIX

CONCLUSIONS AND RECOMMENDATIONS

6.1 Conclusions

Based on the result discussions and interpretations, the following conclusions have been drawn using the combination of data presentation approaches:

The interpreted results of each VES point and correlating the values along the profile line, geoelectic sections reveal resistivity values:

- 7 Ohm-m: top soil
- 6-10 Ohm-m: clay layer
- 26 – 116 Ohm-m: sand and gravel layer
- 8-16 Ohm-m: gravely clay layer
- 21-98: pebble and boulder layer
- 35 – 99 Ohm: weathered volcanic

Out of these layers, the geoelectical sections over each traverse identify the major source of groundwater in the area to be sand – gravely and gravely clay layer. These layers are mainly recharged with water through structural discontinuities like faults beside it are also recharged by overlaying layers pebble and boulder. Over all the potential sites for drillings has been identified within a depth interval of 44 m to 162 m are defined to be a water bearing horizon suggested to be more promising for ground water exploration.

The Geophysical results approve (evidence) the drilling results of well log shown in figure 6.1 that study area is covered by thick alluvial deposit 220 to 238 m. This area having a static water level 7.9 m is dominated by alluvial deposits of coarse size of sand, gravel and boulder.

The electrical and magnetic results correspond very well in mapping structural discontinuities of the study area. It is seen that the area is highly affected by tectonic events that trace NNE-SSW, NE-SW and W-E trending faults. Whereas groundwater is discharged from west to east, as a base flow which is conducted by W-E trending faults.

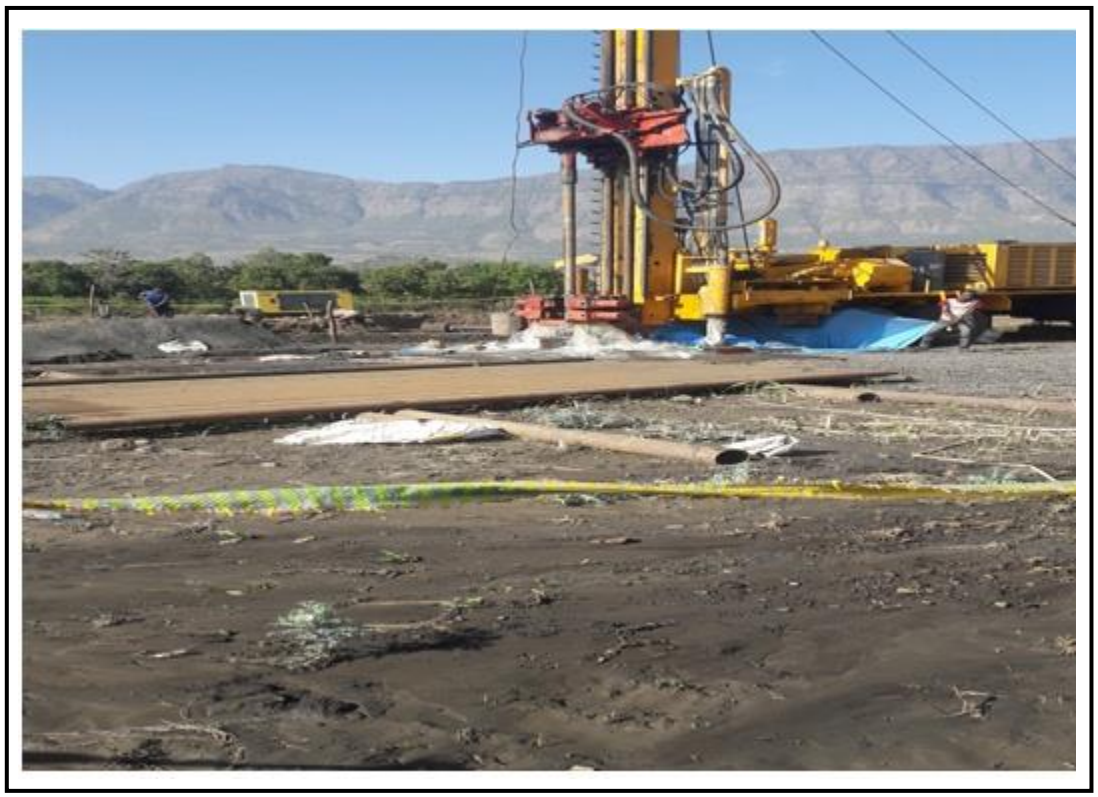

Figure 6.1 Drilling work progress of test well TATW 1, Eastern Amhara Regional State, Ethiopia.

6.2Recommendations

This study proves that the area is highly productive for ground water exploration, special care along the traverse lines should have to be made with a reference of the geoelectric section:

- Geoelectical section Line 2

Over all the layers the third layer within a depth of 120 m to 140 m is defined to be a water bearing horizon suggested to be more promising for ground water exploration. Except the difficulty from the boulder layer above, drillings between VES TAPV 5 and TAPV 4 is better situated position. This layer may contain clay material to some extent or it can be taken as a region of gravely clay layer. Drillings in this layer can face multiple confined aquifers by clay; in this respect protection against subsidence of layers should have to be considered during drillings.

- Geoelectical section Line 3

The third clayey gravel layer with resistivity range 8 to 16 Ohm-m reveals high ground water potential. Drillings in this layer can face multiple confined aquifers by clay; in this respect protection against subsidence of layers should have to be considered during drillings.

- Within all geoelectric sections along the Lines

The resistivity value which is less than 10 Ohm-m can be an indication that the groundwater in the study area can contain highly dissolved mineral. For an effective ground water exploration, further studies using integrated geophysical methods should have to be made in mapping the regional structural as well as for mapping the possible mineralized zone of the study areas.

7. REFERENCES

Amhara Design and Supervision Works Enterprise (ADSWE) (2010).*Eastern Amhara Development Corridor Project Geophysical Survey report for Groundwater Potential Assessment*. Unpublished technical report, Bahirdar, Ethiopia, p.109.

Amhara Design and Supervision Works Enterprise (ADSWE) (2013).*Groundwater Potential Assessment of Eastern Amhara Development Corridor of Awash Basin (Kobo-Robit-Minjar) project.*Unpublished technical report, ADSWE, Bahirdar, Ethiopia, p. 200.

ADSWE**,** 2017; *Well Completion report on wells drilled in Tisabalima water shade*. Unpublished technical report, Bahirdar, Ethiopia.

Bernard, J. (2003).Short notes on the principles of geophysical methods for groundwater investigations.

Charles, R. (2002). *Ground Water Science*. Elsevier Science ltd.Califrnia USA,p.450.

Fetter,C.W.(2001).*Applied Hydrogeology*, Prentice-Hall,Inc.Upper Saddle River,New Jersey 07458, pp.: 66-88.

Gibson, P.J. and George, D.M., (2003). *Environmental applications of geophysical surveying techniques*. Nova Science Publishers, Inc. New York. Africa,pp:57**12(1),** Addis Ababa.

LewamTesfaLidet,(2015). *Application of integrated geophysical techniques to map groundwater potential zones and geological structures at welhe basin, south of Sekota*. MSc thesis, Addis Ababa University, Ethiopia.

Loke, M. H., (2001**).** Electrical *imagine survey for environmental and engineeringstudies: A practical guide to 2D and 3D surveys.*

Milsom, J. (2003). *Field Geophysics*. John Wiley & Sons Ltd, London, England, 3rd edi., p.548.

MulugetaChanie, (2011).*Application of integrated geophysical techniques to mapgroundwater potential zones and geological structures at Gelchet area, Borena zone,South Ethiopia.*MSc thesis, Addis Ababa University.

Never, K.(2009).Ground Water Resources: Sustainability, Management, and Restoration.Mc McGraw-Hill Companies, Inc. New York. United States, p.548.

Pavelic, P.; Giordano, M.; Keraita, B.; Ramesh, V. and Rao, T. (Eds.).(2012). *Groundwater availabilityand use in Sub-Saharan Africa: A review of 15 countries*. Colombo, Sri Lanka: International Water Management Institute (IWMI), pp.:37.

Telford, W.M., Geldart, L.P. and Sheriff, R.E., 1990**;** *Applied Geophysics,* 2nd Edition; Cambridge University Press, Cambridge, UK,p.770.

Tewodros Mulugeta, (2011).*Geophysical Investigation for Groundwater Potential assessment and Mapping Structures at Alidege Plain*, South Afar, Ethiopia, MSc thesis.

TibebeMengesha, (2006).*Integrated Geophysical Investigation for the Evaluation of Groundwater Resources at Ada'a plain Near Debre-Zeit*, MSc thesis.

Reynold, (1997).*An Introduction to Applied and Environmental Geophysics.* John Wiley and Sons limited, England, UK, p. 160.

S.S. Stefanescu, C., (1930).*Schlumberger Distribution of electric field in potential horizontals layers, homogeneous and isotropic*, J.Phys. radium,**7**:132-141.

Vander Velpen B.P.A., (1995)**.***RESIXIP and Win Resist software*, 1st version; Interpex limited company.

Yahya Ali (2011).*Geophysical Investigations of the Gergedi Thermal Springs, North West of Wonji, Main Ethipian Rift*, Addis Ababa University, Addis Ababa, Ethiopia, MSc thesis.

8. ADDENDUM

APPENDIX -1

Interpreted VES Curves

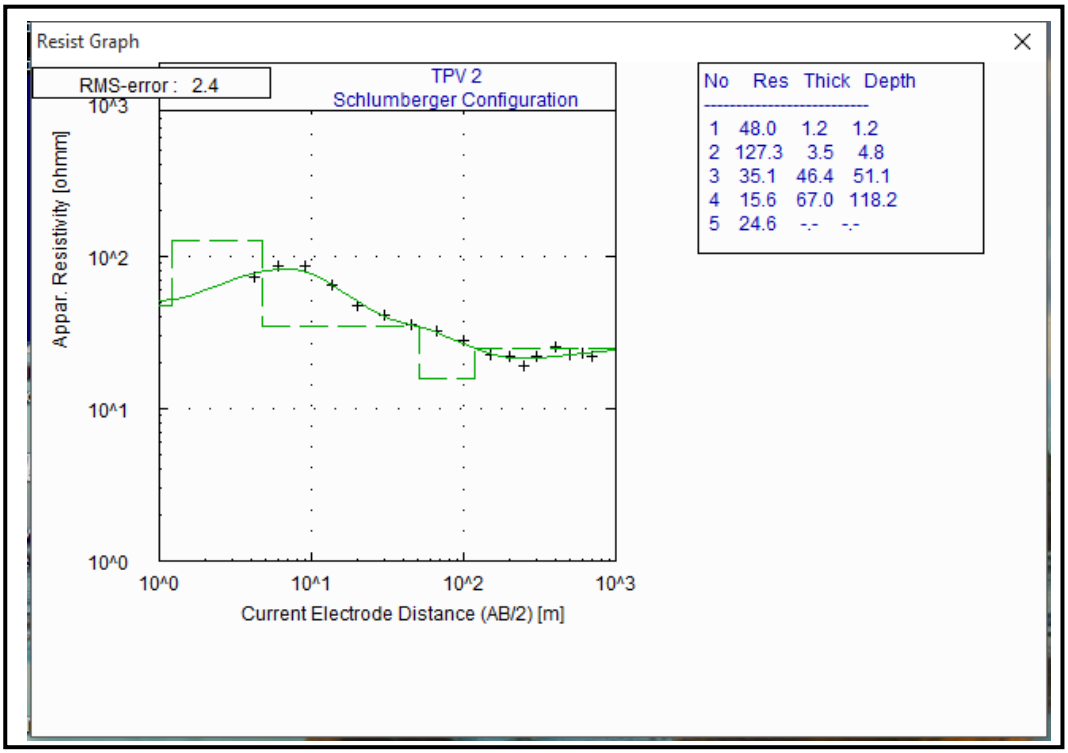

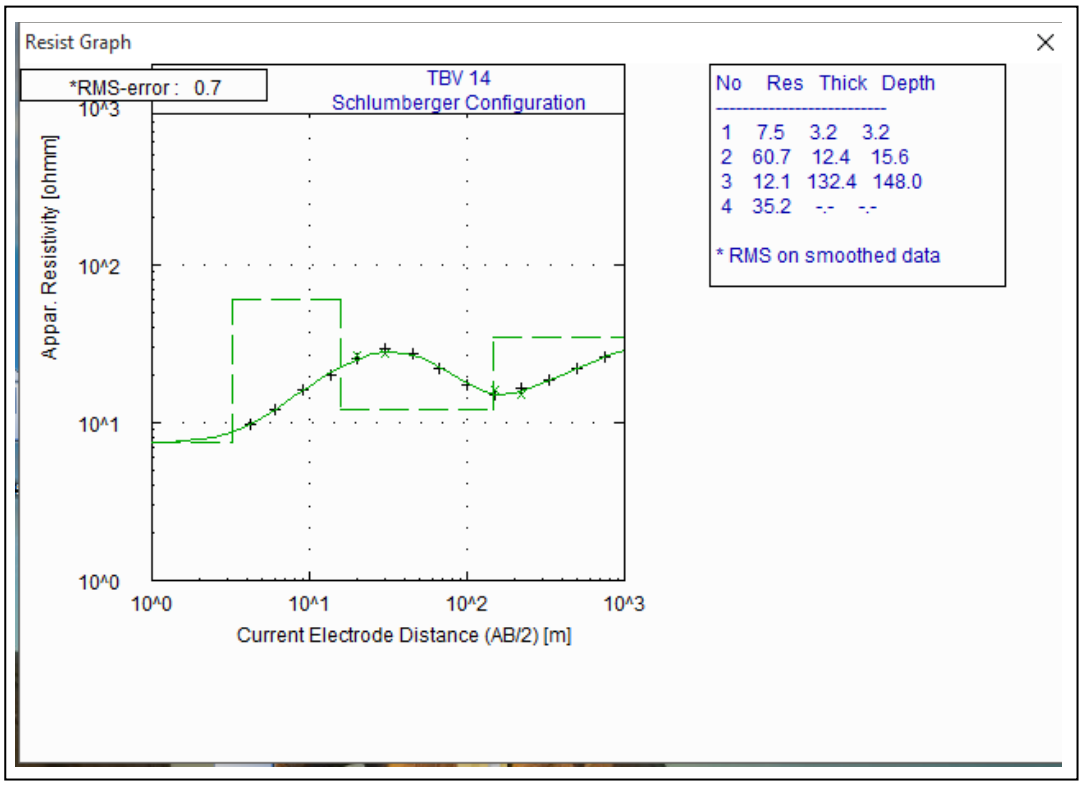

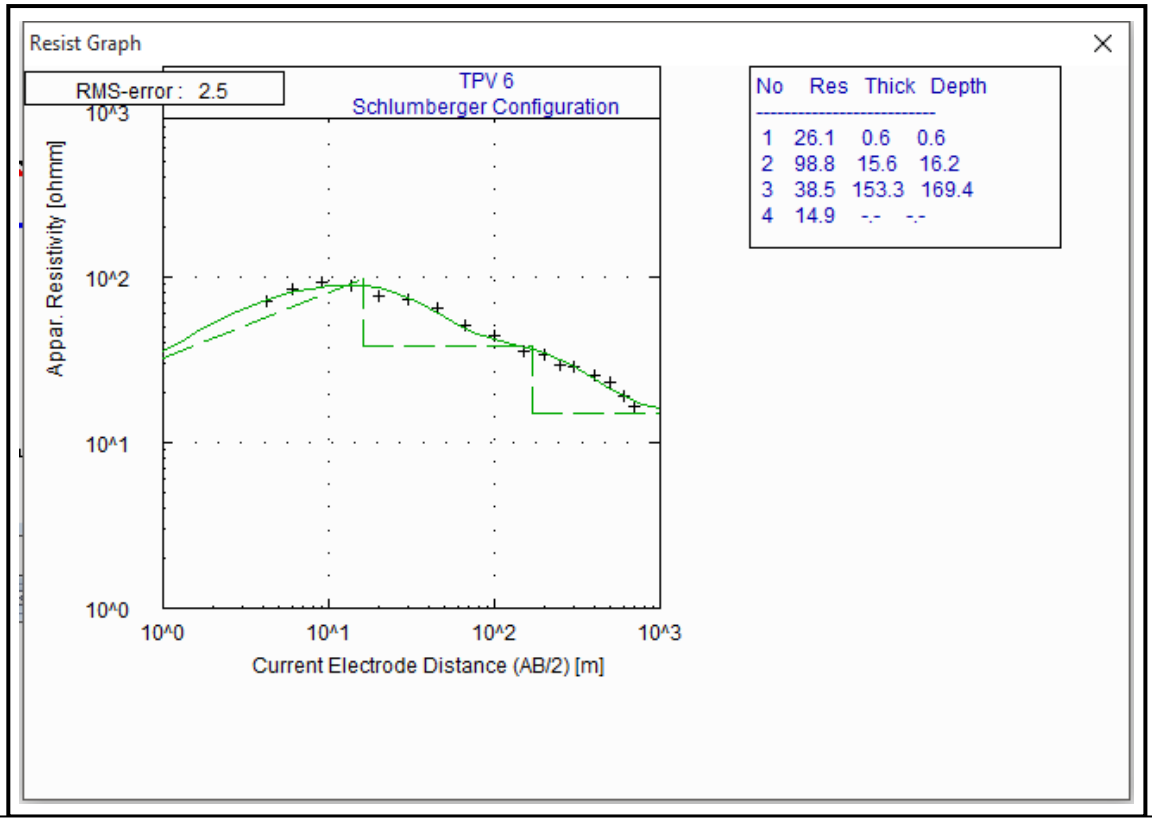
Resist Graph
RMS-error : 2.5
TPV 6
Schlumberger Configuration
No Res Thick Depth
1 26.1 0.6 0.6
2 98.8 15.6 16.2
3 38.5 153.3 169.4
4 14.9 -.- -.-
Appar. Resistivity [ohmm]
10^3
10^2
10^1
10^0
10^0
10^1
10^2
10^3
Current Electrode Distance (AB/2) [m]

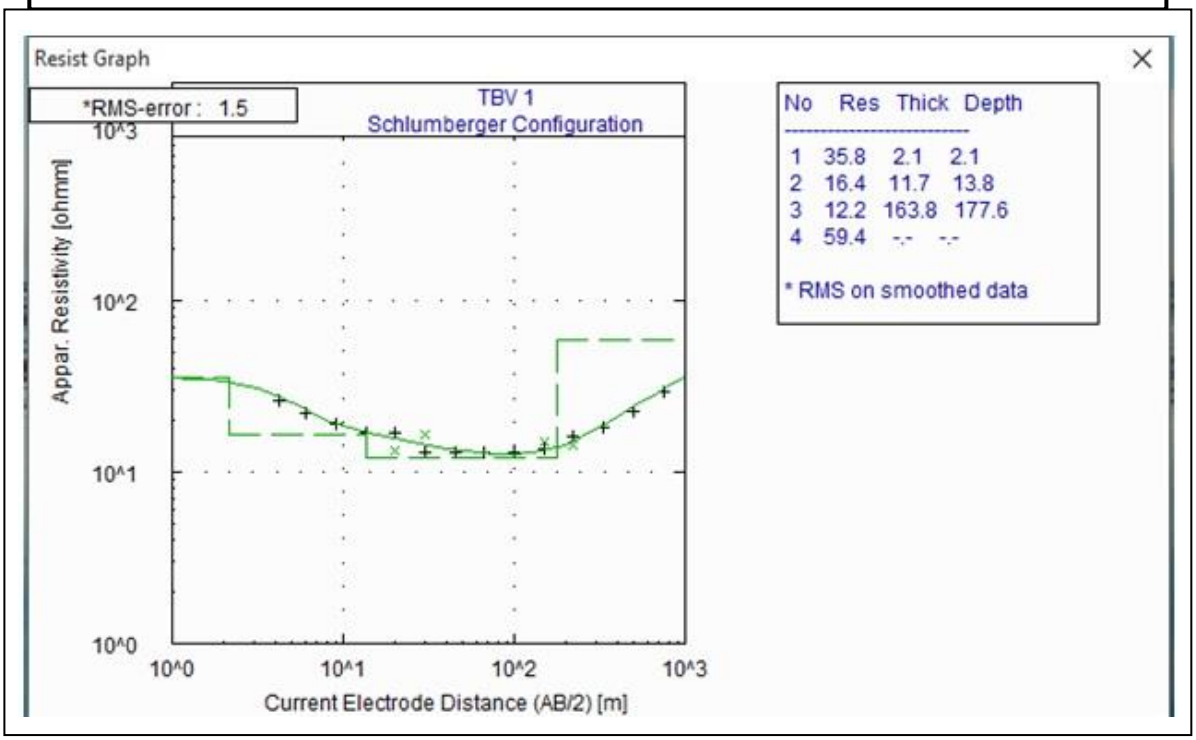
Resist Graph
*RMS-error : 1.5
TBV 1
Schlumberger Configuration
No Res Thick Depth
1 35.8 2.1 2.1
2 16.4 11.7 13.8
3 12.2 163.8 177.6
4 59.4 -.- -.-
* RMS on smoothed data
Appar. Resistivity [ohmm]
10^3
10^2
10^1
10^0
10^0
10^1
10^2
10^3
Current Electrode Distance (AB/2) [m]

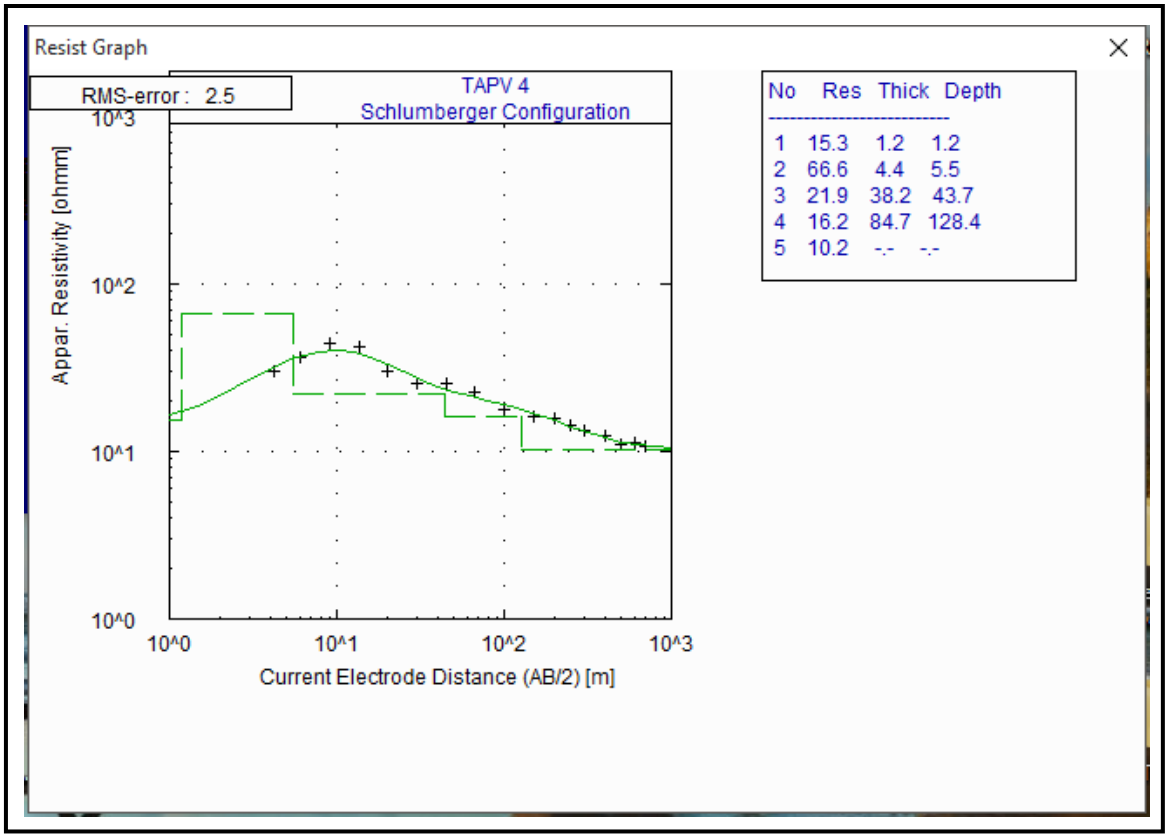

APPENDIX -2

Table 4.3Litho logical description of Borehole TATW1 in meter.

Depth from	to	Lithological Description
0	4	top soil (black cotton soil)
4	8	silt
8	26	gravel and sand
26	28	gravel with some clay
28	38	gravel
38	48	coarse gravel and pebble
48	80	peble and boulder
80	90	gravel with clay
90	94	pebble with boulder
94	98	gravely clay
98	100	gravel
100	104	clayey gravel
104	108	gravel

108	110	clayey gravel
110	112	gravel
112	120	clayey gravel
120	124	gravel
124	130	clayey gravel
130	146	clay
146	148	gravely clay
148	152	gravel
152	156	gravely clay
156	166	clay
166	170	gravely clay
170	184	gravel with some silt
184	190	gravely clay
190	200	clay with some gravel
200	208	gravel and pebble
208	210	clay
210	218	clay with some gravel
218	220	gravel
220	224	decomposed grains gravel
224	228	gravel
228	253	fractured and slightly weathered basalt

Well Design of Well ID TATW1

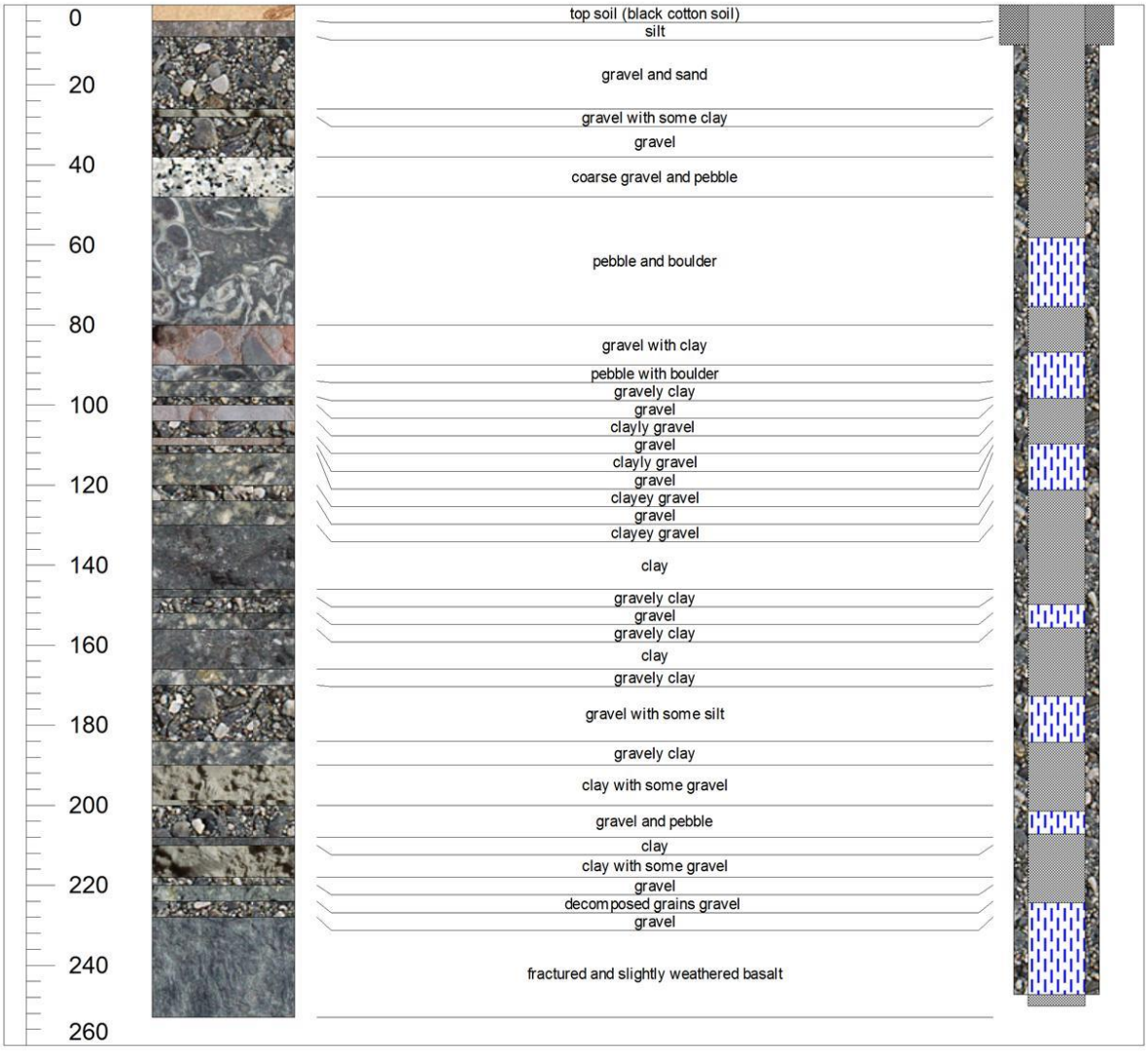

Prepared by Al Nile Business Group

Table 4.4Litho logical description of Borehole-2 in meter.

from	To	
0	6	Top soil
6	36.35	boulder
36.35	66.85	Coarse sand with gravel
66.85	79.05	Coarse sand with clay
79.05	91.25	Clay with minor gravel
91.25	97.35	Coarse sand with gravel
97.35	112.6	Coarse sand with minor silt and clay
112.6	124.8	Coarse sand with minor gravel
124.8	130.9	Boulder
130.9	143.1	Coarse sand
143.1	185.8	Boulder
185.8	204.1	Coarse sand
204.1	213.25	Coarse gravel with clay
213.25	222.4	Coarse gravel
222.4	245	Highly fractured and slightly weathered basalt
245	248	Slightly fractured basalt

WELL ID TATW2

wereda Ambasel
Depth 248m

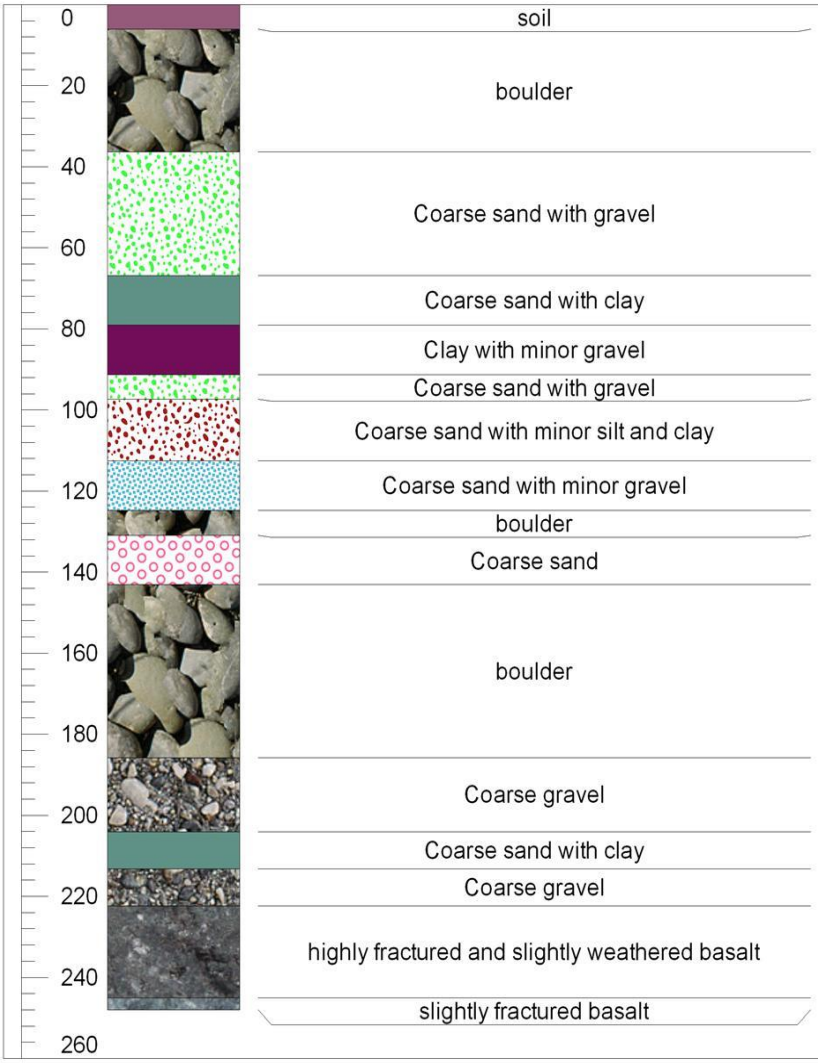

Tis-Abalima test well

9. DECLARATION

I hereby declare that the thesis entitled ‘‘The application of integrated geophysical techniques IN mapping ground water resource at Tisabalima sub basin, eastern Amhara regional state, Ethiopia.” has been carried out by me under the supervision of Prof. Tigistu Haile during the year 2017 as part of Master of Science program in Exploration Geophysics. I further declare that this work has not been submitted to any other University or institution for the award of any degree or diploma and all sources of material used for the thesis have been duly acknowledged.

Tewodros Mulugeta

Signature _____

Date _____

Place and date of submission: School of Earth Sciences, Addis Ababa University

June, 2017

CHAPTER ONE

INTRODUCTION

1.1 General Introduction

Groundwater resource for Pressurized Irrigation Project at Kobo-Robit-Minjar Valley are currently being implemented in Eastern Amhara Development Corridor in parts of the Awash Basin by Ethiopian Construction, Design and Supervision Works Corporation (ECDSWC) Bureau previously known by Water Works, Design and Supervision Enterprise (WWDSE).The Project mainly focuses on the evaluation of the groundwater potential in parts of the Awash Basin. The project as such involves the assessments of the groundwater resources potential of three areas i.e., Woldiya, Mersa, Wirgesa and Tisabalima areas, Gerado, Kombolcha and Harbu areas, Kemissie and Chefa areas. Out of these three areas, the current research work involves the study on the potential area of Tisabalima area within the Woldiya, Mersa, Wirgesa and Tisabalima watershed.

In the past, geophysics has either been used as a tool for groundwater resource mapping or as tool for groundwater character discrimination. For groundwater resource mapping it is not the groundwater itself that is the target of the geophysics rather it is the geological situation in which the water exists. Integrated geophysical techniques, vertical electrical sounding and magnetic, have proved very popular in ground water exploration due to due to the simplicity of the technique and the ruggedness of the instrumentation.

Geoelectrical methods are applied to map the resistivity structure of the underground. Rock resistivity is of special interest for hydrogeological purposes: it allows, e.g., to discriminate between fresh water and salt water, between soft-rock sandy aquifers and clayey material, between hardrock porous/fractured aquifers and low-permeable claystones and marlstones, and between water-bearing fractured rock and its solid host rock (Reichard, 2009).

Magnetic survey measurement along the surface of the earth measure the resultant magnetic field which includes: dipole field, external field and rock magnetism. In magnetic surveying, rock magnetism is one of the interests because it relates to the existence of subsurface rocks of contrasting susceptibilities (high or low magnetic susceptibilities).Magnetic measurements can be used to locate subsurface rocks having high magnetic susceptibilities by mapping variations in the

strength of the magnetic field at the Earth's surface. The magnetic method can be used in groundwater exploration mapping of fractures in crystalline rocks and bedrock aquifers under alluvial cover, delineating volcano-sedimentary belts concealed by recent formations, and associated to local tectonic structures (faults, fractures/shears).

Every research project has its strength and weaknesses and the choice of the best topic is sometimes difficult. The selection of research project was made mainly based on criteria which are primarily the interest and willingness of researcher, availability of field site activities to collect primary geophysical data (electrical resistivity sounding and magnetic).Further, integerated geophysical investigation in the area (Tisabalima sub basin) has never been done until now. In this respect, the application of integrated geophysical techniques in ground water resource mapping and identifying the geological structures in which the water exists at Tisabalima sub basin (parts of Eastern Amhara Regional State) is selected for MSc thesis study.

During this study, resistivity [Vertical Electrical Sounding (VES)] secondary data collected by Ethiopian Construction, Design and Supervision Works Corporation and primary magnetic data have been used to define the ground condition of the subsurface.. Since the area is not well studied, this thesis will be an important contribution for defining the ground water condition of the sub basin.

The thesis has been organized in Five Chapters. The First Chapter is Introduction and presents general insight on the location, objective and general geologic, hydrogeologic and tectonic aspects of the study area. Chapter Two discusses the basic principles of the geophysical methods resistivity and magnetics. Chapter Three discusses data acquisition, processing and presentation. Finally Chapter four discussions about the field work, data reduction, interpretation, conclusion and recommendation of the studies.

1.2 Description of the Study Area

1.2.1 Location and topography

The study area is located within Eastern Amhara Regional State which is part of the Awash River catchment (Figure 1.1). The study area lies on UTM Geographical coordinate between latitudes Northing 1257436 to 1270701 and longitudes Easting 562692 to 571800 in meter.

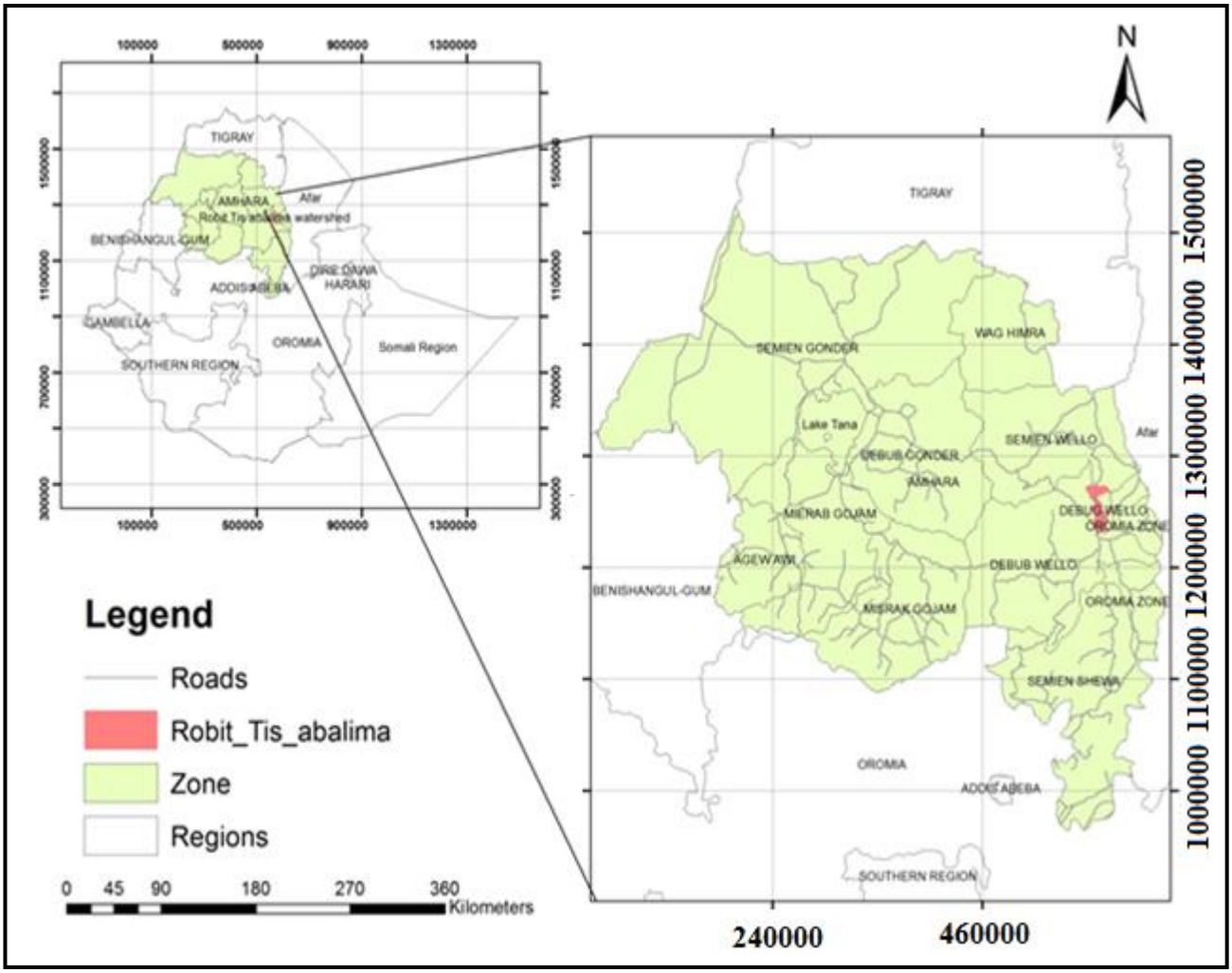

Figure 1.1 Location map of Tisabalima, the study area in the research work.

1.3 Objectives and Scope of the Study

1.3.1General Objective

The main objective of the study is identifying the groundwater potential zone of Tisabalima sub basin and locates potential sites for the drilling of test boreholes that are favorable for sustainable yield of ground water.

1.3.2 Specific Objectives

The specific objectives of the research work include

- Identify the major subsurface geoelectrical/geological units in the area and map possible water bearing horizons.
- Mapping subsurface structure like faults, fractures and fissures that acts conduits or barriers for groundwater flow.
- Identify potential sites for the drilling of test boreholes that are favorable for sustainable yield of ground water.

1.4 Previous Works

Geophysical studies namely Vertical Electrical Sounding (VES) surveys were conducted by Amhara Design and Supervision Works Enterprise, with the aim of identifying the groundwater potential assessment for test and/or production well drilling and also provision of subsurface information. The geoelectric section developed along two profiles TPV 1, TPV 2, TPV 3 and TPV 6, TPV 2, TAPV 4, TAPV 8 shown in Figure 1.2 and 1.3 revealed that the area has four to five major layers. The locations of these sounding profiles and the sounding points are indicated in Figure 3.1.

The first profile along TPV 1, TPV 2, and TPV 3 comprises of:

- Top dry soil
- sand and gravel layer
- silt layer
- weathered and fractured basalt layer
- bottom paleo soil (clay)

These layers layer vary in thickness from1-5 m, 40-50 m, 75-125 m, 125-150 m respectively. Whereas geo-electric section produced along VES points TPV 6, TPV 2, TAPV 4, and TAPV 8 reveal top dry clay soil having a resistivity 10 to 25 ohm-m underneath, the second layer comprises of sandy layer, with resistivity range 6-16 ohm- m and gravel (boulder) layer with resistivity range 30-64 ohm- m.

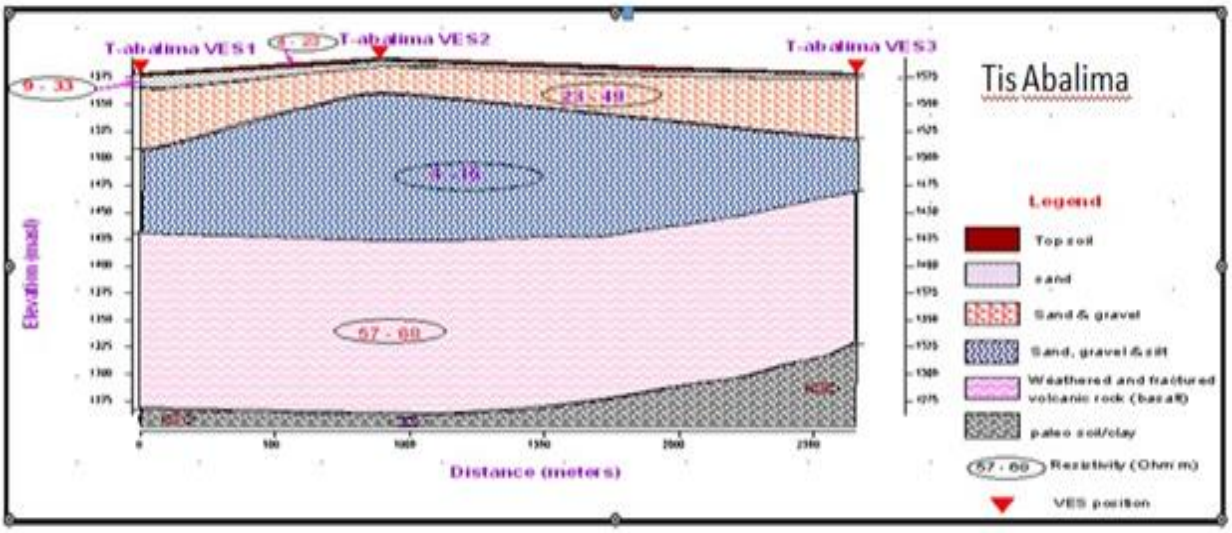

Figure 1.2 Geoelectrical Sections along the survey traverse consisting of VES pointsTPV 1, TPV 2 and TPV 3, Tisabalima sub basin (from AmharaDesignand Supervision Works Enterprise, 2013).

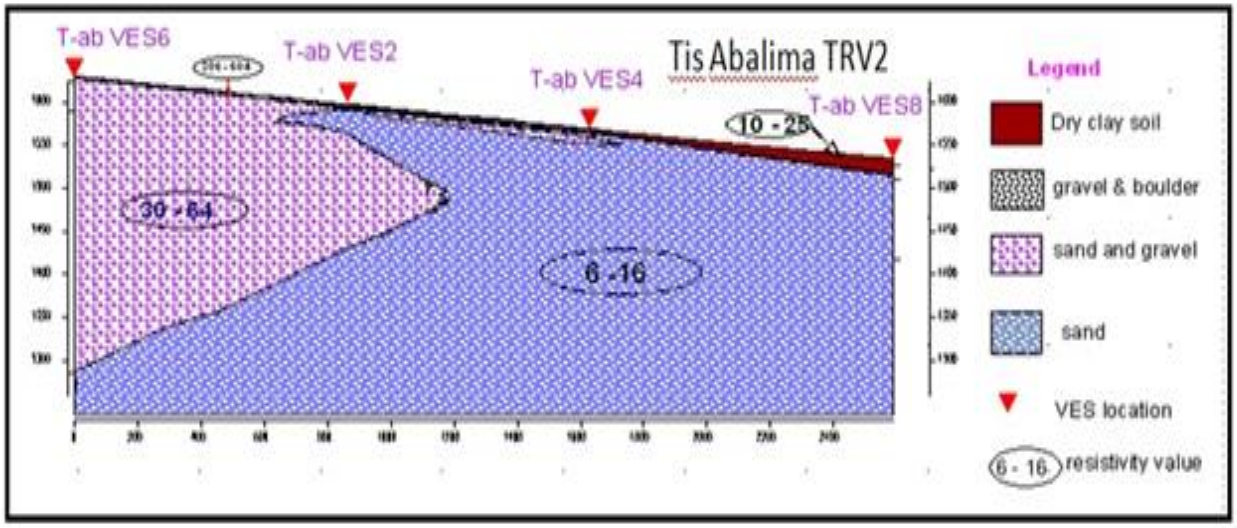

Figure 1.3 Geoelectrical Sections along the survey traverse consisting of VES points TPV 6, TPV 2, TAPV 4, TAPV 8, Tisabalima sub basin (from AmharaDesign and Supervision Works Enterprise, 2013).

This study is limited on electrical sounding survey along two profiles which makes it difficult to define zones of saturation (aquifer) of the study area. Due to a limitation in financial resources, an in integrated geophysical technique electrical and magnetic is mainly made to study the area that are located in between easting from 563553 to 569313 and northing 1264188 to 1271489 UTM geographical coordinate. To study the regional ground water flow in the area further magnetic survey should have to be made.

CHAPTER TWO

GEOLOGICAL, STRUCTURAL AND HYDROLOGICAL REVIEW

2.1 Regional Geology and Tectonic Setting of the Study Area

The ground water potential assessment of Kobo-Robit-Minjar unpublished report 2013 is reviewed for the study area as a reference. The general lithological units identified in the Kobo, Dessie,

Kemissie sheet are shown in Figure 2.1 revealing 23 rock types with separate lithological code. These units are shown on the geological maps of the study area. These mappable lithological rock units are listed below: -

- Upper sandstone (Ka)
- Ashange basalt (E3as)
- Aiba basalt (E2ai)
- AlajiSirro rhyolite, trachyte, ignimbrite & tuff (E2ajs)
- AlajiMolale rhyolite, trachyte, ignimbrite & tuff (E2ajm)
- Anchar basalt (NlAn)
- Termaber – Guassa basalt (E3tg)
- Dermaber – Megezez basalt (E3tm)
- Ataye Rhyolite & domes (Nlar)
- Granite Intrusion (Nlgt)
- Kessem formation (Nlkf)
- Fursa Rhyolite (NlFs)
- Mabla rhyolite (Nlma)
- Albuko rhyolite (Nlab)
- Dalha basalt (Nldh)
- Rasa basalt (Nlrb)
- Balchi rhyolite, ignimbrite, tuff (Nlbr)

- GaraBokan older rhyolitic domes & flows (QlGb)
- K'one Felsic volcanics (lavas, domes, pyroclastics) (Q1kv)
- Recent basalt flows & scoria cones (Q2rb)
- Fluvio-lacustrine sediments (Q1us)
- Alluvium (Qus)

Of these rock units, the dominant lithological units that feature in the Tisabalima area are the Alluvium (Qus) deposits.

Alluvium deposits (Qus)

This deposit is observed to occur in almost all of the marginal grabens of Tisabalima areas. The sub-basins have thick unconsolidated deposit that overlay the bedrock. The loose and unconsolidated sediments that are re-deposited in the sub-basins are thick enough to have implications on groundwater availability and movement. These deposits are very young sedimentary materials that are transported by the river that exists in the area.

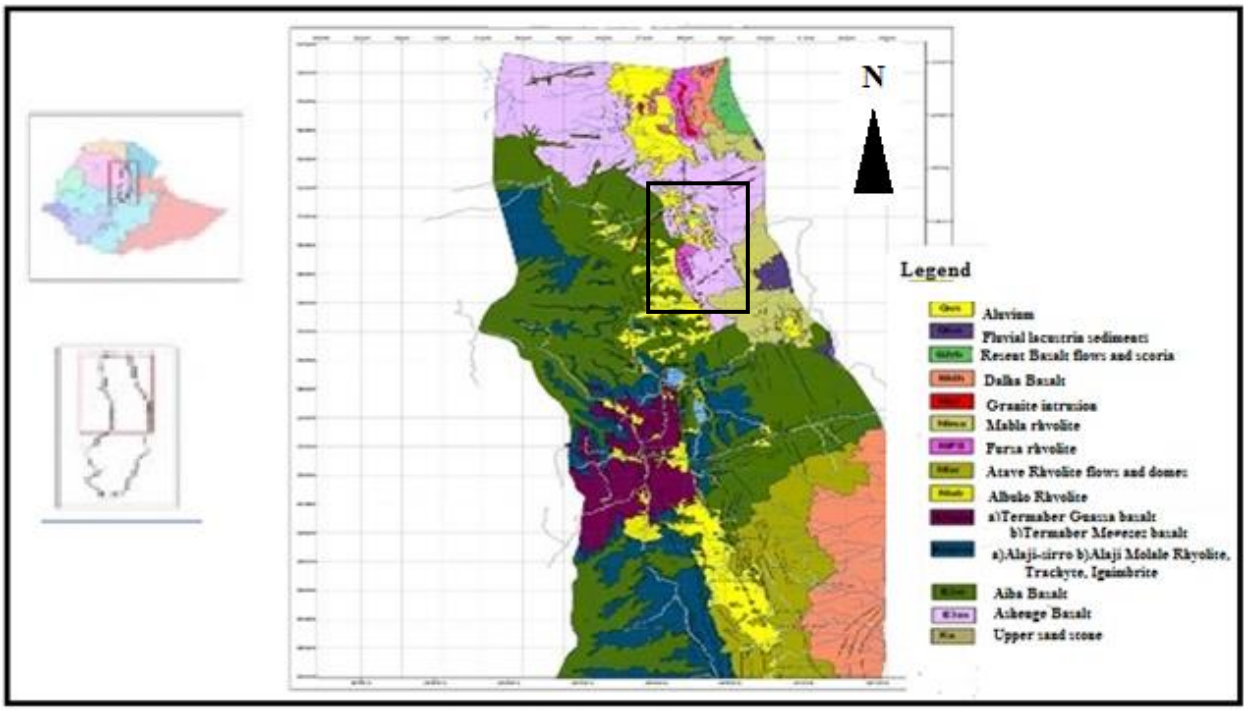

Figure 2.1 Geological Map of Kobo, Dessie, Kemissie Sheet, 1:250, 000scale (from Amhara Design and Supervision Works Enterprise, 2013).

Rivers have the capacity to erode, transport and deposit earth materials such as rocks and sediments. Fluvial processes are related to the hydrosphere and belong to the exogenous processes that shape the relief, sometimes by acting constructively land creation through accretion and other times by acting destructively, resulting in lowering of relief (erosion).

The formation of the drainage network in the marginal grabens or basins begins with the down faulting of the rifting processes. When the initial inclinations of the resulting escarpment are small, erosion processes are limited. With time, the escarpment continues to rise up its inclination dramatically, thus erosion becomes more intense and fluvial deposits more abundant. In general the river or stream flow directions are west to east from the plateau and bordering escarpments drain towards the rift.

When the solid supply of a stream is high and the transfer capacity is not adequate for the transportation of the corresponding solid material, flow speed is reduced and deposition of the heavier solid material (boulders, gravels) begins to be deposited in the upstream areas (towards the western sector of the marginal grabens near the Escarpments). As one goes towards downstream due to a decrease in inclination of the terrain, a decrease of a water stream's transfer capacity occurs and as a result finer and lighter materials (sand, silts, and clays) are deposited on the eastern part of the marginal grabens forming wide alluvial plains.

2.2 Geological structures

Several researchers agree that crustal extension had been commenced by 18Ma in the southern Main Ethiopian Rift (MER), but most of the present rift morphology was developed after 12 Ma. The age of the first stage basins in the northern Main Ethiopian Rift (MER) is considered to be 11 Ma; whereas the basins in the Southern Red Sea are 15 Ma older than those in the northern MER. The Main Ethiopian Rift is a narrow rift segment of 700 Km long, 80km wide volcanically active rift situated between the northwestern and southeastern Ethiopian plateaus bordered by the great border faults. The eastern margin border faults are characterized by rift-ward en échelon; right-stepping normal faults with a NNE-SSW & NE-SW strike directions. They are defined by multiple faults with cumulative displacement greater than100m on each of the fault, where as the

western margin is marked by a elevated escarpment with an exposed throw of 1.5 Km. Between these border faults, the central rift valley is marked by approximately 20 km-wide right-stepping, en echelon chains of eruptive volcanic centers, extension cracks, fissures and N15E striking, small offset normal faults. These right stepping en échelon faults, fissures and chains of Quaternary eruptive centers were collectively referred to as the Wonji Fault Belt (WFB).

Three distinct structural patterns are depicted in Kobo-Robit-MINJAR area are shown in Figure 2.2. These are, NNW to SSE trending structures are observed starting from Kobo up to Kara Kore area that is parallel to Red Sea Rift, the NE – SW structures that corresponds to the Main Ethiopian Rift trend, which characterizes the southern part, and N – S trending border faults from Kara-Kore up to Debresina-Ankober area where both the Main Ethiopian Rift and Red Sea Rift interact. Additionally ENE -WSW trending structures of the Gerado,-Meticolo – Degan- Bati areas and Ambo - Kessem fault that parallels the Gulf of Aden Ridge are also observed.

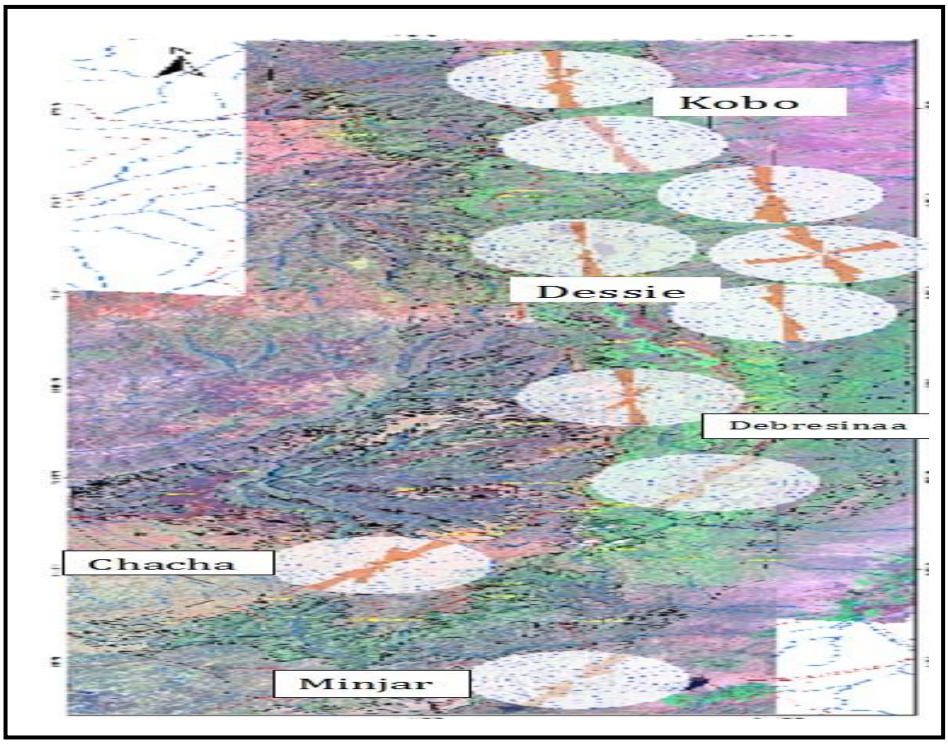

Figure 2.2 Strike variation of the major faults trend within the Kobo, Robit and Minjar(from Amhara Design and Supervision Works Enterprise, 2013).

2.3 Hydrogeology

2.3.1 Recharge and discharge area

Generally, the major sources of groundwater recharge are mainly high land plateau, fault block high lands and escarpments, shield volcanoes, high land plateau, isolated domes within the valleys, whereas marginal graben basins, low land and faulted plains are the discharge areas where groundwater is released in various ways.

2.3.2 Hydrogeological Set up of Tisabalima Sub basin

This area is located downstream of Kete stream catchment. It is wide E-W elongated intermountain valley plain area started from the foot of Ambassel Mountain (Tisabalima) along Mille stream up to Seglen area. Kete, Nibo (Chirecha) &Gomora streams begin from south west of Tisabalima area and join at about 2 km SW of Jarri village and form one big stream called Mille. This stream flows to north direction through highly faulted gorge to Tis Abalima plain area and later bends east to Seglen area. Since the western escarpment of Rift valley is highly affected by tectonic activities; most of the streams follow weak zone and transport huge volume of rock fragment (boulder, pebble, coble, sand, silt and clay). These transported earth material settle gradually at plain area based on grain size and fills intermountain valleys. Wide plain area south of Wuchale town and around Tisabalima town have coarser deposit and the base flow from the plain area of the unconsolidated sediments feeds the Mille stream. Rhyolitic and basaltic ridges around Wuchale town, Mille bridge, south and south west of Jari area, along the road to Marye-silassie, had been highly affected and crushed by north – south trending parallel faults and this situation provides a highly permeable condition for groundwater recharge and circulation. The presence of Bededo, Itecha, Passo-Mille, Jari and other high discharge springs indicate the role of tectonic effect on the groundwater recharge and circulation in the area.

Other intermountain valley plain area is along Burka intermittent stream begins north of Haik Lake and flows NE to Mille stream. This plain area starts from Kistane and extend to Seglen area with good prevailing geological and morphological circumstances for groundwater occurrence.

CHAPTER THREE

GEOPHYSICAL METHODS

3.1 General

3.2 Electrical Methods of Prospecting

3.2.1. Vertical Electrical Sounding (VES) Principle

In Vertical Electrical Sounding (VES), the positions of electrodes are changed with respect to a fixed point (known as the sounding point) and the measured values reflect the vertical distribution of resistivity values on a geologic section.

Vertical electrical sounding consists of a symmetrical electrode array used to determine the resistivity of the subsurface which is assumed to be consisting of horizontally stratified layers. The procedure is used to determine the variations in resistivity in the vertical direction and is also called electrical drilling or commonly vertical electrical sounding (VES). By expanding symmetrically the distance between current electrodes about a point called the sounding point, while keeping the potential electrodes MN at the same position, provides a sounding curve corresponding to the apparent resistivity versus depth of the location.

The measured potential becomes very low and the distance between the potential electrodes is increased. Increasing the potential electrode spacing produces a 'step' in the apparent resistivity curve and it is good practice to obtain an overlap between the curve segments by obtaining two readings at different potential electrode spacing for two adjacent current electrode spacing. Segments obtained at larger potential electrode spacing can be shifted in order to produce a smooth curve (Gibson and George, 2003). In electrical prospecting to determine the depth and electrical resistivity of a series of horizontal or nearly horizontal ground, it is difficult to measure both parameters. In order to solve this problem, we should calculate the potential and the electric field, due to a point source of current, at any point on the surface of a stratified earth. This has advantages because of enables one to use axial symmetry of the potential filed about the vertical axis through the current source and the additive property of the potential is also be used. Let us choose a cylindrical system of coordinate with the origin at the point source a direct current located on the surface. The subsurface consists of infinite number of layers separated by

horizontal boundary planes, the deepest layer existing to infinite depth and the other layers have finite thickness $h_i = h_1, h_2, h_3 \ldots h_n$ and resistivity's $\rho_i = \rho_1, \rho_2, \rho_3, \ldots, \rho_n$. Each of the layers is electrically homogeneous and isotropic.

The derivative of the potential based on the above conditions was first due to (Stefanescus et al., 1930).

The electrical potential field V for direct current satisfies the differential equation of Laplace, which is

$$\frac{\partial 2_V}{\partial x^2} + \frac{\partial 2_V}{\partial y^2} + \frac{\partial 2_V}{\partial z^2} = 0 \qquad (3.1)$$

The potential field has a cylindrical symmetry with respect to the vertical axis line through the current source. Therefore, Laplace equation in cylindrical coordinate is most appropriate.

For a solution symmetrical with respect to the vertical axis $\frac{\partial V}{\partial \theta} = \frac{\partial^2 v}{\partial \theta^2} = 0$ so,

$$\frac{\partial^2 V}{\partial X^2} + \frac{1}{r}\frac{\partial V}{\partial r} + \frac{\partial^2 V}{\partial Z^2} = 0 \qquad (3.2)$$

The particular solution of equation (3.2) can be obtained using the method of separation of variables and can be assumed to be of the form

$$V(r,z) = U(r)W(z) \qquad (3.3)$$

Substituting equation (3.3) to (3.2) and divide throughout by the product U(r) W (z) gives

$$\frac{1}{U(R)}\frac{\partial^2 U(r)}{\partial r^2} + \frac{1}{rU(r)}\frac{\partial U(r)}{\partial r} + \frac{1}{W(z)}\frac{\partial^2 W(Z)}{\partial z^2} = 0 \qquad (3.4)$$

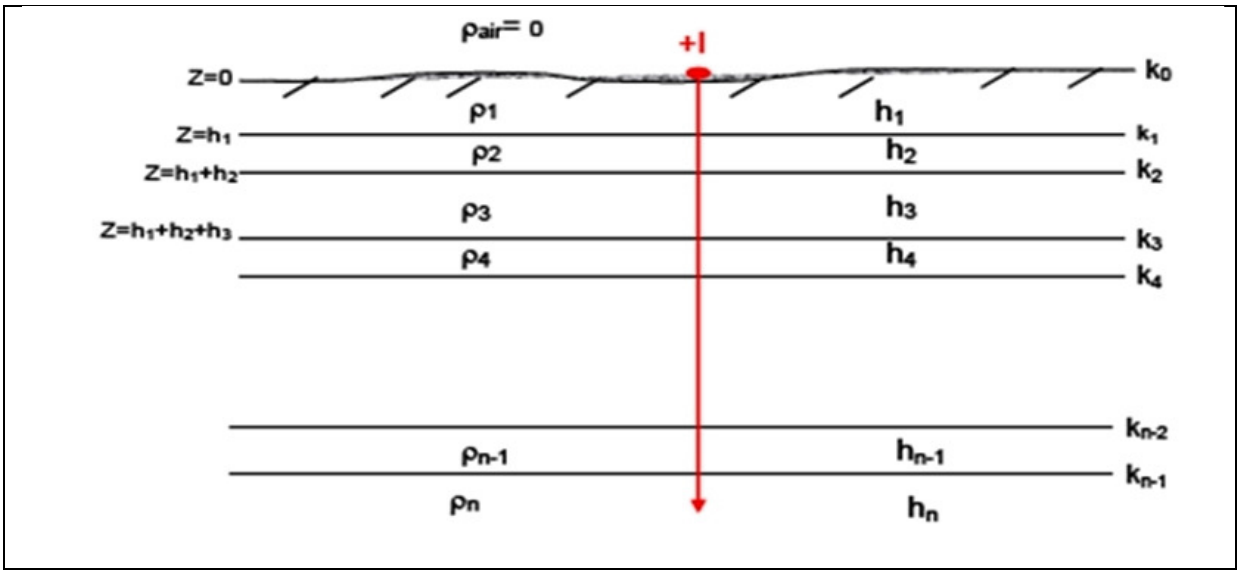

Figure 3.1 Problem presentation for sounding over multi-layered Earth**.**

This equation is satisfied if and only if

$$\frac{1}{U(R)}\frac{\partial^2 U(r)}{\partial r^2}+\frac{1}{rU(r)}\frac{\partial U(r)}{\partial r}=\lambda^2\ and \tag{3.5}$$

$$\frac{1}{W(z)}\frac{\partial^2 W(Z)}{\partial z^2}=-\lambda^2 \tag{3.6}$$

where λ is an arbitrary constant. The solution of equation (3.6) may be given as:

$$W(z)=C_1e^{-\lambda z}andW(z)=C_1e^{+\lambda z} \tag{3.7}$$

and that of equation (3.5) is given as

$$U(r)=C_3J_O(\lambda r) \tag{3.8}$$

where **J0** is the Bessel function of order zero.

The combination of equation (3.7) and (3.8) gives the particular solution of the differential equation given by equation (2.9), which is

$$V(r,z)=C_4e^{+\lambda z}J_O(\lambda r)\ and \tag{3.9}$$

$$V(r,z) = c_4 e^{-\lambda z} J_o(\lambda r)$$

where **c** and $\lambda$are both constants in the last of these equations.

Since, by theory of differential equation, every linear combination of the particular solution is also a solution, one can make λ to rough all possible values from zero toinfinity and allowing the constant "c" to very independence of λ the general solution of equation (3.2) can be obtained as

$$V(r,z) = \int_0^\infty [\phi(\lambda)\, e^{+\lambda z} + \psi(\lambda) e^{-\lambda z}]\, J_O(\lambda r) d\lambda \tag{3.10}$$

Here$\phi(\lambda)$ and $\psi(\lambda)$are arbitrary functions of the boundary conditions control the special form of these equations. From basic theory, the potential generated by a single point source of current intensity "I" located at the surface of an electrically homogeneous earth is given by

$$V = \frac{I\rho}{2\pi} \frac{1}{\sqrt{r^2+z^2}} \tag{3.11}$$

Where ρ is the resistivity of homogeneous Earth. Equation (3.11) can be written in integral form by using the so-called Lipchitz integral (also called the Weber Integral Formula) in theory of Bessel function as

$$\int_0^\infty e^{-\lambda z} J_O(\lambda r) d\lambda = \frac{1}{\sqrt{r^2+z^2}} \tag{3.12}$$

So that equation (2.12) gives

$$V = \frac{I\rho}{2\pi} e^{-\lambda z} J_O(\lambda r) d\lambda \tag{3.13}$$

Equation (3.13) is also a solution of equation (3.12). Therefore, the combined solutions will also be a solution to the equation, that is

$$V(r,z) = \frac{I\rho}{2\pi} \int_0^\infty [e^{-\lambda z} + X(\lambda) e^{+\lambda z} + \Theta(\lambda)\, e^{+\lambda z}] J_O(\lambda r) d\lambda \tag{3.14}$$

Where $\Theta(\lambda)$ and $X(\lambda)$ are arbitrary function. Solutions of equation (3.14) are valid in all the layers of the subsurface. However, necessarily it is the same in different layers of the subsurface. Therefore, the potential due to a point source of current at the surface of a horizontally layered earth must in each layer satisfy

$$V_I = \frac{I\rho}{2\pi}\int_0^\infty [e^{-\lambda z} + X_i(\lambda)e^{+\lambda z} + \Theta_i(\lambda)\, e^{+\lambda z}]J_O(\lambda r)d\lambda \qquad (3.15)$$

This equation is called the Stefanescu Integral, with 'i' referring to the several layers of the subsurface.

Boundary conditions

For a potential set up by a single source of current at the surface of a horizontally stratified earth, the following boundary conditions are fulfilled.

1. At each of the boundary planes in the subsurface, the electrical potential must be the same

$$V_i = V\ at\ Z = h_i \qquad (3.16)$$

2. The vertical component of the current density must be continuous on each boundary plane (the current density normal to the boundary planes …)

$$(J_I)_N = (J_{i+1})_N$$

$$\frac{1}{\rho_i}\frac{\partial v_i}{\partial z} = \frac{1}{\rho_{i+1}}\frac{\partial v_{i+1}}{\partial z} \qquad (3.17)$$

the current source. In air J air = 0 and from condition (3.17), the vertical component of the current density at depth zero must be zero. Near the current source the potential must not approach infinity (must remain finite) as

$$V = \frac{I\rho}{2\pi}\frac{1}{\sqrt{r^2+z^2}} \qquad (3.18)$$

3.2.2 Basic Principles of Resistivity for Groundwater

The most common minerals forming soils and rocks have very high resistivity in a dry condition, and the resistivity of soils and rocks is therefore normally a function of the amount and quality of water in a pore spaces and fractures. The degree of connection between the cavities is also important. The following considerations can be used to determine the resistivity of rocks.

- Sandstones and limestones saturated with water have lowest resistivities, where as the highest resistivities values represent strongly consolidated sedimentary rock or dry rock above the ground surface.

- Sand, gravel and sedimentary rock pore spaces filled with salin water may have very low resistivities.

- Dry sand without water is very resistive.

- Additionally weathering commonly produces conductive clay-rich Saprolite geological formation causes to have low resistivity value to occur.

- Impermeable clay layer, which is wet, has low resistivity but may not contain enough yields for successful groundwater exploitation.

To identify the conditions necessary for the presence of groundwater from resistivity measuremts , the absolute value of the ground resistivity must be considered. Usual target for aquifer resistivity can be between 50 Ohm-m to 2000 Ohm-m (Bernard, 2003).

Generally the resistivity data against geological documentation, for example surface mapping, test pits or drillings are calibrated to define the variation in characteristics of geological material. The amount of water in a material depends on the porosity, which may be divided into primary and secondary porosity. Primary porosity consists of pore spaces between the mineral particles, and occurs in soils and sedimentary rocks. Secondary porosity may also be important in certain sedimentary rocks, such as limestone.

The resistivity of the pore water is determined by the concentration of ions in solution, the type of ions and the temperature. A range of resistivities for different types of water is given in table 2.1

Table 3.1 Electrical resistivity of some types of natural waters (ABEM instruction manual, 2009)

Types of water	Resistivity (Ohm-m)
Surface water, in areas of igneous rock	30-500
Surface water, in areas of sedimentary rock	10-100
Groundwater, in areas of igneous rock	30-150
Groundwater, in areas of sedimentary rock	>1

3.3 ELECTRODE CONFIGURATIONS

The two potential and current electrodes disposed over the ground in various ways. The disposition of the four electrodes system gives rise to what are known as electrode arrays, configurations, layouts or arrangements.

The arrangement of current and potential electrodes and the distances between showed in figure 2.1 displays the general form of four electrodes system. The potential difference between the position P_1 and P_2 is founded by:

The Potential at $V_{P1} = \frac{I}{2}\frac{\rho}{\Pi}\left(\frac{1}{r_1} - \frac{1}{r_2}\right)$

Similarly, the potential at $V_{P2} = \frac{I}{2}\frac{\rho}{\Pi}\left(\frac{1}{r3} - \frac{1}{r_4}\right)$

And the potential difference

$$\Delta V = \frac{I}{2}\frac{\rho}{\Pi}\left(\frac{1}{r1} - \frac{1}{r_2} - \frac{1}{r3} + \frac{1}{r_4}\right) \quad (2.1)$$

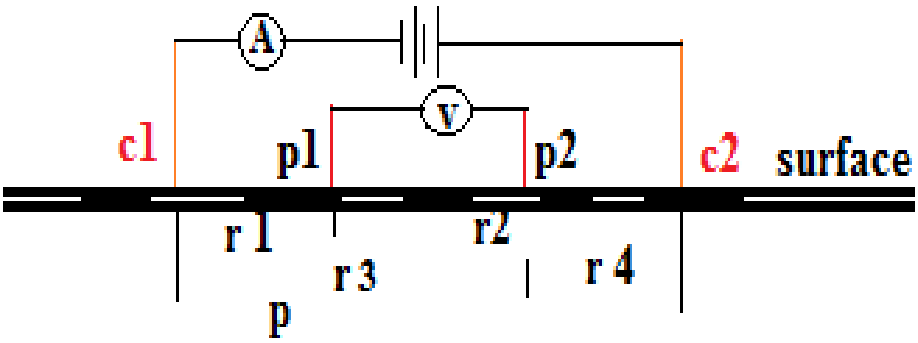

Figure 2.1 The arrangement of current and potential electrodes in a four electrodes system.

3.3 Magnetic Method of Prospecting

The other method employed in the work is the magnetic method of prospecting. Geomagnetic methods can be used in a wide variety of applications and range from small-scale investigations to locate pipes, cables and metallic objects in the very near surface, and engineering site investigations, through to large scale regional geological mapping to determine gross structure, such as in hydrocarbon exploration (Reynolds, 1997).

3.3.1 Basic concepts and units of Geomagnetism

Within the vicinity of a bar magnet a magnetic flux is developed which flows from one end of the magnet to the other (Figure 2.6).This flux can be mapped from the directions assumed by a small compass needle suspended within it. The points within the magnet where the flux converges are known as the poles of the magnet. A freely-suspended bar magnet similarly aligns in the flux of the Earth's magnetic field.

The pole of the magnet which tends to point in the direction of the Earth's North Pole is called the north-seeking or positive pole, and this is balanced by a south-seeking or negative pole of identical strength at the opposite end of the magnet (Kearey et al., 2002).

Magnetic poles always exist in pairs of opposite sense to form a dipole. When one pole is sufficiently far removed from the other so that it no longer affects the other, the single pole is referred to as a monopole (Reynolds, 1997).

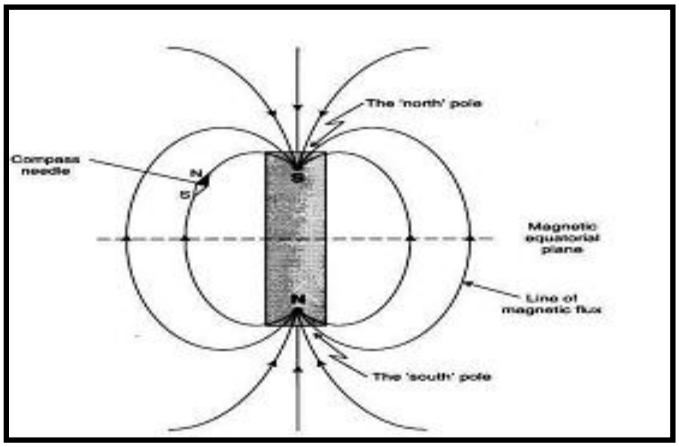

Figure 3.3 Lines of magnetic flux around a bar magnet (after Reynolds, 1997).

The force F between two magnetic poles of strengths m_1 and m_2 separated by a distance 'r' is given by

$$F = \frac{\mu_0 m_1 m_2}{4\pi\mu_R r^2} \tag{2.20}$$

where μ_0 and μ_R are constants corresponding to the magnetic permeability of vacuum and the relative magnetic permeability of the medium separating the poles (Kearey et al., 2002).The force is attractive if the poles are of different sign and repulsive if they are of like sign.

The magnetic field B due to a pole of strength *m* at a distance *r* from the pole is defined as the force exerted on a unit positive pole at that point

$$B = \frac{\mu_0 \mathrm{m}}{4\pi\mu_\mathrm{R} \mathrm{r}^2} \tag{2.21}$$

Magnetic fields can be defined in terms of magnetic potentials in a similar manner to gravitational fields. For a single pole of strength *m*, the magnetic potential *V* at a distance *r* from the pole is given by

$$V = \frac{\mu_0 m}{4\pi\mu_R r} \tag{2.22}$$

The magnetic field component in any direction is then given by the partial derivative of the potential in that direction.

The SI unit of B is expressed in Vsm^{-2}(Weber (Wb)m^{-2}). The unit of the Wbm^{-2} is designated the Tesla (T). The c.g.s unit of magnetic field strength is the gauss (G), numerically equivalent to 10^{-4}T.

Common magnets exhibit a pair of poles and are therefore referred to as dipoles. The *magnetic moment M* of a dipole with poles of strength *m* a distance *l* apart is given by

$$M = ml \tag{2.23}$$

The magnetic moment of a current-carrying coil is proportional to the number of turns in the coil, its cross sectional area and the magnitude of the current, so that magnetic moment is expressed in Am^2.
The intensity of induced magnetization J_i of a material is defined as the dipole moment per unit volume of material:

$$J_i = \frac{M}{LA} \tag{2.24}$$

Where M is the magnetic moment of a sample of length L and cross-sectional area A. J_i is consequently expressed in Am^{-1}.

The induced intensity of magnetization is proportional to the strength of the magnetizing force H of the inducing field:

$$J_i = kH \tag{2.25}$$

where k is the magnetic susceptibility of the material. Since $J_i$and H are both measured in Am^{-1}, susceptibility is dimensionless in the SI system.

In a vacuum the magnetic field strength B and magnetizing force H are related by $B=\mu_0 H$ where μ_0 is the permeability of vacuum ($4\pi \times 10^{-7} Hm^{-1}$). Air and water have very similar permeability to μ_0 and so this relationship can be taken to represent the Earth's magnetic field when it is undisturbed by magnetic materials (Kearey et al., 2002).

When a magnetic material is placed in this field, the resulting magnetization gives rise to an additional magnetic field in the region occupied by the material, whose strength is given by $\mu_0 J_i$. Within the body the total magnetic field, or magnetic induction, B is given by

$$B = \mu_0 H + \mu_0 J_i \tag{2.26}$$

Substituting equation (2.26)

$$B = \mu_0 H + \mu_0 kH = (1 + k)\mu_0 H = \mu_R \mu_0 H \tag{2.27}$$

where μ_R is a dimensionless constant known as the relative magnetic permeability. The magnetic permeability μ is thus equal to the product of the relative permeability and the permeability of vacuum, and has the same dimensions as μ_0. For air and water μ_R is thus close to unity.

3.3.2 Nature of the Geomagnetic Field

The geomagnetic field of the Earth is composed of three parts:

The main field or Dipole field $\mathbf{B_D}$, which is produced in the fluid outer core of the earth and accounts for the very large regional variations in the total field intensity and direction.

The external magnetic field $\mathbf{B_{ext}}$, which is produced by electric currents in the earth's ionosphere consisting of particles ionized by solar radiation and put into motion by the solar tidal force.

The anomalous magnetic field which is produced by ferromagnetic minerals and rocks in the earth's crust or rock magnetism $\mathbf{B_{rm}}$.Therefore the Earth's total magnetic field $\mathbf{B_T}$ is given by

$$B_T = B_{ext} + B_D + B_{rm} \tag{3.28}$$

3. 3.3 The Earth's Magnetic Elements

A vector is used to represent the earth's magnetic field at an observation site. At any point on the Earth's surface, the magnetic field **B** has some strength and points in some direction. This vector quantity has a vertical component **Z** and a horizontal component **H** in the direction of the magnetic north. The horizontal component **H** of the magnetic field **B** can be further decomposed into a component **X** in the geographic north direction and a component **Y** in the geographical east direction. The terms which are used to describe the direction of the magnetic field **B** are declination (**D**), the angle between geographic and the magnetic north. The angle of declination is measured positive through east and varies from 0 to 360 degrees, and inclination (**I**), the angle between the horizontal **H** and field **B**. Angle of inclination **I** varies from -90^0 to 90^0. These seven magnetic elements are related in the following ways (Figure 3.4).

3.4 Data Reduction and Processing

Data reduction and processing is the series steps taken to remove both signal and spurious noise from the data that are not related to the geology of the site. This process there by prepares the dataset for interpretation by reducing the data to only contain signal relevant to the task. These steps are summarized below:

i. **Data checking and editing:** involves the removal of spurious noise and spikes from the data that was caused by high tension power cable.

ii. **Diurnal removal:** corrects for the temporal variation of the Earth's main field which was achieved by subtracting the time synchronized signal, recorded at a stationary base magnetometer from the survey data.

iii. **IGRF removal:** removes the strong influence of the Earth's main field. This was achieved by subtracting a calculated of main field from the diurnal corrected survey data.

$$B^2 = H^2 + Z^2 = X^2 + Y^2 + Z^2 \quad \mathrm{B}^2 = \mathrm{H}^2 + \mathrm{Z}^2 = \mathrm{X}^2 + \mathrm{Y}^2 + \mathrm{Z}^2$$

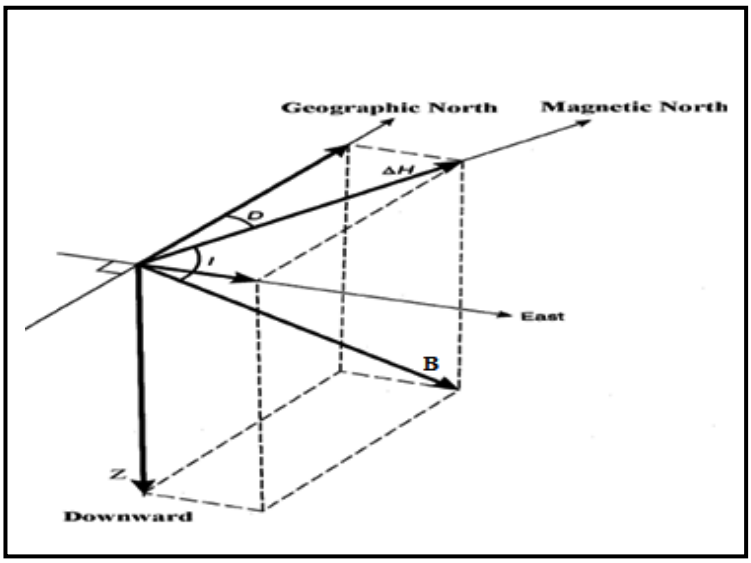

$$H = B\cos i$$

$$Z = B\sin i$$

$$\tan i = Z / H \quad (3.22)$$

$$X = H\cos D$$

$$Y = H\sin D$$

Figure 3.4 The Earth's magnetic field elements (from Reynolds1997).

CHAPTER FOUR

DATA ACQUISITION, PROCESSING AND PRESENTATION

4.1 The Resistivity Method

4.1.1 Field procedure and data acquisition

The Schlumberger array is mostly used in vertical electrical sounding for its better depth penetration and that it is less sensitive for lateral inhomogeneities because the potential electrodes remain fixed during a number of successive measurements with expanding current electrodes.

For this study the symmetrical Schlumberger array which is the secondary data which is vertical electrical sounding (VES) among 4 lines are shown in Figure 4.1. The VES were carried out with maximum current electrode spacing (AB/2) of 750 m by injecting electrical current in to the ground by means of two outer electrodes, and the resulting potential difference were measured by a second pair of potential electrodes placed near the center of the outer electrodes.

Electrical resistivity survey using ABEM SAS 1000 Terrameter was used to collect the data within an average distance of 880 m. The current electrode spacing AB/2: 1.5, 2.1, 3.0, 4.2, 6.0, 9.0, 13.5, 20.0, 30.0, 45.0, 66.0, 100.0, 150.0, 220.0, 330.0,500.0 and 750.0 meter and the potential electrodes spacing were MN/2 1.0, 12.0 and 90.0 were used to collect data during field work. The overlap readings AB/2: 20.0, 30.0, 150.0 and 220.0 m were taken in order to avoid the ambiguity of in homogeneity of the subsurface.

4.1.2 Data reduction

The apparent resistivity values are plotted on logarithmic transparent paper. In processing of the collected data, the apparent resistivity values were written on the ordinate and the electrode separation (AB/2) on the abscissa. The resistivity measurements were made by progressively increasing the potential electrode distance (MN/2) relatively large increment of the current electrode distance (AB/2).In most cases the sounding curve is segmented due to overlap

measurement and cannot be interpreted as it is. To have precise interpretations the segmented curves were shifted to the small MN curve points, so that the effect could be quantified and corrections could be made in order to obtain a single smooth curve that could be processed with the computer software known as “RESIXIP” software.

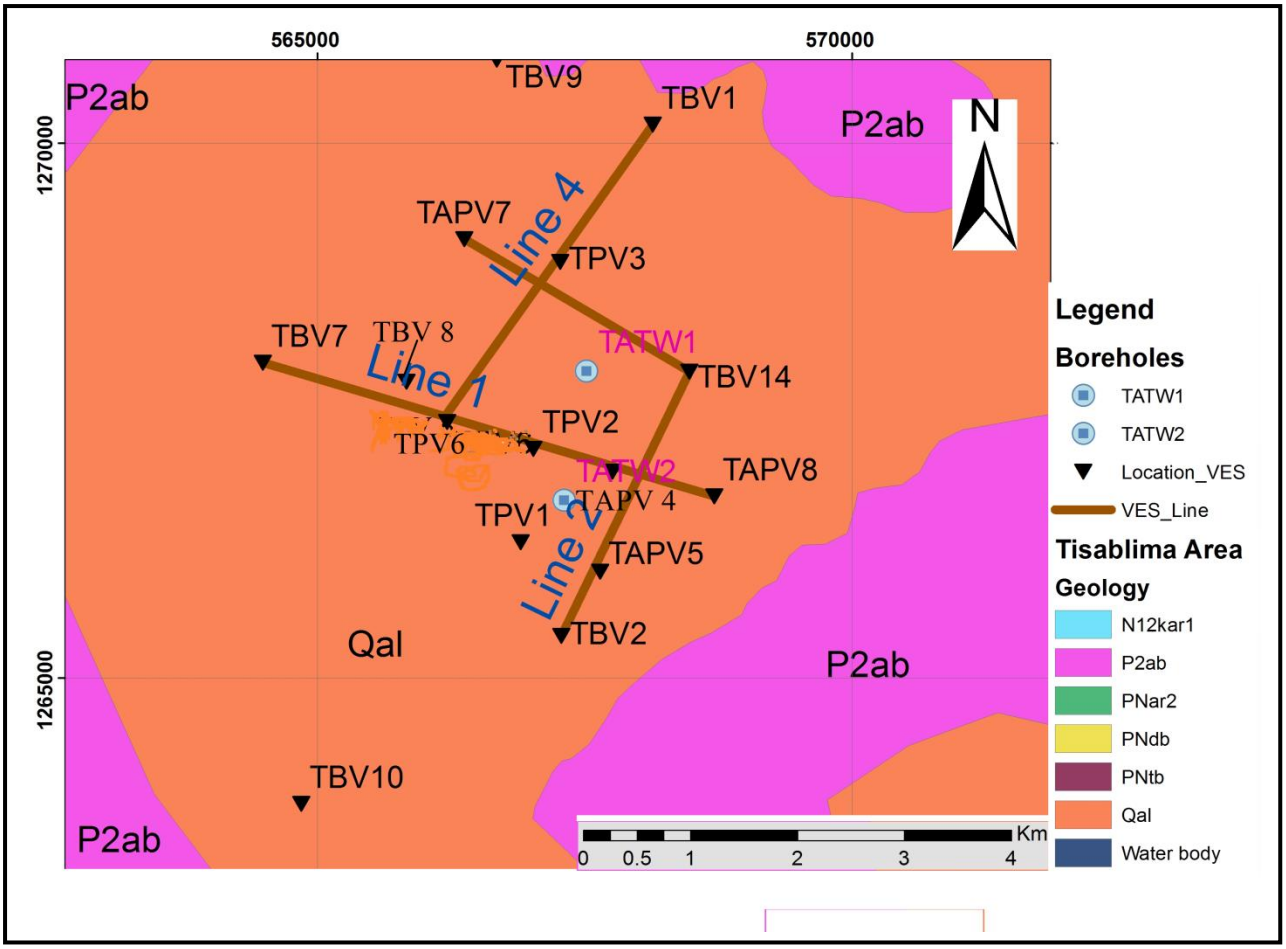

Figure 4.1 Location of the Vertical Electrical Sounding (VES) points along the four traverse lines at Tisabalima sub basin, Eastern Amhara Regional State Ethiopia.

4.1.3 Data processing and presentation

The electrical sounding data collected in the field work were plotted on a bi- logarithmic paper and interpreted by using two layer master curves and auxiliary charts to find out initial model parameters for the thickness and electrical resistivity of the possible layers mapped with survey. These parameters obtained from curve matching techniques arranged and analyzed with litho logical units

of existing boreholes were used as initial model in the WIN RESIST inversion software which resulted in improved and reliable electrical parameters under the area of investigation as depicted in the interpreted sounding resist curves. Consequently, from the results of these interpreted geoelectric parameters. The depth, thickness and resistivity parameters acquired by the mentioned software program of vertical electrical sounding curves were used to construct geoelectric sections for each VES to show the distribution of different lithological unit in vertical direction using the software AutoCAD, 2007 programs. Geoelectric Sections are constructed according to the traverses they positioned. Available lithological logs from boreholes TATW 1 and TATW 2 in proximity of the surveyed traverses have been used for calibration and further refining the results. Thus, interpreted VES points at existing well sites are employed for calibrating the sounding points with in the area.

4.2 The Magnetic Methods

4.2.1 Field procedures and data acquisition

To gain the field target (anomaly), Total magnetic field measurements with spacing interval 50 meter along traverse line 1, line 2, line 3 and line 4 was made. These traverses are on the same lines as that of the VES points as can be seen in the figure 3.1.During each measurement GPS location and time of measurements were taken. Total magnetic field measurements with GSM-19 magnetometer having a resolution 0.01 nT has been used. For each survey a base station was carefully selected and established in an area away from the magnetic noise like stores, iron sheet buildings. The location of the base station is within the study area in order to facilitate easy and quick reoccupation. At each station the location, time and reading were recorded, as well as any relevant topographic or geological information and details of any visible or suspected magnetic sources. Readings at the base stations were taken within an hour are used to correct the diurnal variation of the earth magnetic field.

The GSM-19 is a portable high-sensitivity Overhauser effect magneto meter designed for hand-held, towed or base station use. In contrast to a standard proton magnetometer sensor that uses a proton-rich liquid, an Overhauser Effect sensor has a free radical added. This free radical ensures the presence of free unbound electrons that couple with protons, producing a two-spin system. A strong RF magnetic field is used to disturb the electron-proton coupling. By saturating free electron resonance lines, the polarization of protons in the sensor liquid is greatly increased. The

Overhauser effect offers a more powerful method of proton polarization than standard DC polarization (GSM 19 v7.0 Instruction Manual, 2008).

The diurnal variation was removed from the observed magnetic field data using the Microsoft excel 2007. The main magnetic field at the base station is obtained from the International Geomagnetic Reference Field (IGRF). The IGRF value at the base station is subtracted from the diurnal corrected total magnetic field of each station. The magnetic field anomaly map was gridded and contoured using the Geosoft Oasis Montaj mapping software.

4.2.2 Data processing and presentation

During a survey, magnetic base readings were taken within intervals of two hours, so that diurnal corrections for total magnetic field readings along the profiles were corrected using Microsoft excel 2007. Additionally by using Microsoft excel 2007 IGRF correction for each total magnetic reading along the profiles were corrected by referring to online IGRF calculator.

The corrected magnetic data were processed using a standard Geosoft Oasis Montaj were used program and presented as: Total magnetic field intensity map, Residual map Magnetic analytic signal map are presented in chapter 4.These maps are used to define qualitative interpretations in terms subsurface anomalous magnetic source that are favorable for ground water occurrences.

4.2.3 Data enhancement

Data enhancement techniques for residual magnetic anomaly field data like analytical methods were used for highlighting the contrast between magnetic anomalies generated by deep-seated and shallow origin anomalous geologic bodies. The residual magnetic map was used to enhance the analytical signal magnetic map of the study area and the resulting plots were interpreted in terms of the objectives of the work.

CHAPTER FIVE

RESULTS, DISCUSION AND INTERPRETATION

5.1 Results and Interpretation of Resistivity Data

To gain the greatest amount of change over the anomaly, a total of 15 vertical electrical soundings (VES) data are used to develop five survey lines are shown in Figure 3.1. Four of the survey lines that form a grid are used to identify the major subsurface geological units in the area and map possible water saturated horizons.

From the interpreted individual VES curves, the results of geoelectrical surveys along the lines are presented and discussed in the presiding sections in terms of interpreted individual VES curves, apparent resistivity pseudodepth sections, and geoelectric sections. The apparent resistivity pseudodepth section along the selected lines are mapped from raw data using surfer 10 software and the resistivity sounding geoelectric sections along the selected line are constructed from the interpreted layer parameters of each VES points(sample interpretations of the individual VES are shown in Annex-1). In the preside sections, Interpretation of a sample curve VES-TPV 2, the apparent resistivity pseudo depth and geoelectric sections on each line are presented and discussed separately.

5.1.1 Interpreted VES curves

A typical interpreted sounding curve, for example VES-TPV 2 of Line 1 is as shown in the Figure 4.1. By plotting the apparent resistivity with electrode spacing on a bi-log scale the initial model of VES-TPV 2 is obtained using RESIXIP and IPI2Win software. Further by using the nearby borehole TATW 2 (Annnex-2) the initial model parameter such as static water level of the study area 7.9 m, the depth of the boulder layer 6-36 m, gravel layer 36-66 m and clayey sediments within a depth 66-112 m are used as a standard to calibrate VES-TPV 2.Finally by using the inversion software (WINRESIST)and litho-logical description final model parameters are defined in terms of geo-electric layers and its depth obtained by the resistivity survey.
The interpretation of the resistivity data revealed five layers with resistivity contrast between 24.6 and 127.3 Ohm-m (Figure 4.1).The first tiny layer having a thickness 1m and resistivity

value 48 Ohm-m is interpreted to be top clayey layer. Below it two consecutive layers located at a depth of 4.8 m and 51.1 m having resistivity value 127.3and 35.1 Ohm-m is characterized by highly permeable gravel and boulder layers. Similarly beneath these layers, the fourth layer clayey gravel shows low resistivity response (15.6 Ohm-m) than the underlying unit gravel.

Generally the interpreted VES-TPV 2 represents a five layer subsurface each of varying thickness and resistivity. A very good data quality and interpretation is obtained with RMS error of 2.4 %.

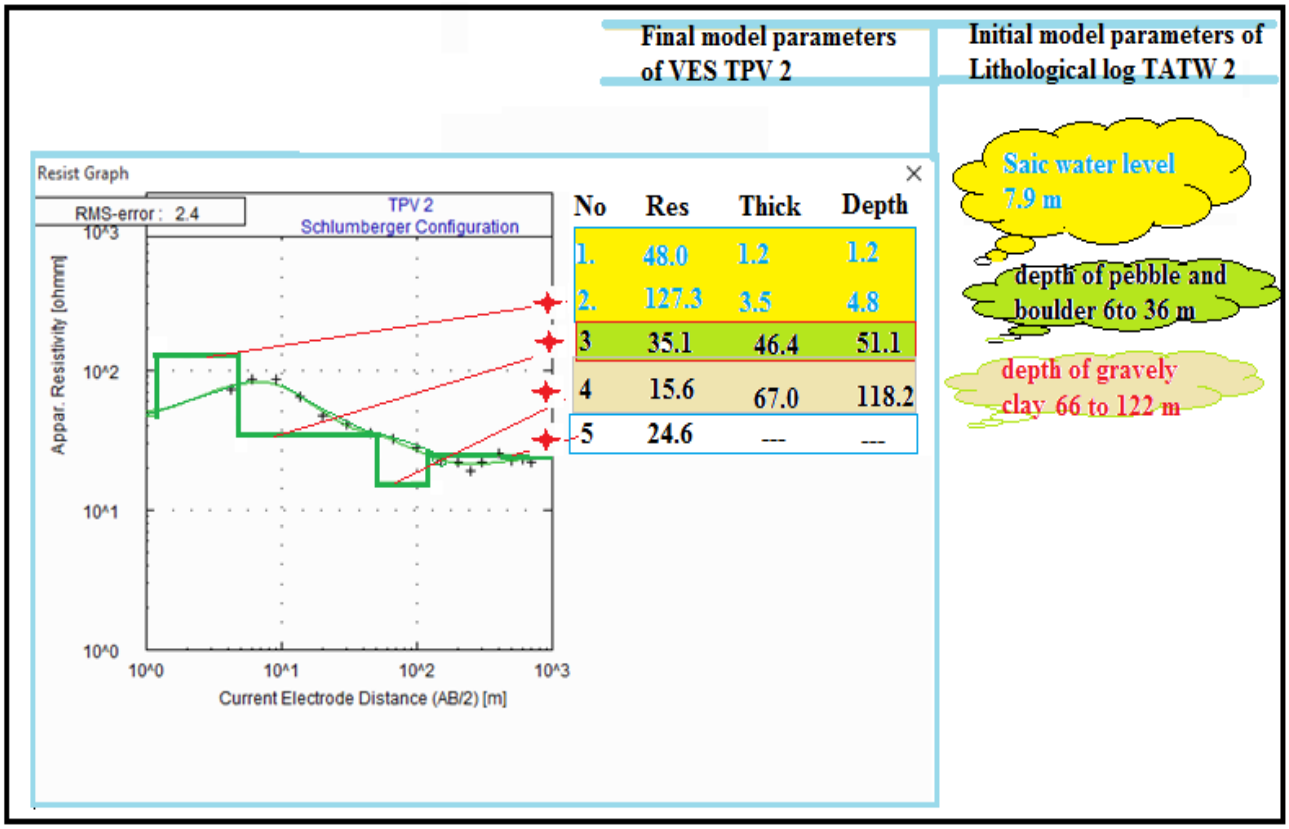

Figure 5.1 An example of interpreted sounding curve VES-TPV 2, on Line 1, Tisabalima Eastern Amhara Regional State, Ethiopia.

5.1.2 Pseudo depth section and Geoelectric Section of the Profiles

Using the 15 VES, Pseudo depth and geoelectric sections mapped along profile lines 1 to line 4 are constructed from software surfer 10 and Auto CAD, 2007 respectively. On average each VES points distant within 1204 m are used to represent the area. The designations of VES on each

line and its location are given in the Table 5.1.

5.1.2.1 Traverse Line 1

Traverse line-1 positioned near the middle of the basin is oriented NW to SE direction. This line with total length 4487 m consists of 6 VES points that lie on the traverse. Each VES with average spacing 747 m has an advantage to cross the widest part of the anomaly.

Table 45.1 Location of the VES sounding points along each traverse and total traverse length.

Line		UTM Location			Total line/Profile lengths in meter
		Easting	Northing	Elevation(m)	
1	TBV 7	564489	1267947	1725	4500
	TBV 8	565834	1267769	1639	
	TPV 6	566212	1267395	1625	
	TPV 2	567020	1267144	1593	
	TAPV 4	567758	1266931	1565	
	TAPV 8	568710	1266699	1530	
2	TBV 2	567281	1265395	1565	2823
	TAPV 5	567643	1265995	1550	
	TAPV 4	567758	1266931	1565	
	TBV 14	568477	1267866	1555	
3	TAPV 7	568477	1267866	1555	2500
	TPV 3	567270	1268889	1579	
	TBV 14	566374	1269101	1657	
4	TPV 6	566212	1267395	1625	3380
	TPV 3	567270	1268889	1579	
	TBV 1	568137	1270173	1610	

A. Pseudodepth section of traverse Line 1

From Pseudodepth section shown in Figure 5.2. Except the top layer mapped between VES point TBV7 and TBV8 along the traverse Line 1; all layers are covered by lower resistivity values. Overall, the vast portions of the section are covered by low resistivity values that lie between 3 to 23 Ohm-m. These layers are expected to be a high yield aquifer for ground water exploration.

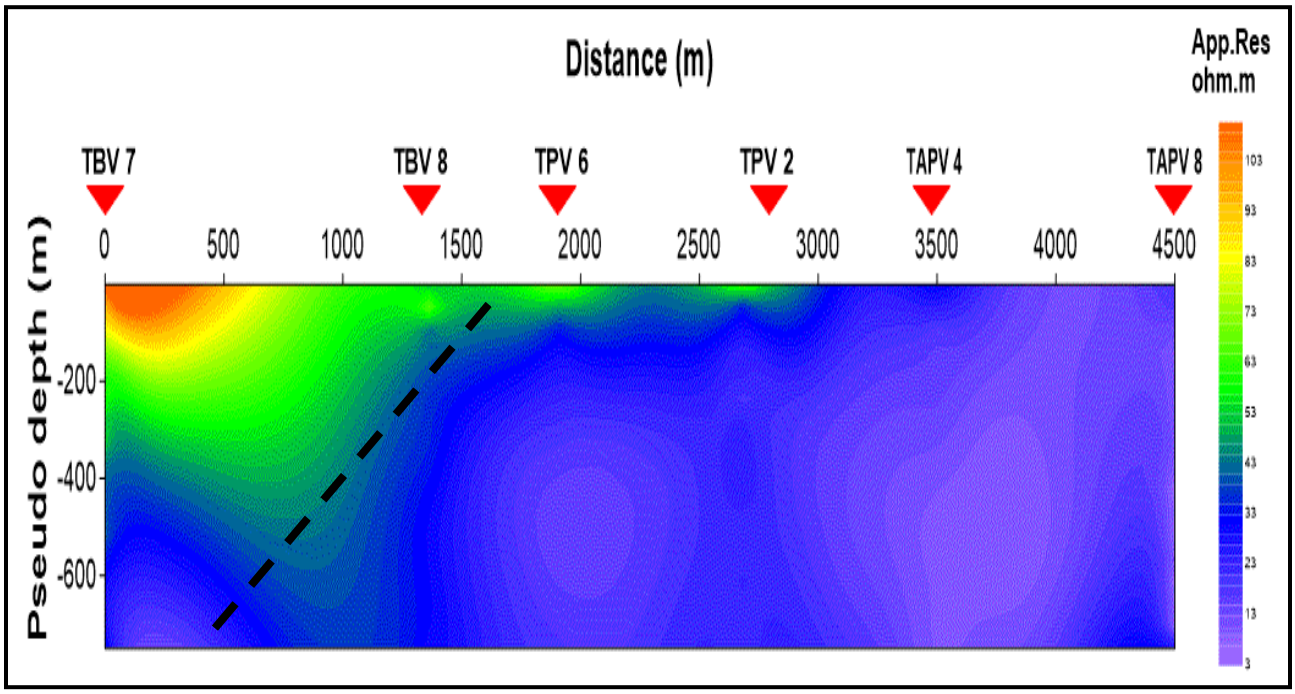

Figure 45.2.Apparent resistivity pseudodepth section along traverse Line 1,Tisabalima Eastern Amhara Regional State, Ethiopia.

B. Geoelectric section along traverse Line 1

Geoelectric section along traverse Line 1 shown in Figure 5.3 is constructed from the interpreted layer parameters of six VES. Among these, discussion on sample interpretations of VES curve TPV 2 which is near the bore hall TATW 2 is given on appendix-2.. As the standard VES TPV 2 has been used as an initial model to interpret and model VES TBV 8, TPV 6 and TAPV 4.Where as other VES-TBV 7 and VES- TAPV 8 are interpreted initially using two layers Master curve. Finally geoelectric section along traverse line 1 is mapped using a priori information (data) such as bore hall, thickness of the aquifer static water level 7.9 m, and thickness of alluvial deposit dominantly coarse size of sand, gravel and boulder 220 m to 238 m are adopted from Kobo-Robit-Minjar project report (ADSWE, 2013).The geoelectric section developed along traverse line 1 are discussed as follows:

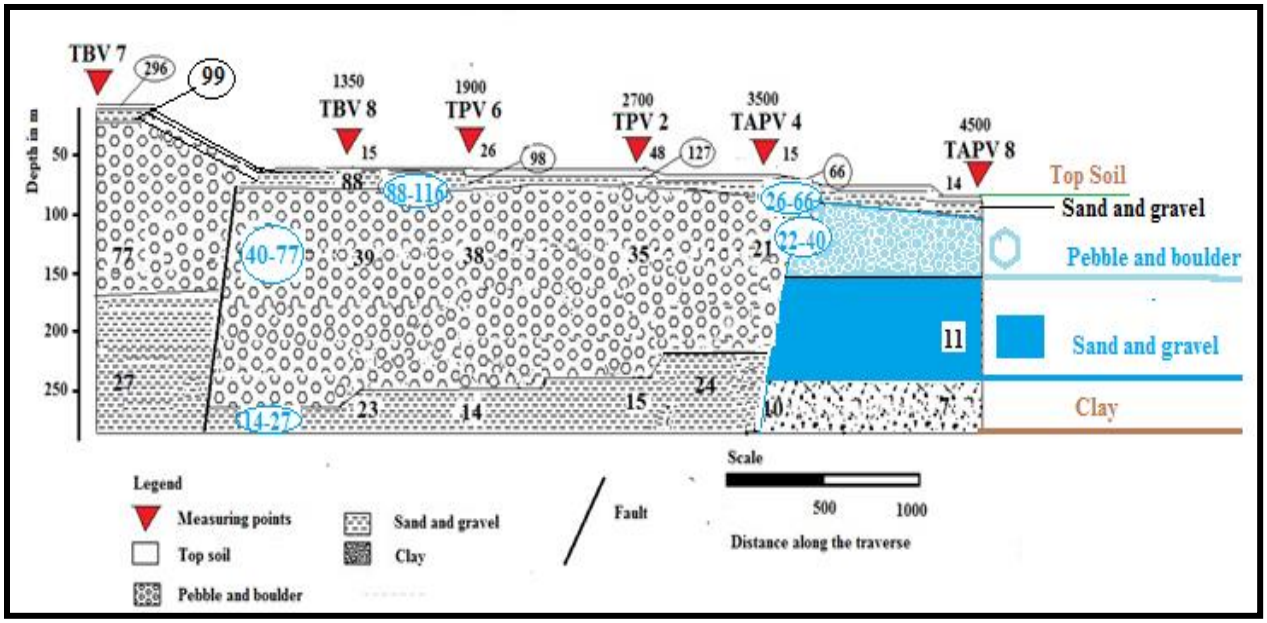

Figure 5.3 Geoelectric section along traverse Line 1, Tisabalima Eastern Amhara Regional State, Ethiopia.

The geoelectric section along the traverse Line 1 is represented by four to five layers of simple structures which dip along the traverse. The first layer having variable resistivity ranges 14 to 126 Ohm-m is represented by top clay soil. This layer extends on the top of traverse has an average thickness of 1 m.

The second layer located within VES point TBV 7 and TPV 2 has resistivity ranges from 88 to 116 Ohm-m is characterized by highly permeable sand and gravel. This layer having an average thickness 17 meter is highly porous and has an advantage in ground water recharging. Beyond the VES point TPV 2, this layer with resistivity range 26 to 66 Ohm-m extends down has a thickness from 4 to 20 meter.

The third layer oriented from VES point TBV 7 and TBV 6 is represented by pebble and boulder additional of sediments with a proportion nearly one fourth has high resistivity value within a range 40 to 77 Ohm-m. This layer with an average thickness 160 meter dominated the region is best situated area for ground water circulation within the neighboring layers. Due to a variation in moisture content of sub surface soil, this layer decreases its resistivity to range 22 - 40 Ohm-m indicated that moisture content increases along the region from VES point TPV 6 to TAPV8.

The fourth layer beyond the depth of 167 m decreases its resistivity from 14 to 27 Ohm-m beneath VES point TBV 7 to TAPV 8.The resistivity value indicates the layer to be a high yield aquifer sand and gravel. Below this layer, the fifth layer located between VES point TAPV 4 and TAPV 8; has a very low resistivity range 7 to 9 Ohm-m is considered to be moist clay.

Of all the layers mapped with the survey over this traverse, the fourth layer which is located beneath VES-TAPV4 and TAPV 8 within depth interval of 43m-140m and 20m-126m respectively, are suggested to be more promising for ground water exploration.

5.1.3Traverse Line 2

Traverse Line 2 oriented on direction of SW-NE has a total length of 2800 m. This line consists of 4 VES points that lay within an average VES point spacing 933 m.

A. Pseudodepth section along Line 2

Four VES points shown in Figure 5.4 aligning namely TBV 2, TAPV 5, TAPV 4 and TBV 14 are used in defining the Pseudodepth section along the traverse line 2.

Except the region at the top of VES TPV 2 and bottom of VES TBPV 14, all regions is covered by low resistivity zone. This low resistivity region having alluvial deposit is expected to have ground water potential in the region. In contrast, the high resistivity region beneath VES point TBV 2 is expected to be slightly weathered and fractured basalt.

B. Geoelectric section along traverse line 2

The geoelectric section along traverse Line 2 shown in Figure 5.5 reveals four main layers. Except in the middle of the profile, the upper most layer is covered by high resistive dry top soil .This layer having an average thickness 2 m; is considered to be variable in moisture content of the sub soil changes within resistivity of range of 7 to 44 Ohm-m.

Except between VES point TBV 2 and TAPV 5, the second layer having high resistive 21 to 66 Ohm-m is interpreted as pebble and boulder. This layer increases its thickness along the profile from 42 m at VES point TAPV 4 to 12 m at TBV 14.

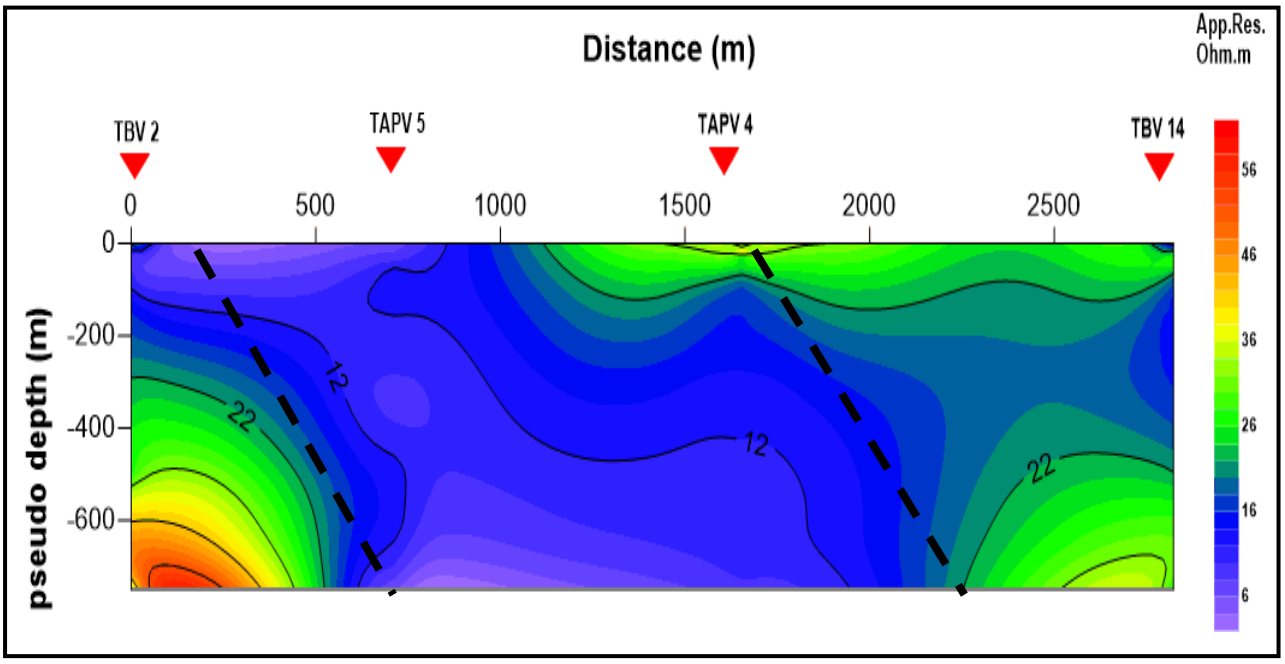

Figure 5.4 Pseudodepth sections along traverse Line 2, Tisabalima Eastern Amhara Regional State, Ethiopia.

In contrast, the third layer located between VES point TAPV 5 and TAPV 4 is dominated by unconsolidated thick gravely clay layer (46 to 120 m). This layer with resistivity range 12-15 Ohm-m is defined to be a high yield aquifer for ground water exploration.

Except beneath VES point TAPV 5 and TAPV 4, the forth layer with resistivity 35 and 41 Ohm-m) is characterized highly weathered and fractured basalt. Whereas beneath the point TAPV 5 and TAPV 4, low resistive mineralized clay (9 Ohm-m) is sandwiched by highly weathered and fractured basalt. The variation in resistivity indicates the possible position of structure can be depicted in between VES point TBV 2 and TAPV 4.

For ground water exploration purpose the third gravely clay layer which is located between the VES point TAPV 5 and TAPV 4 is the best position where ground water can be tapped.

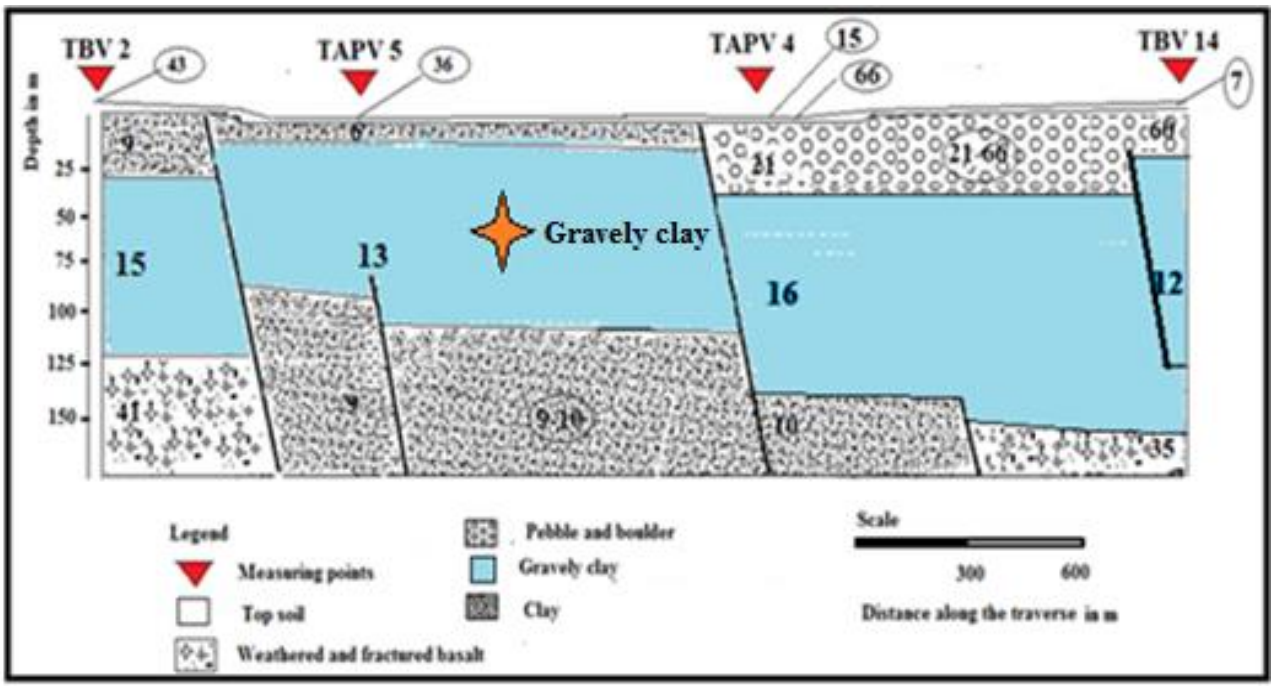

Figure 5.5 Geoelectric section along traverse Line 2, Tisabalima Eastern Amhara Regional State Ethiopia.

4.1.4 Traverse Line 3

This line shown in figure1.3 is oriented in NW to SE direction. This with a total length of 2506 m is identified by 3 VES points namely TAPV7, TPV3 and TBV14 .The average distance between each VES point is nearly equal to be 1253 m.

A. Pseudodepth section along traverse line 3

AT the shallower depth level between VES point TAPV 7 and TAPV 3 (Figure 4.6.), the region are dominated by high resistivity value which corresponds to dry silt and clay.

At deeper depth point VES TBV14, it is covered by high resistivity value which corresponds to fresh basalt. In contrast the low resistivity region is related to geological formation having high yield aquifer.

B. Geoelectric section along traverse Line 3

The geoelectric section along the traverse Line 3 (Figure 5.7.) is represented by three or four layers of simple structures which dip along the traverse. The first layer with resistivity ranges 7 to 28 Ohm-m is represented by dominantly top soil clay. This layer extends on the top of traverse varies with thickness from 1.3 m to 6.4 m is considered to be so thin that its contribution for ground water distribution is inconsiderable.

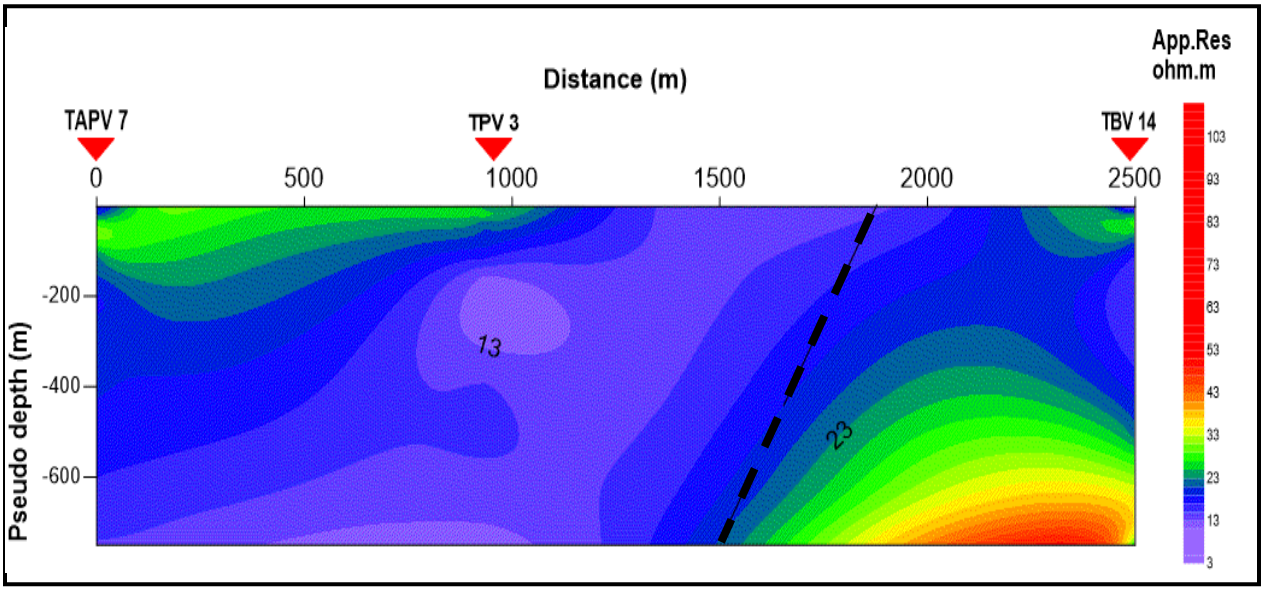

Figure 5.6 Apparent resistivity pseudodepth section along traverse Line 3, Tisabalima Eastern Amhara Regional State Ethiopia.

The second layer with resistivity ranges 25 to 40 Ohm-m is characterized by highly permeable pebble and boulder. This layer with average thickness of 31 m covers the whole traverse dips in the NE direction. Due to its permeability, this layer may acts like a conduit for ground water movement dawn to the traverse line.

At deeper depth point below VES TBV 14, the last layer is covered by resistivity value 40 Ohm-m which corresponds to slightly weathered and fractured basalt. In contrast the low resistivity layer below VES TAPV 7 and TPV 3 has resistivity range 8 to 16 Ohm-m is related to geological formation having high yield aquifer sand, gravel and clay (Gravely).

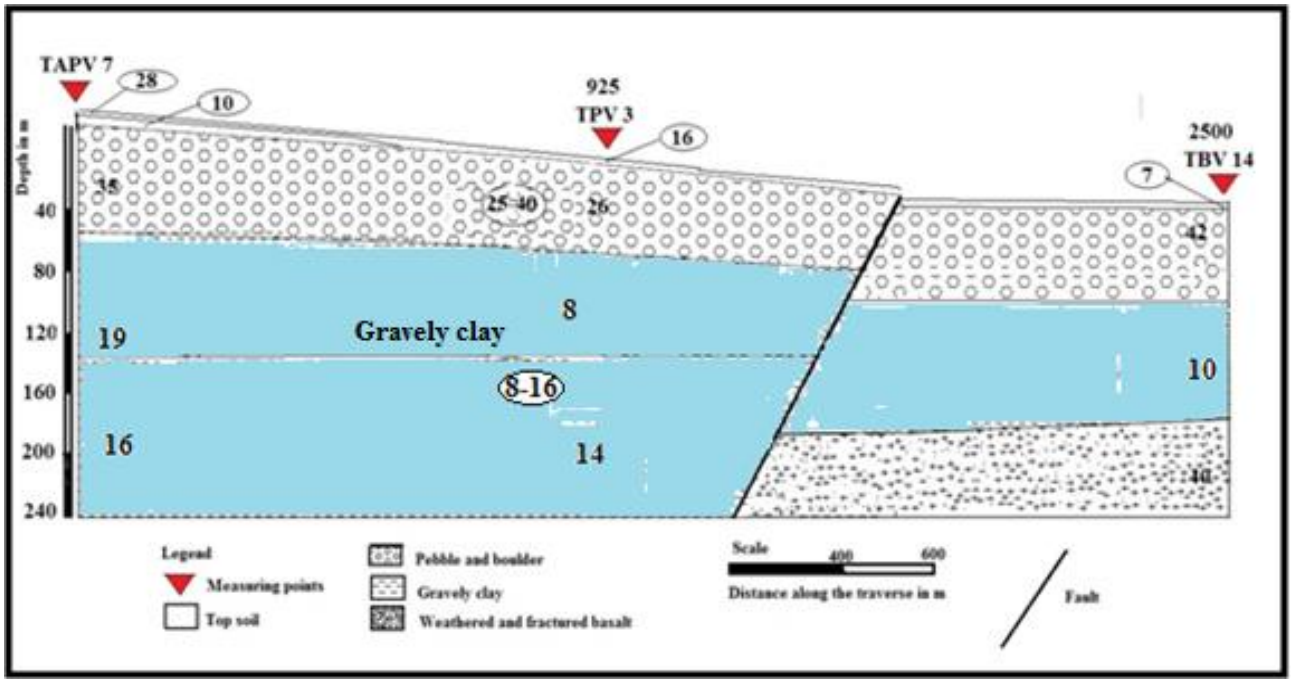

Figure 5.7 Geoelectric section along traverse Line 3, Tisabalima Eastern Amhara Regional State, Ethiopia.

4.1.5 Traverse line 4

This line is oriented in south west to north east direction. The line has a total length of about 3381m and having 3 VES points namely VES point TPV6, TPV3 and TBV1.The average distance between each VES point is nearly equal to 1253 m.

A. Pseudo depth section along Line 4

AT the shallower depth level between VES point TPV6 and TPV3 is dominated by high resistivity value which corresponds to dry silt and clay. At deeper depth VES point TBV1 there is a high resistivity value which corresponds to fresh basalt. The contrast between low to high resistivity region is related to top dry soil and the bed rock is an indication of faults which is located at a distance of 1500 m and 3000 m on the survey line.

B. Geoelectric section along traverse line 4

The geolelectric section developed along traverse line 4 is characterized by litho logical unit clay, boulder, sand (gravel) and weathered or fractured basalt.

The first geoelectric layer with resistivity range 26 to 35 Ohm-mis defined to be top soil clay. This layer which covers the upper most geoelectric section with an average thickness 1m is considered to have less effect for ground groundwater occurrences in the area. Beneath this layer, the second geoelectric layer located beneath VES point TPV 6 having a thickness 16 m showed highly resistive pebble and boulder layer (98 Ohm-m).It spans horizontally within a distance of 800 m act as a medium for ground water recharging.

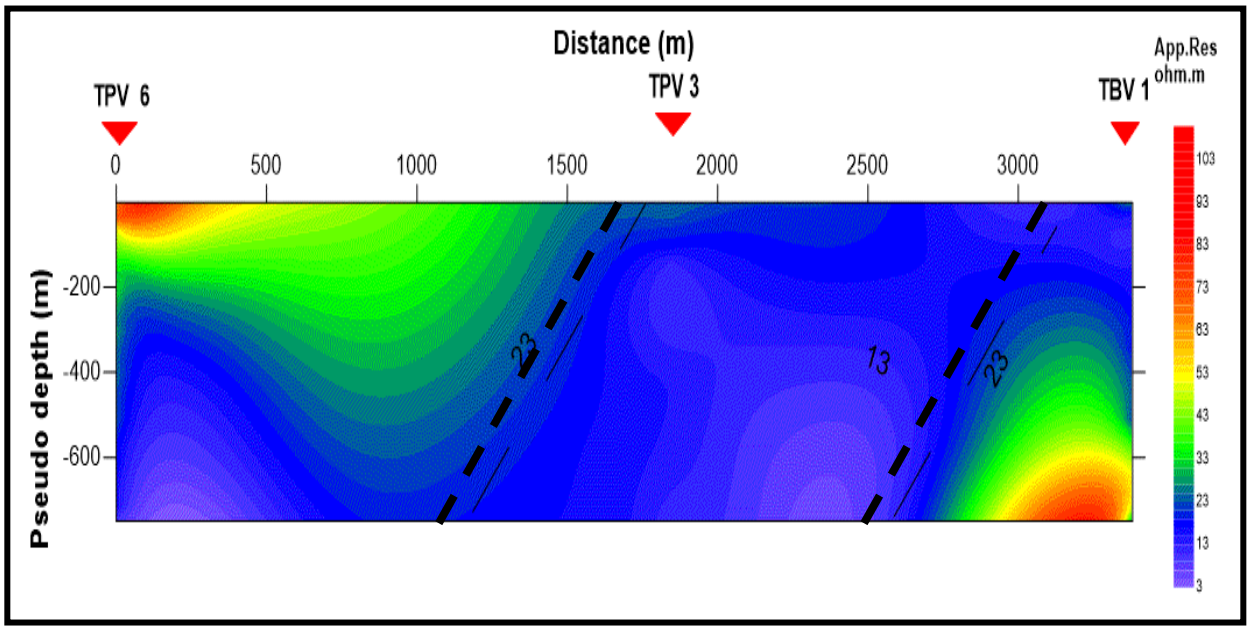

Figure 5.8.Pseudodepth sections along traverse Line 4, Tisabalima Eastern Amhara Regional State, Ethiopia.

Whereas the third geoelectric layer having variable thickness 9 to 137 m cover the whole section from VES point TPV 6 to TBV 1 .This layer with resistivity range 16 to 38 Ohm-m is interpreted to be sand and gravely layer.

Except at end of VES point TBV 1, the fourth geoelectric layer is characterized by having very low resistive clayey layer with a range 8 to 14 Ohm-m. This layer which is located beneath the VES point TPV 6, TPV 3 and TBV 1 respectively can serve as a dam for accumulation of ground water. In contrast the fourth layer is highly resistive (60 Ohm-m) and it is interpreted to be slightly weathered and fractured basalt.

From the geoelectric section shown the third layer lying between the VES point TPV 6 and TPV 3 is considered to be potential source for ground water (aquifer zones).This layer having resistivity value 38 Ohm-m is considered to be a high yield aquifer. This layer which is sandwiched by overlain highly permeable boulder layer and underlain clayey layer makes it preferable for ground water exploration.

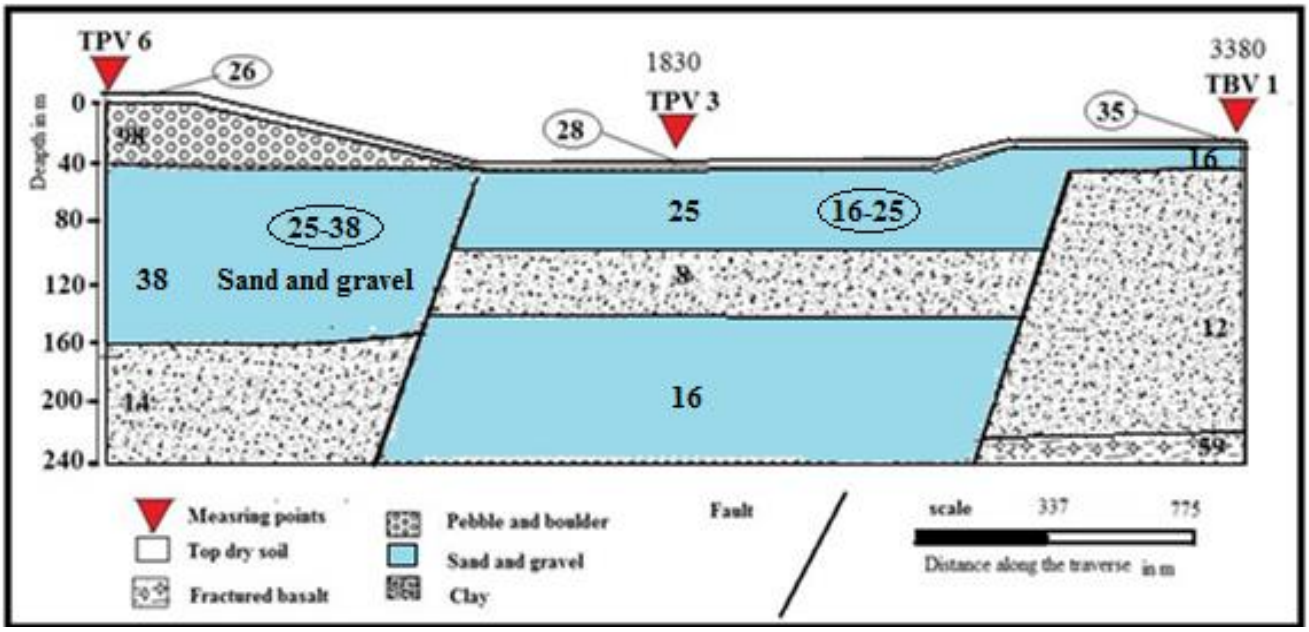

Figure 5.9 Geoelectric section along traverse Line 4, Tisabalima Eastern Amhara Regional State Ethiopia.

5.2 RESULT AND INTERPRETATION OF MAGNETIC DATA

5.2.1 Total magnetic field anomaly and analytical signal maps

The total magnetic field intensity map plotted shown in Figure 5.10, are corrected for diurnal variation shows variation of rock magnetization at their respective locations. The total magnetic field intensity map can be revealed within three magnetic anomaly patterns. The first pattern which is represented in region **A** shows low magnetic intensity 35444 nT to 35787 nT is represented to be sediment geological formation. In contrast, the high magnetic intensity (36096 nT to 36459 nT) located within a region **C;** is related to be tertiary volcanic rocks .This region is highly affected by dislocation trends SW-NE direction. Between a region **A** and **C**, an intermediate magnetic intensity35787nT to36096nTdepicted in region B (green and yellow pattern) define the directions of the lineaments to be SW-NE, SE-NW and E-W.

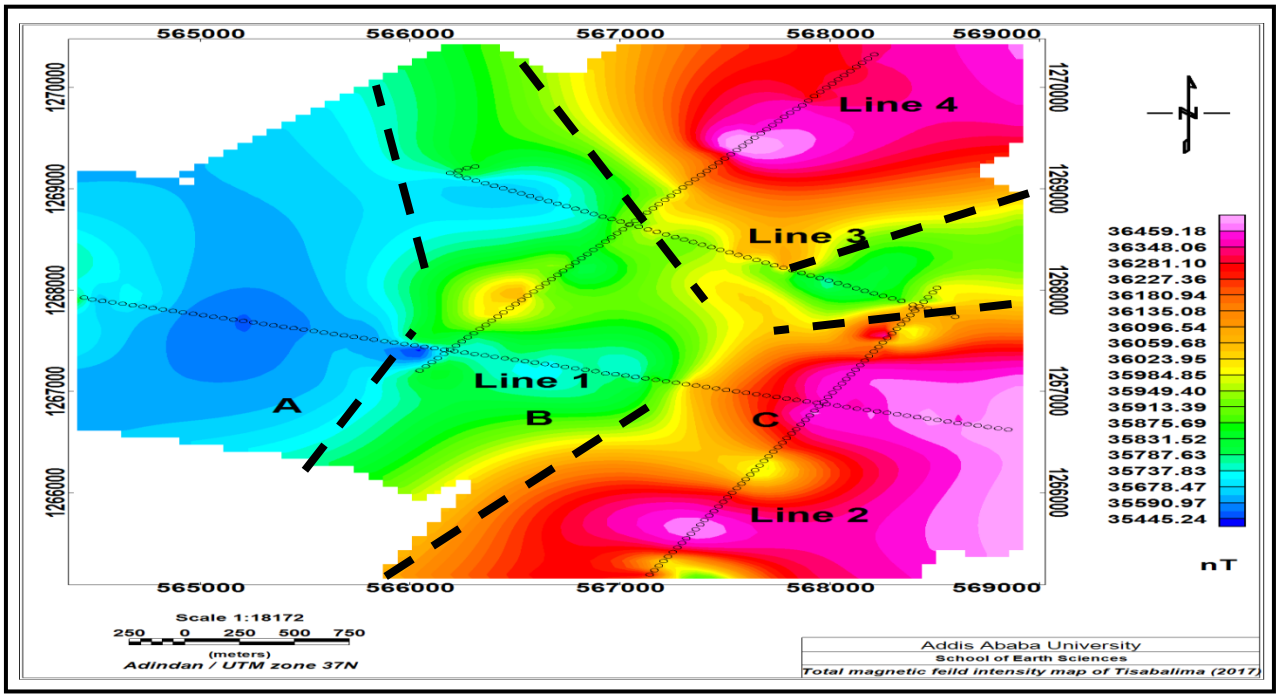

Figure 5.10 Total magnetic field intensity map of Tisabalima, Eastern Amhara Regional State, Ethiopia.

5.2.2 Residual magnetic field anomaly map

Magnetic anomalies, on the other hand, are a function of two independent parameters: the subsurface distribution of susceptibility and the orientation of the Earth's main magnetic field. Change one of these parameters will change the resulting magnetic anomaly. That is magnetic anomalies over the same susceptibility distribution will be different if the distribution is in a different location, say one located beneath the equator versus one located beneath the north pole. Additionally, the magnetic anomaly over a two-dimensional body will look different depending on the orientation of targeted object.

Strong remanent magnetization is abundantly observed with young volcanic rocks, while in sedimentary and metamorphic rocks the remanent magnetization is in general much lower than the induced magnetization (Reinhard et al., 2009).

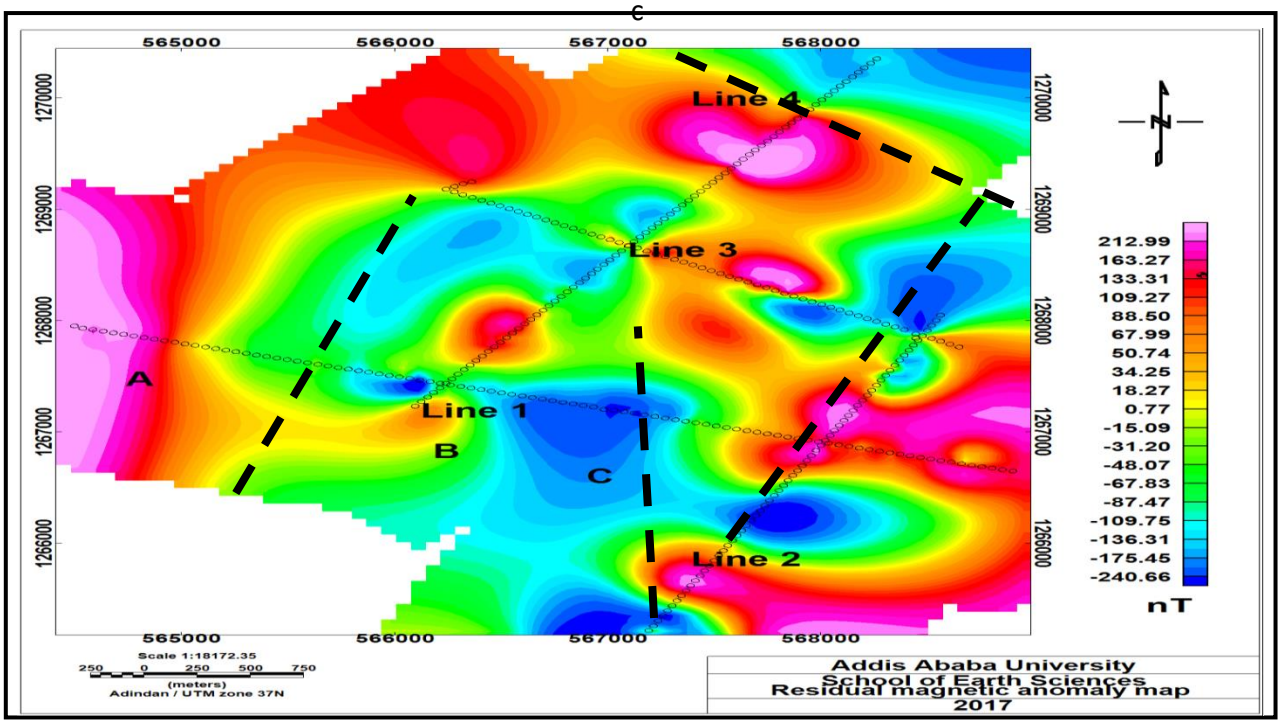

Figure 5.11Residual magnetic anomaly map of Tisabalima, Eastern Amhara Regional State, Ethiopia.

The residual magnetic anomaly map Figure 5.11 and 5.12 of the study area are compiled by applying a linear fit and Gaussian residual filter to the diurnally corrected total magnetic field intensity map of the study area (Figure 5.10).

These map shows relatively high residual magnetic anomaly represented in the region **A** (red and yellow pattern). This high magnetic response is could be magnetization of tertiary volcanic rocks basalt which is represented in the area. Whereas, the low magnetic responses represented by blue and green pattern B and C, could arise due to alluvial deposits located in the region. From the ground potential report of Kobo-Robit-Minjar, the alluvial deposits of the study area can reach from 100 to 200 m depth is dominant with coarse grain size (boulders, gravels and coarse sand).

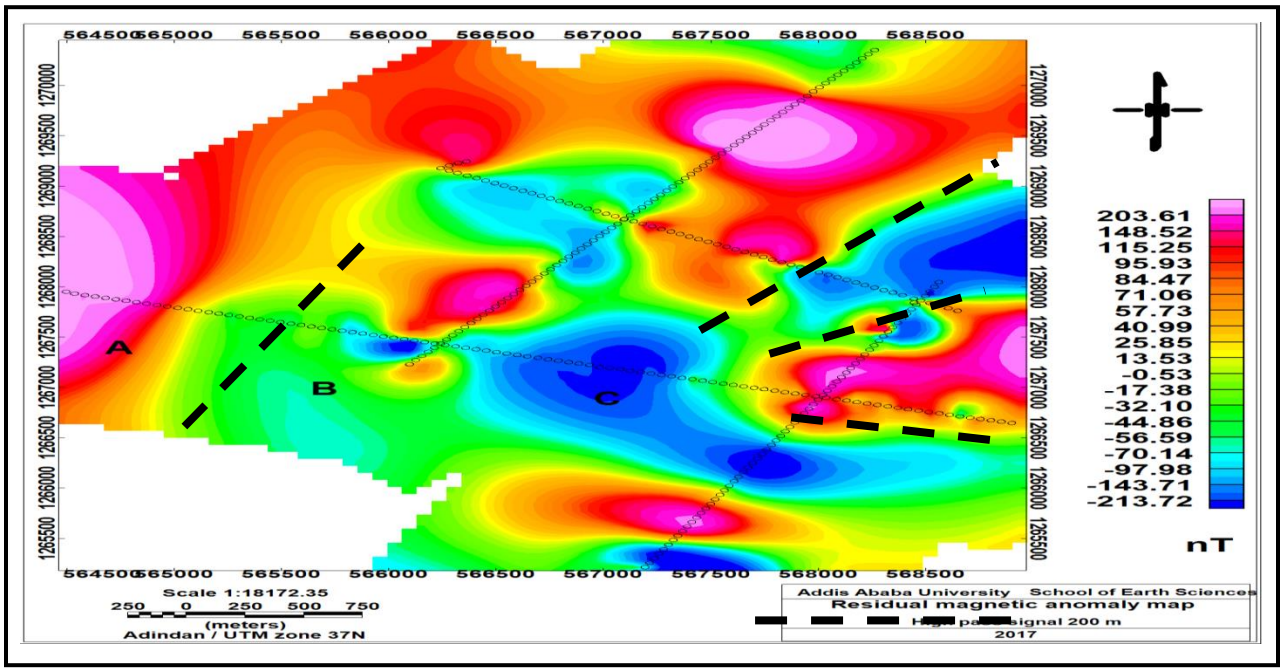

Figure 5.12 High pass filtered (200m cut off frequency) residual magnetic anomaly map of Tisabalima, Eastern Amhara Regional State, Ethiopia.

5.2.3 Residual magnetic anomaly trend along selected profiles

Residual magnetic anomaly profiles along the traverse line 1, 2 and 3 shown in Figure 5.12, 5.13 and 5.14are constructed from the residual magnetic anomaly map. These profiles are intended to

define faulted plains or a possible geological contact that acts as discharge areas for ground water release.

Residual magnetic profile line 1shown in Figure 5.12 is intended to define the faults that lie within Ethiopian Main Rift. Along the profile line 1 shown in Figure 5.12, high residual magnetic contrast to low evidence SSW-NNE two trending faults are confirmed to lie within Ethiopian Main Rift.

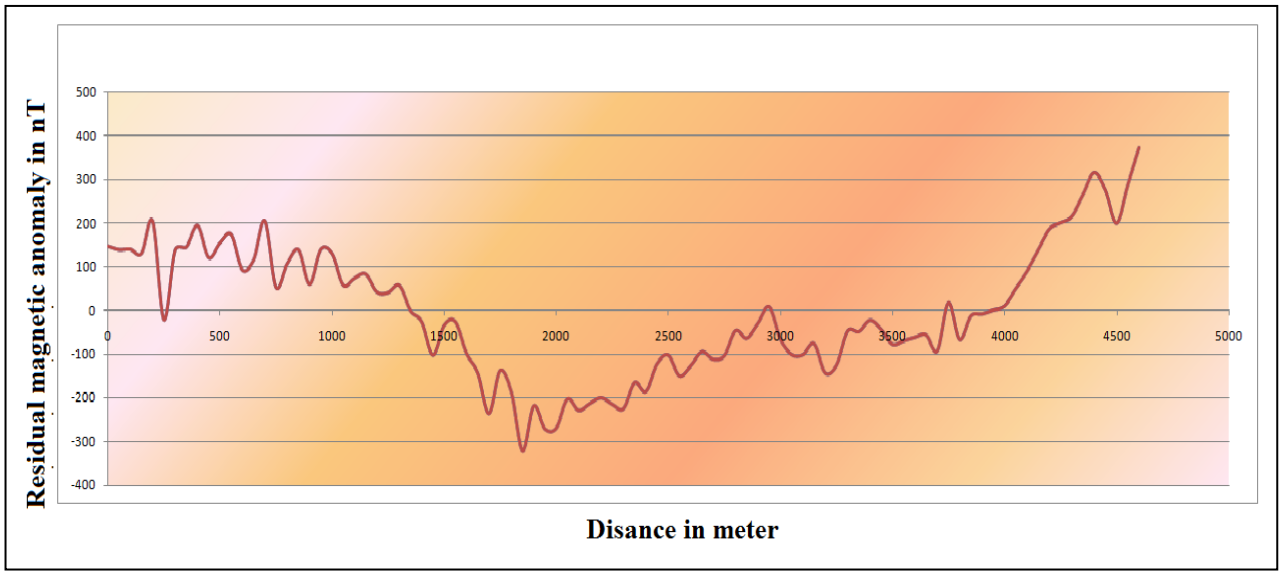

Figure 5.13 Magnetic profile plot along Line 1.

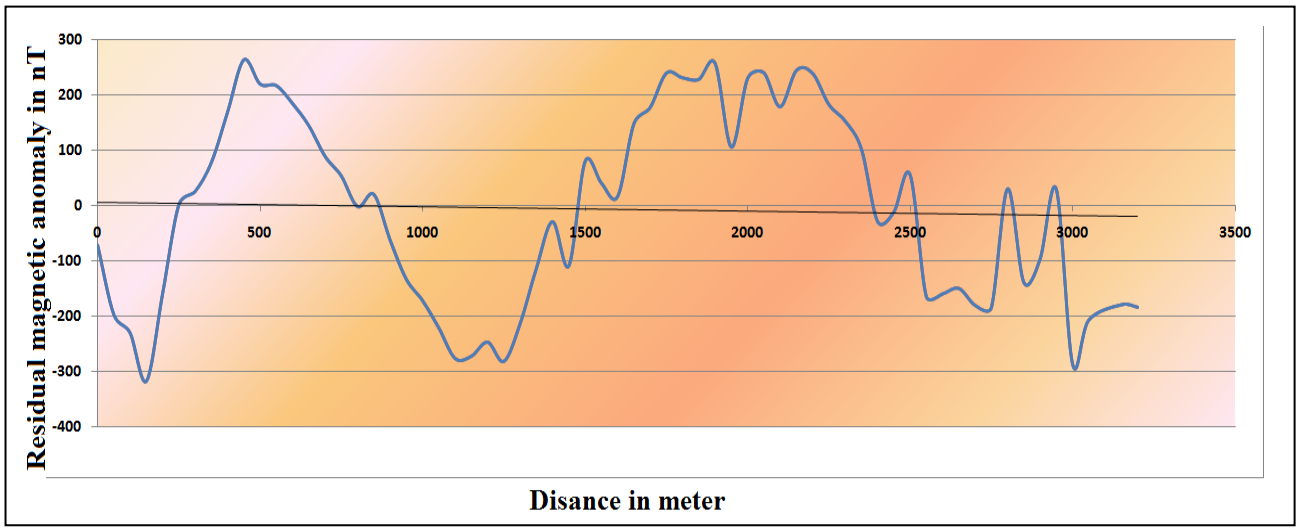

Figure 5.14 Magnetic profile plot along line 2.

Whereas, the contrast between high residual magnetic profiles (line 2) to low shown in Figure 5.13 define four possible geologic contacts. This is mainly caused by E-W trending faults elongated in a direction along the Gulf of Aden Ridge. Similarly residual magnetic profile of line 4 confirms four geologic contacts oriented in E-W.

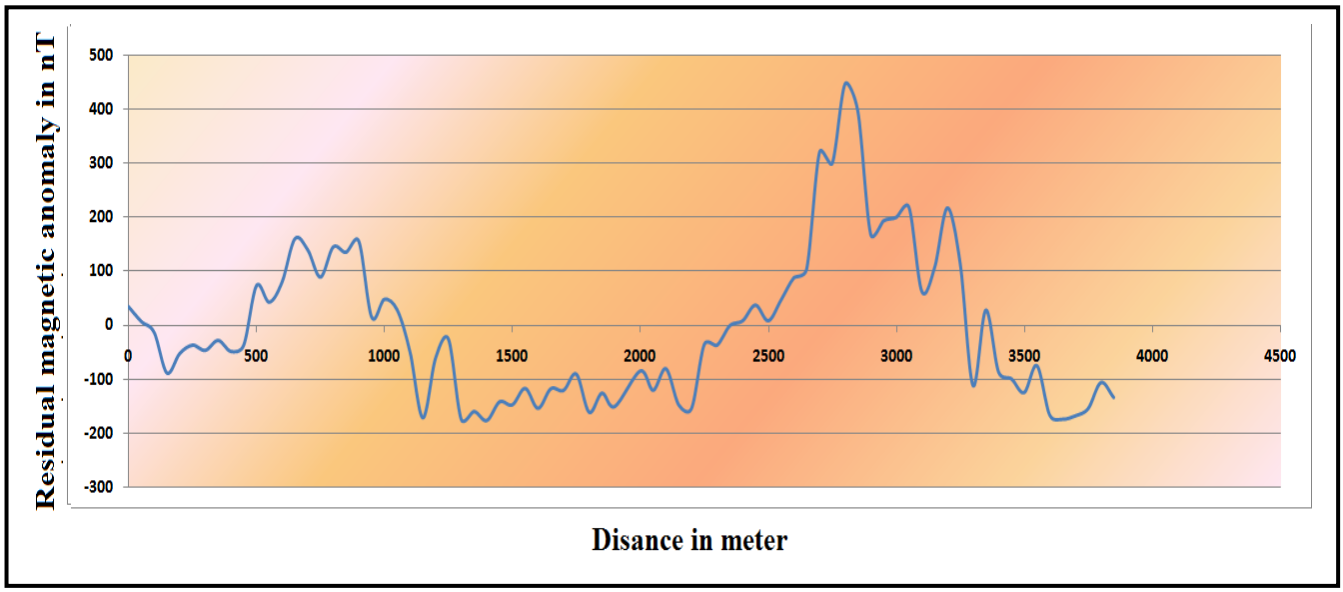

Figure 5.15 Magnetic profile plot along Line 4.

5.2.4 Magnetic analytical signal map

The analytical signal map Figure 5.16 is formed through a combination of horizontal and vertical gradients of a residual magnetic anomaly map. The analytic signal has a form over causative bodies that depend on the locations of the bodies but not their directions of magnetization.

The analytic signal method, known also as the total gradient method, as defined here produces a particular type of calculated gravity or magnetic anomaly enhancement map used for defining in a map sense the edges (boundaries) of geologically anomalous density or magnetization distributions (e.g., basement fault block boundaries, basement lithology contacts, fault/shear zones, igneous and salt diapirs, etc.).

The amplitude of analytic signal of the magnetic anomaly of a 3D source can be given by the following formula:

$$|AS(x,y,z)| = \sqrt{(\frac{\partial M}{\partial x})^2 + (\frac{\partial M}{\partial y})^2 + (\frac{\partial M}{\partial z})^2}$$

In contrast to the sediments deposited in the area, High analytical signal gradient oriented in a direction SSW-NNE and W-E is caused by High Susceptibility contrast of basalt. Whereas low magnetic anomalies values around region **c,** located in residual anomaly map; shows contrasting high analytical signal values. This is believed to be a structure that oriented towards NNE direction can acts like a barrier for ground water circulation.

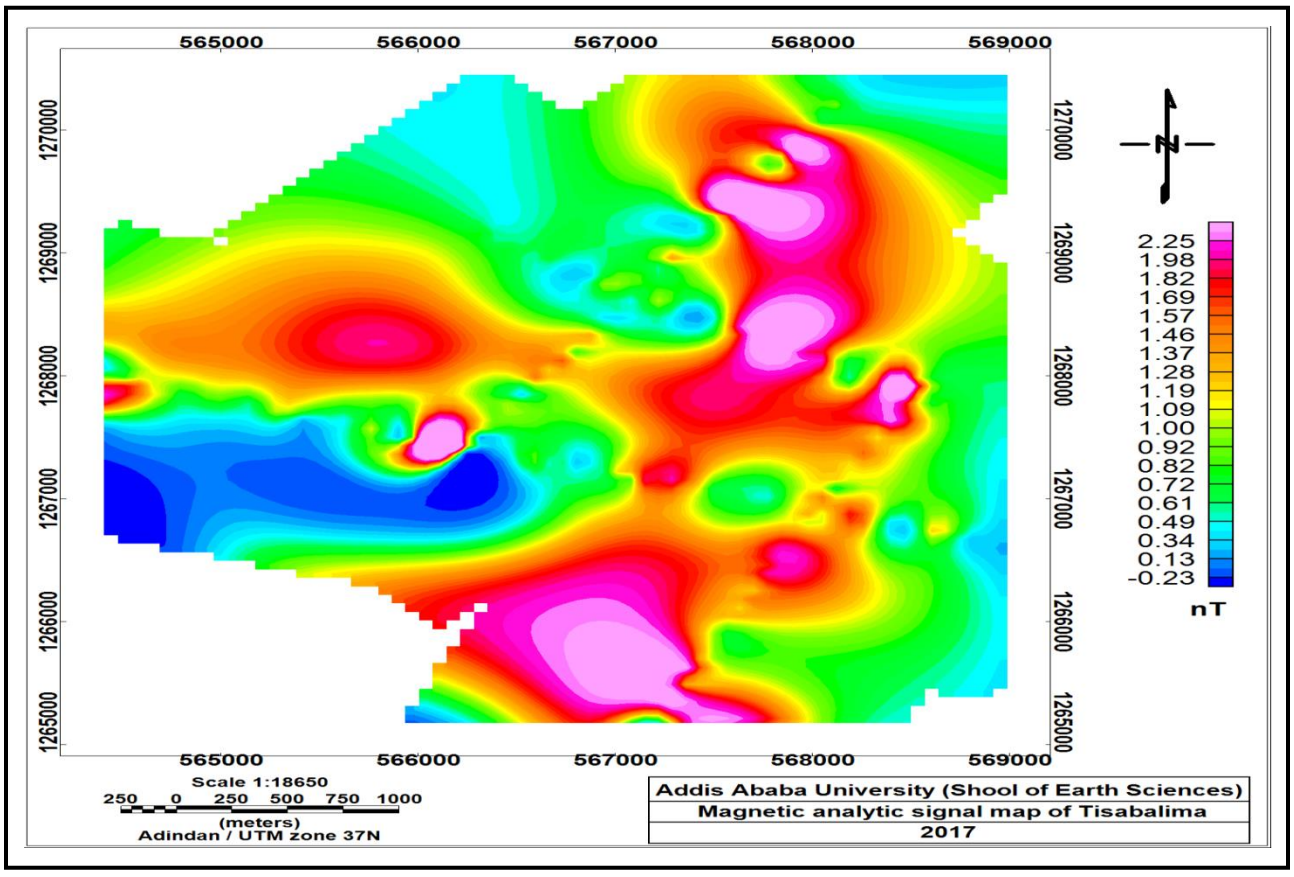

Figure 5.16 Magnetic analytical signal map of Tisabalima, Eastern Amhara Regional State, Ethiopia.

CHAPTER SIX

CONCLUSIONS AND RECOMMENDATIONS

6.1 Conclusions

Based on the result discussions and interpretations, the following conclusions have been drawn using the combination of data presentation approaches:

The interpreted results of each VES point and correlating the values along the profile line, geoelectic sections reveal resistivity values:

- 7 Ohm-m: top soil
- 6-10 Ohm-m: clay layer
- 26 – 116 Ohm-m: sand and gravel layer
- 8-16 Ohm-m: gravely clay layer
- 21-98: pebble and boulder layer
- 35 – 99 Ohm: weathered volcanic

Out of these layers, the geoelectical sections over each traverse identify the major source of groundwater in the area to be sand – gravely and gravely clay layer. These layers are mainly recharged with water through structural discontinuities like faults beside it are also recharged by overlaying layers pebble and boulder. Over all the potential sites for drillings has been identified within a depth interval of 44 m to 162 m are defined to be a water bearing horizon suggested to be more promising for ground water exploration.

The Geophysical results approve (evidence) the drilling results of well log shown in figure 6.1 that study area is covered by thick alluvial deposit 220 to 238 m. This area having a static water level 7.9 m is dominated by alluvial deposits of coarse size of sand, gravel and boulder.

The electrical and magnetic results correspond very well in mapping structural discontinuities of the study area. It is seen that the area is highly affected by tectonic events that trace NNE-SSW, NE-SW and W-E trending faults. Whereas groundwater is discharged from west to east, as a base flow which is conducted by W-E trending faults.

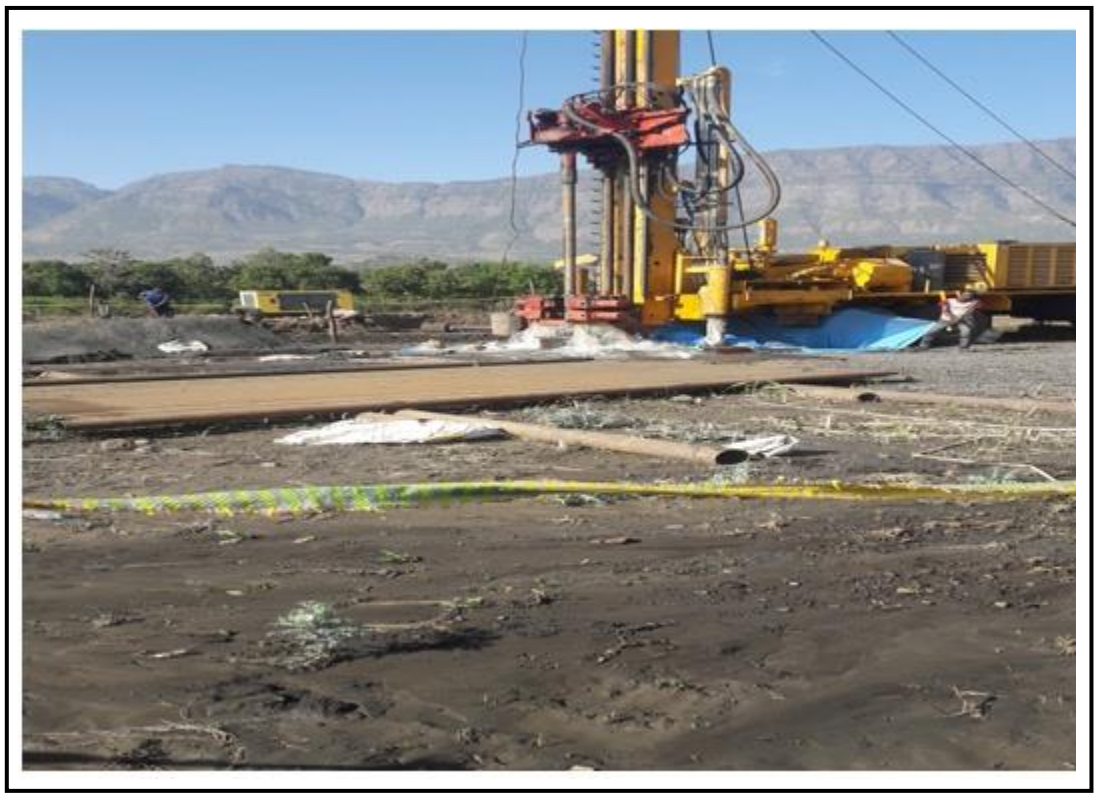

Figure 6.1 Drilling work progress of test well TATW 1, Eastern Amhara Regional State, Ethiopia.

6.2Recommendations

This study proves that the area is highly productive for ground water exploration, special care along the traverse lines should have to be made with a reference of the geoelectric section:

- Geoelectical section Line 2

Over all the layers the third layer within a depth of 120 m to 140 m is defined to be a water bearing horizon suggested to be more promising for ground water exploration. Except the difficulty from the boulder layer above, drillings between VES TAPV 5 and TAPV 4 is better situated position. This layer may contain clay material to some extent or it can be taken as a region of gravely clay layer. Drillings in this layer can face multiple confined aquifers by clay; in this respect protection against subsidence of layers should have to be considered during drillings.

- Geoelectical section Line 3

The third clayey gravel layer with resistivity range 8 to 16 Ohm-m reveals high ground water potential. Drillings in this layer can face multiple confined aquifers by clay; in this respect protection against subsidence of layers should have to be considered during drillings.

- Within all geoelectric sections along the Lines

The resistivity value which is less than 10 Ohm-m can be an indication that the groundwater in the study area can contain highly dissolved mineral. For an effective ground water exploration, further studies using integrated geophysical methods should have to be made in mapping the regional structural as well as for mapping the possible mineralized zone of the study areas.

7. REFERENCES

ABEM (2009).ABEM instruction manual for SAS 4000/ SAS 1000. ABEM instruction AB, Allen 1, S-17266 Sundbyberg, Sweden.

Amhara Design and Supervision Works Enterprise (ADSWE) (2010).*Eastern Amhara Development Corridor Project Geophysical Survey report for Groundwater Potential Assessment*. Unpublished technical report, Bahirdar, Ethiopia, p.109.

Amhara Design and Supervision Works Enterprise (ADSWE) (2013).*Groundwater Potential Assessment of Eastern Amhara Development Corridor of Awash Basin (Kobo-Robit-Minjar) project.*Unpublished technical report, ADSWE, Bahirdar, Ethiopia, p. 200.

ADSWE**,** 2017; *Well Completion report on wells drilled in Tisabalima water shade*. Unpublished technical report, Bahirdar, Ethiopia.

Bernard, J. (2003).Short notes on the principles of geophysical methods for groundwater investigations.

Charles, R. (2002). *Ground Water Science*. Elsevier Science ltd.Califrnia USA,p.450.

Fetter,C.W.(2001).*Applied Hydrogeology*, Prentice-Hall,Inc.Upper Saddle River,New Jersey 07458, pp.: 66-88.

Gibson, P.J. and George, D.M., (2003). *Environmental applications of geophysical surveying techniques*. Nova Science Publishers, Inc. New York. Africa,pp:57**12(1),** Addis Ababa.

LewamTesfaLidet,(2015). *Application of integrated geophysical techniques to map groundwater potential zones and geological structures at welhe basin, south of Sekota*. MSc thesis, Addis Ababa University, Ethiopia.

Loke, M. H., (2001**).** Electrical *imagine survey for environmental and engineeringstudies: A practical guide to 2D and 3D surveys.*

Milsom, J. (2003). *Field Geophysics*. John Wiley & Sons Ltd, London, England, 3rd edi., p.548.

Mulugeta Chanie, (2011).*Application of integrated geophysical techniques to mapgroundwater potential zones and geological structures at Gelchet area, Borena zone,South Ethiopia.*MSc thesis, Addis Ababa University.

Never, K.(2009).Ground Water Resources: Sustainability, Management, and Restoration.Mc McGraw-Hill Companies, Inc. New York. United States, p.548.

Pavelic, P.; Giordano, M.; Keraita, B.; Ramesh, V. and Rao, T. (Eds.).(2012). *Groundwater availabilityand use in Sub-Saharan Africa: A review of 15 countries*. Colombo, Sri Lanka: International Water Management Institute (IWMI), pp.:37.

Telford, W.M., Geldart, L.P. and Sheriff, R.E., 1990**;** *Applied Geophysics,* 2nd Edition; Cambridge University Press, Cambridge, UK,p.770.

Tewodros Mulugeta, (2011).*Geophysical Investigation for Groundwater Potential assessment and Mapping Structures at Alidege Plain*, South Afar, Ethiopia, MSc thesis.

TibebeMengesha, (2006).*Integrated Geophysical Investigation for the Evaluation of Groundwater Resources at Ada'a plain Near Debre-Zeit*, MSc thesis.

Reynold, (1997).*An Introduction to Applied and Environmental Geophysics.* John Wiley and Sons limited, England, UK, p. 160.

S.S. Stefanescu, C., (1930).*Schlumberger Distribution of electric field in potential horizontals layers, homogeneous and isotropic*, J.Phys. radium,**7**:132-141.

Vander Velpen B.P.A., (1995)**.***RESIXIP and Win Resist software*, 1st version; Interpex limited company.

Yahya Ali (2011).*Geophysical Investigations of the Gergedi Thermal Springs, North West of Wonji, Main Ethipian Rift*, Addis Ababa University, Addis Ababa, Ethiopia, MSc thesis.

William L. (2007). Fundamentals of Geophysics, Cambridge University Press, United states of America New York p.381.

`8. ADDENDUM

APPENDIX -1

Interpreted VES Curves

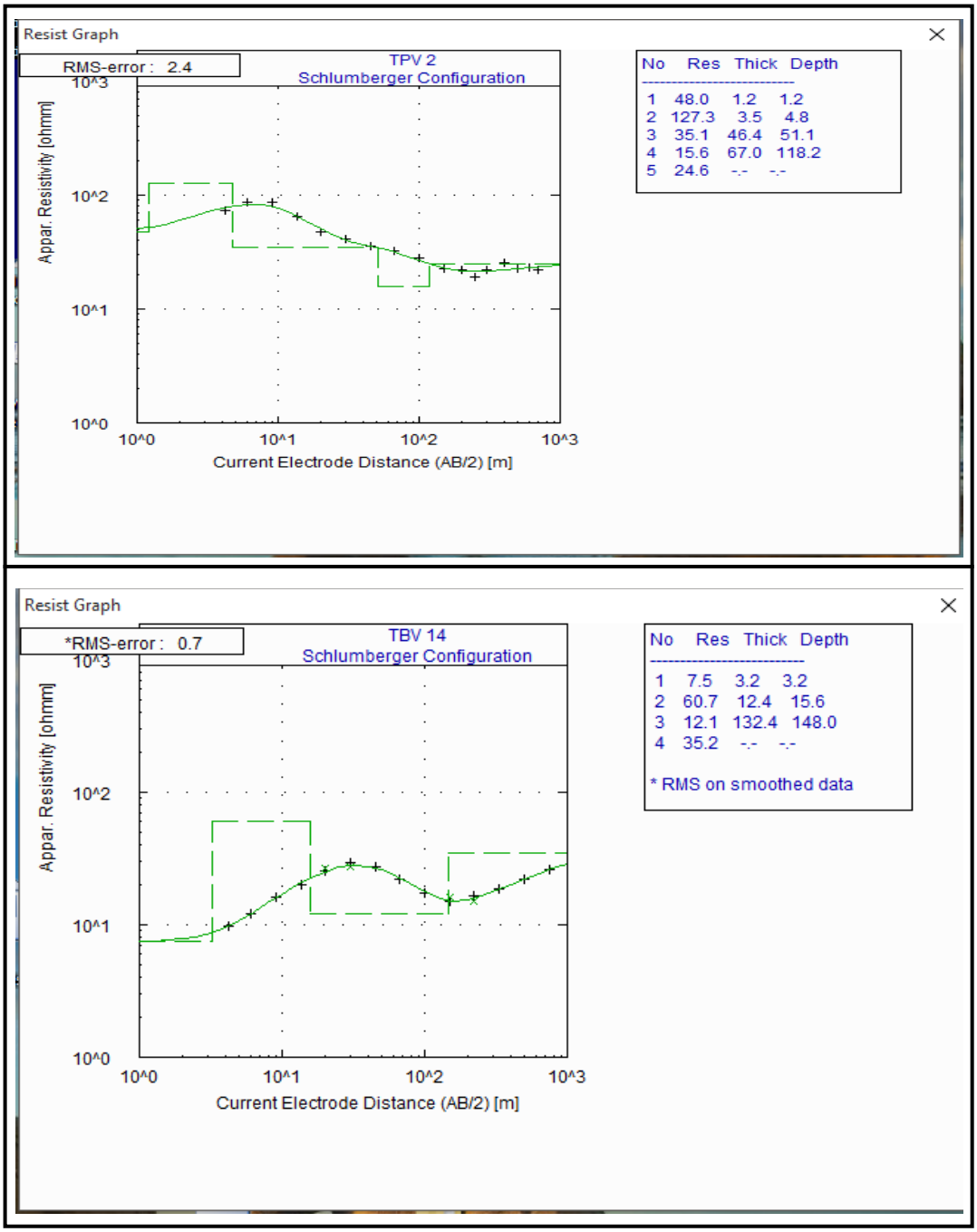

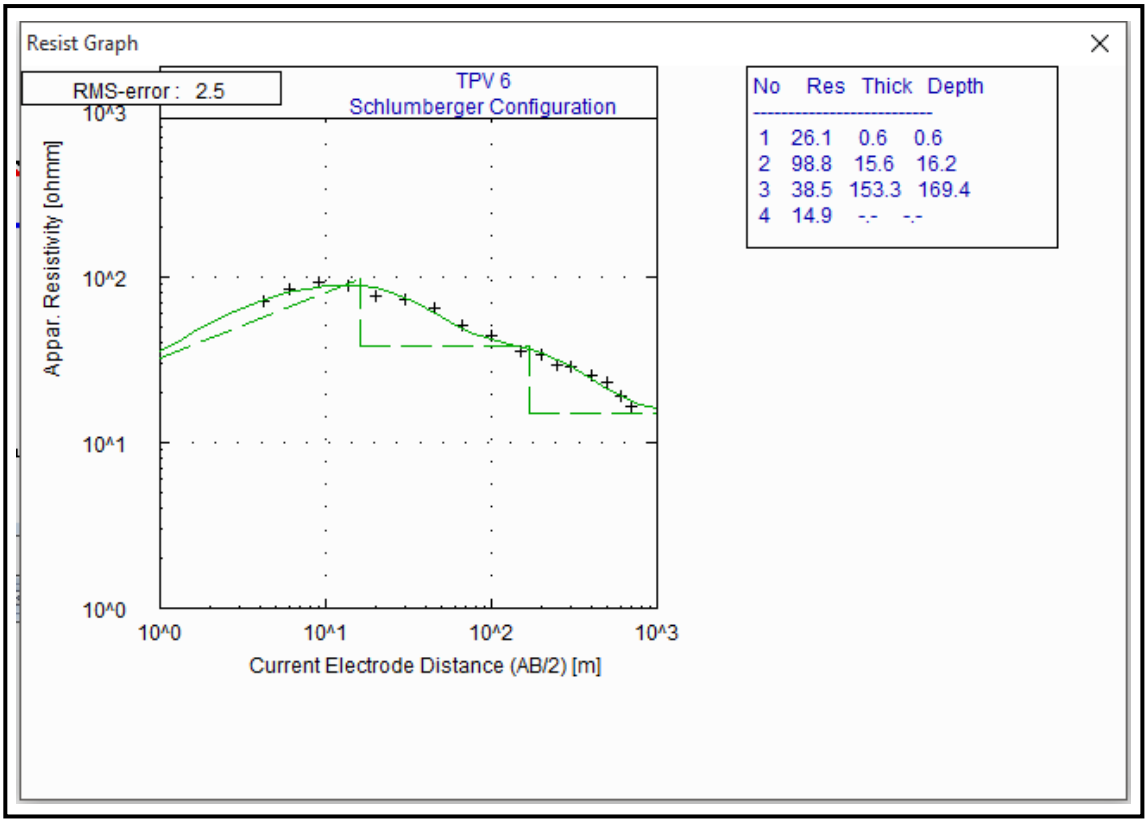
Resist Graph
RMS-error : 2.5
TPV 6
Schlumberger Configuration
No Res Thick Depth
1 26.1 0.6 0.6
2 98.8 15.6 16.2
3 38.5 153.3 169.4
4 14.9 -.- -.-
Appar. Resistivity [ohmm]
10^3
10^2
10^1
10^0
10^0 10^1 10^2 10^3
Current Electrode Distance (AB/2) [m]

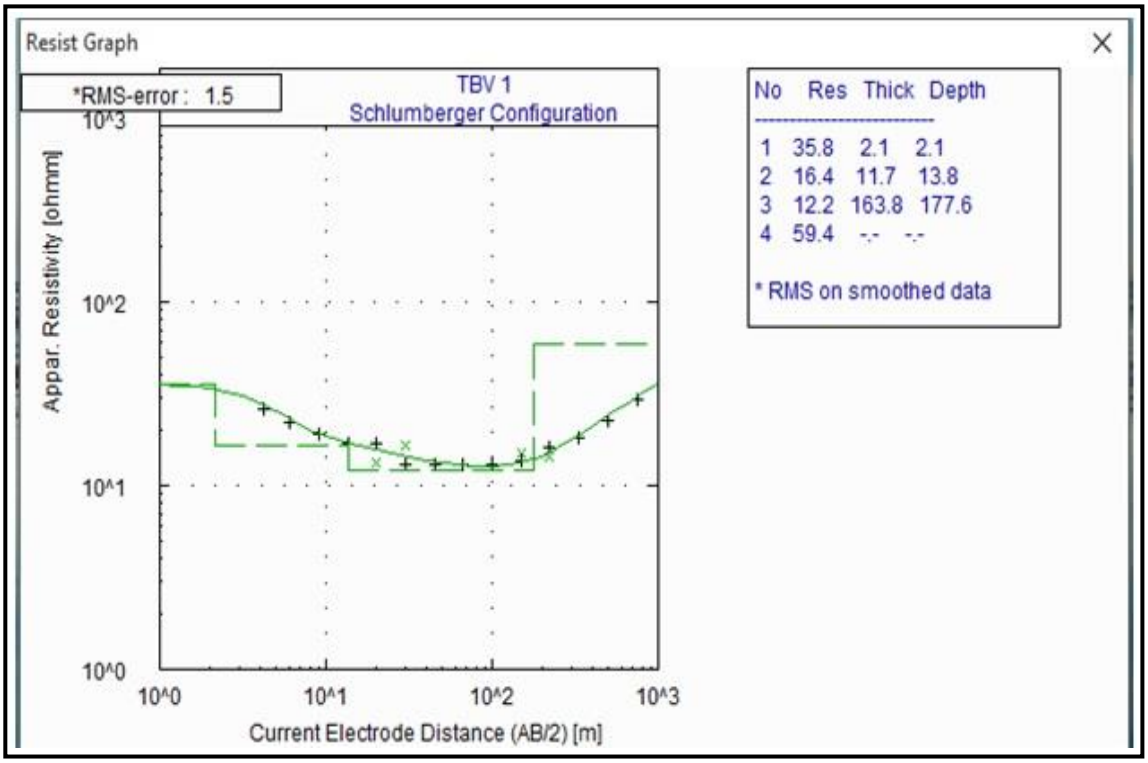
Resist Graph
*RMS-error : 1.5
TBV 1
Schlumberger Configuration
No Res Thick Depth
1 35.8 2.1 2.1
2 16.4 11.7 13.8
3 12.2 163.8 177.6
4 59.4 -.- -.-
* RMS on smoothed data
Appar. Resistivity [ohmm]
10^3
10^2
10^1
10^0
10^0 10^1 10^2 10^3
Current Electrode Distance (AB/2) [m]

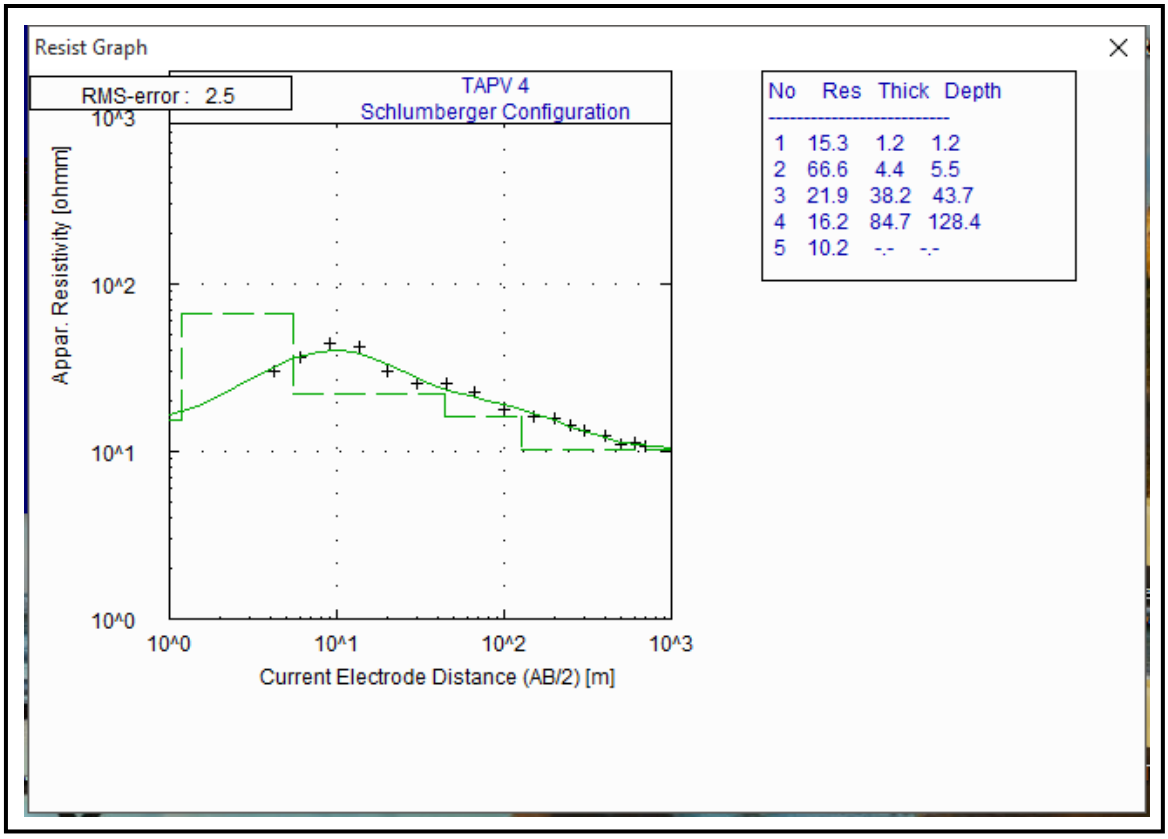

APPENDIX -2

Table 4.3Litho logical description of Borehole TATW1 in meter.

Depth from	to	Lithological Description
0	4	top soil (black cotton soil)
4	8	silt
8	26	gravel and sand
26	28	gravel with some clay
28	38	gravel
38	48	coarse gravel and pebble
48	80	peble and boulder
80	90	gravel with clay
90	94	pebble with boulder
94	98	gravely clay
98	100	gravel
100	104	clayey gravel
104	108	gravel

108	110	clayey gravel
110	112	gravel
112	120	clayey gravel
120	124	gravel
124	130	clayey gravel
130	146	clay
146	148	gravely clay
148	152	gravel
152	156	gravely clay
156	166	clay
166	170	gravely clay
170	184	gravel with some silt
184	190	gravely clay
190	200	clay with some gravel
200	208	gravel and pebble
208	210	clay
210	218	clay with some gravel
218	220	gravel
220	224	decomposed grains gravel
224	228	gravel
228	253	fractured and slightly weathered basalt

Well Design of Well ID TATW1

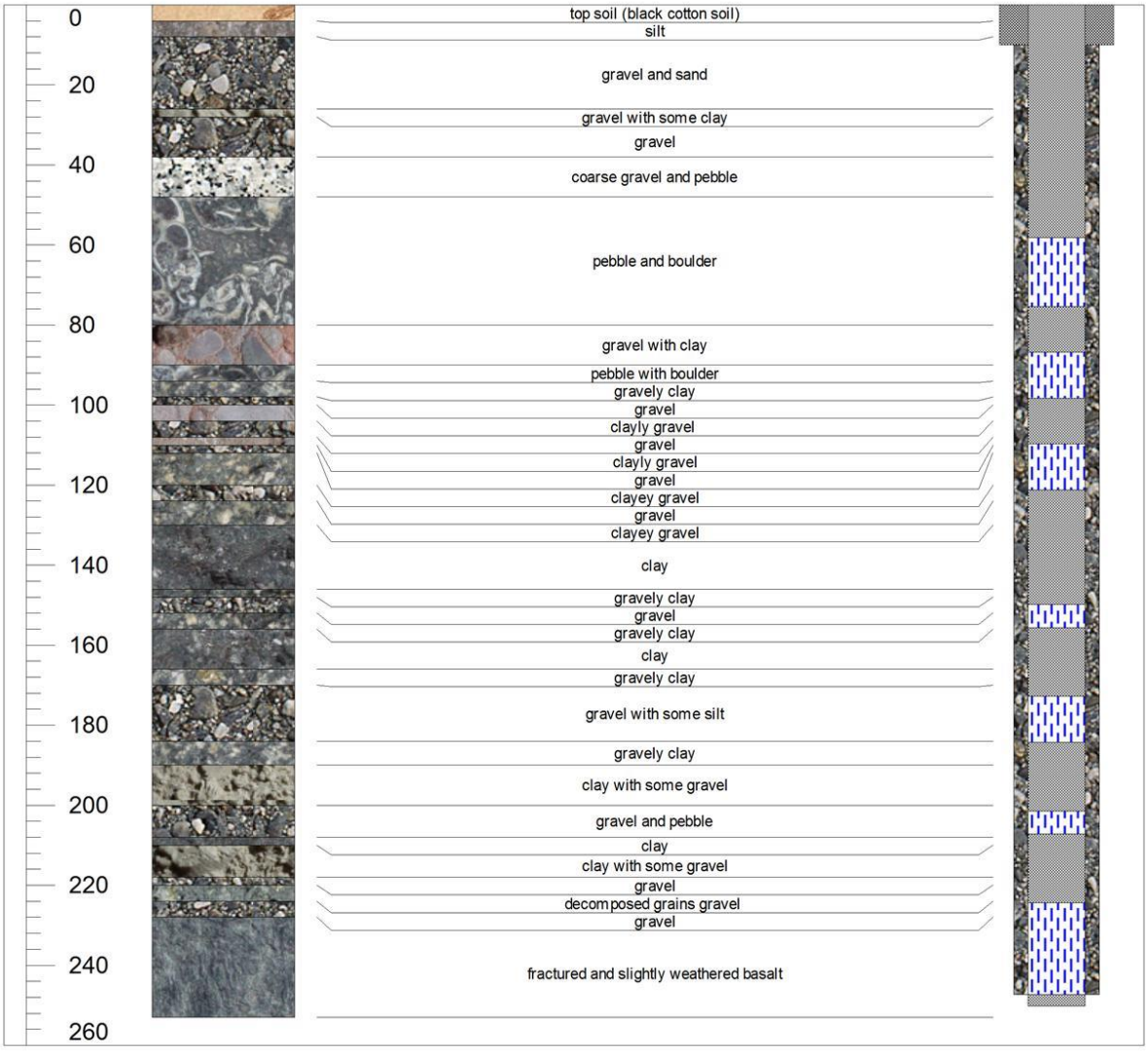

Prepared by Al Nile Business Group

Table 4.4Litho logical description of Borehole-2 in meter.

from	To	
0	6	Top soil
6	36.35	boulder
36.35	66.85	Coarse sand with gravel
66.85	79.05	Coarse sand with clay
79.05	91.25	Clay with minor gravel
91.25	97.35	Coarse sand with gravel
97.35	112.6	Coarse sand with minor silt and clay
112.6	124.8	Coarse sand with minor gravel
124.8	130.9	Boulder
130.9	143.1	Coarse sand
143.1	185.8	Boulder
185.8	204.1	Coarse sand
204.1	213.25	Coarse gravel with clay
213.25	222.4	Coarse gravel
222.4	245	Highly fractured and slightly weathered basalt
245	248	Slightly fractured basalt

WELL ID TATW2

wereda Ambasel
Depth 248m

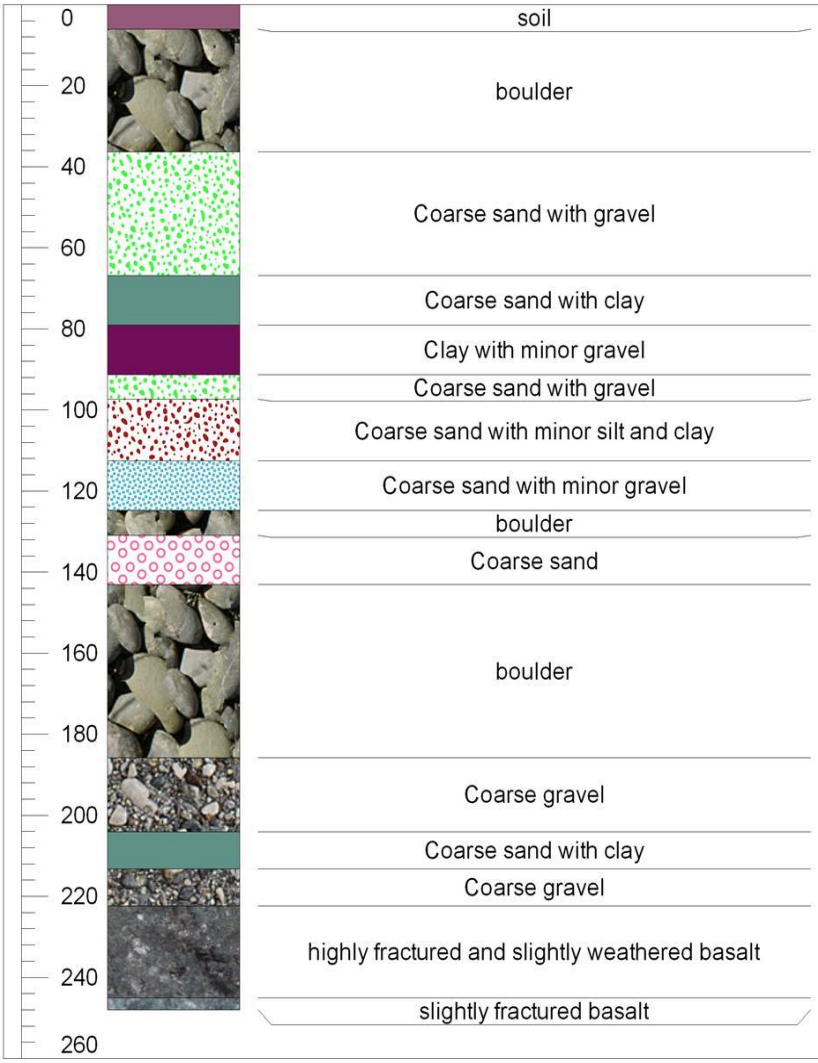

Tis-Abalima test well

9. DECLARATION

I hereby declare that the thesis entitled ‘‘The application of integrated geophysical techniques IN mapping ground water resource at Tisabalima sub basin, eastern Amhara regional state, Ethiopia.” has been carried out by me under the supervision of Prof. Tigistu Haile during the year 2017 as part of Master of Science program in Exploration Geophysics. I further declare that this work has not been submitted to any other University or institution for the award of any degree or diploma and all sources of material used for the thesis have been duly acknowledged.

Tewodros Mulugeta

Signature _____

Date _____

Place and date of submission: School of Earth Sciences, Addis Ababa University

July, 2017